

Department of Physics and Astronomy

University of Heidelberg

Master thesis

in Physics

submitted by

Martin Vökl

born in Filderstadt

2012

**Study of the Transverse Momentum Spectra
of Semielectronic Heavy Flavor Decays
in pp Collisions at $\sqrt{s} = 7$ TeV
and Pb-Pb Collisions at $\sqrt{s_{NN}} = 2.76$ TeV
with ALICE**

This Master thesis has been carried out by Martin Völkl

at the

Physikalisches Institut der Universität Heidelberg

under the supervision of

Prof. Dr. Johanna Stachel

Acknowledgements:

I would like to thank Prof. Dr. Johanna Stachel for supervising this project and enabling me to work in this field at a very exciting time for the study of the quark-gluon plasma. I would like to thank MinJung Kweon for her seemingly endless patience in discussions about physics and measurement strategies as well as for the supervision of the work presented here. Finally, I want to thank Yvonne Pachmayer, the KP ALICE group at the PI, the Heavy Flavor Electron group, and the ALICE collaboration for the support of the project, answers to numerous questions and great dedication to the research done in the ALICE experiment.

Contents

1. Introduction	7
1.1. Introduction to Quark-Gluon Plasma Physics	7
1.1.1. Approaches to Measurement	8
1.1.2. Measurement of Heavy Quarks	9
1.1.3. Measurable Quantities	12
1.2. The ALICE Experiment	13
1.2.1. The Inner Tracking System	14
1.2.2. The Time Projection Chamber	15
1.2.3. The Time of Flight Detector	16
1.2.4. The Transition Radiation Detector	17
2. Analysis of Electrons from Heavy Flavor Hadron Decays	18
2.1. Analysis Strategy for the Measurement of Inclusive Heavy Flavor Electron Transverse Momentum Spectra	18
2.1.1. Data Set, Event and Track Selection	18
2.1.2. Electron Identification	19
2.1.3. Cocktail Estimation	19
2.2. Estimating the Hadron Contamination	19
2.2.1. Energy Loss of Charged Particles in a Gas Detector	22
2.2.1.1. The Landau Approximation	25
2.2.2. The ALICE TPC Signal	26
2.2.2.1. TPC Clusters	26
2.2.2.2. The Truncated Mean Cut	27
2.2.2.3. Monte Carlo Reproduction of the Energy Loss Distribution	29
2.2.3. Fitting Binned Data	30
2.2.3.1. Fitting Binned Data using the χ^2 -measure	30
2.2.3.2. The Maximum Likelihood Method	31
2.2.4. Fitting the TPC Signal	32
2.2.4.1. Gaussian Approximation Efforts	32
2.2.4.2. Alternative Methods	37
2.2.4.3. Refinement of the Fit Quality	45
2.2.5. Fit Results	50
2.2.5.1. Electron Centers	50
2.2.5.2. Contamination and Efficiency	51
2.3. Measurement of Electrons from Beauty Decays	53
2.3.1. The RHIC Heavy Quark Energy Loss Puzzle	53

Contents

2.3.2.	The Impact Parameter	53
2.3.2.1.	Decay Vertices	53
2.3.2.2.	The Impact Parameter	54
2.3.2.3.	Contributing Processes	55
2.3.2.4.	Modeling the IP Shapes	57
2.3.3.	A Beauty Hadron Decay Electron Measurement Strategy	58
2.3.4.	Fits with Monte Carlo Templates	59
2.3.4.1.	A Modified χ^2 Method	60
2.3.4.2.	Likelihood Method	61
2.3.4.3.	Information Content of the Diagrams	61
2.3.4.4.	Issues with the Conversion Electrons	63
2.3.4.5.	Error Estimation	64
3.	Results and Discussion	72
3.1.	Results in pp	72
3.2.	Results in Pb-Pb	77
4.	Summary and Outlook	80
4.1.	Summary	80
4.2.	Outlook	81
A.	Notes on the Poisson Distribution	83
B.	Centrality Selection	85
C.	Glossary of Terms	87
	Bibliography	89

Abstract

The measurement of the transverse momentum spectra of hadrons containing heavy quarks in heavy ion collisions is important for understanding the properties of the quark-gluon plasma. In this analysis proton-proton ($\sqrt{s} = 7 \text{ TeV}$) and lead-lead ($\sqrt{s_{NN}} = 2.76 \text{ TeV}$) collisions performed at the LHC and measured with ALICE were investigated. The measurement was performed in the semielectronic decay channel of charm and beauty hadrons $H_c, H_b \rightarrow e + X$. Electron candidates were identified via the particle identification capabilities of the ALICE subdetectors. In this study, the adequate modeling of the TPC signal is discussed, leading to a simple model for the signal distribution. Application of the model via a fit of the free model parameters to the data well estimates the contamination of the final sample and efficiency of the selection for electrons.

Additionally, a method to separate the beauty and charm contributions to the electron spectrum is presented. It is based on the decoupling of the contributions from different sources via a fit of the impact parameter distribution using Monte Carlo generated distribution templates. The resulting systematic and statistical errors resulting from this approach are discussed in detail. They are found to be strongly dependent on the statistics available for both data and the Monte Carlo templates. A comparison with independent methods in pp collisions suggests great usefulness of this method for the currently investigated application to Pb-Pb collision measurements.

Übersicht

Die Messung der transversalen Impulsspektren von Hadronen mit schweren Valenzquarks (Charm/Bottom) in Schwerionenkollisionen hilft, die Eigenschaften des Quark-Gluon-Plasmas besser zu verstehen. In dieser Arbeit wurden diese für Proton-Proton- ($\sqrt{s} = 7 \text{ TeV}$) und Blei-Blei-Kollisionen ($\sqrt{s_{NN}} = 2.76 \text{ TeV}$) untersucht, die am LHC stattfanden und mit ALICE untersucht wurden. Die Messung wurde im semielektronischen Zerfallskanal der Hadronen $H_c, H_b \rightarrow e + X$ durchgeführt. Die Auswahl der Elektronen fand durch Nutzung der Teilchenidentifikationsfähigkeiten der Subdetektoren von ALICE statt. In dieser Arbeit wird hierzu die angemessene Modellierung des TPC-Signals untersucht, die zu einem einfachen Modell führt. Die Anwendung dieses Modells über einen Fit seiner freien Parameter ermöglicht eine gute Abschätzung der Verunreinigung der Elektronenauswahl und der Effizienz der Auswahlkriterien.

Desweiteren wird eine Methode vorgestellt, den Beitrag der beauty- und charm-Quarks enthaltenden Hadronen zu separieren. Diese basiert auf einer Entkoppelung der Beiträge über die zusätzliche Information aus dem Stoßparameter über einen Fit auf der Basis Monte Carlo generierter Verteilungsvorlagen. Die daraus resultierenden statistischen und systematischen Fehler werden im Detail besprochen. Sie zeigen eine starke Abhängigkeit von der Datenfülle sowohl der gemessenen als auch der Monte Carlo generierten Daten. Ein Vergleich mit unabhängigen Methoden in Proton-Proton-Kollisionen lässt gute Ergebnisse auch in den momentan untersuchten Blei-Blei-Kollisionen erwarten.

1. Introduction

In the high energy collisions of lead nuclei at the Large Hadron Collider (LHC), a new state of matter is created. This so-called Quark-Gluon Plasma (QGP) is of great interest to physics as it occurred in the earliest moments of the universe. Investigation of its properties will improve the understanding of the development of the early universe and of the properties of the strong interaction under extreme conditions. As no direct measurement of the universe at that time is possible, recreation in the collisions of heavy nuclei is the only viable experimental approach. Due to the small spatial extent and short duration of the QGP in the experiment, all information about its properties must be deduced from the particles created in the collision, which are measured in detectors such as ALICE (A Large Ion Collider Experiment). A particularly interesting quantity is the transverse momentum spectrum of particles containing beauty and charm valence quarks (beauty and charm hadrons). For the analysis presented here, the electrons from the semileptonic decays of beauty and charm hadrons were measured. Comparison of the resulting spectra in pp and Pb-Pb collisions yields information about the properties of the quark-gluon plasma which can be extracted via comparison to theoretical predictions.

This first chapter will give an introduction to the quark-gluon plasma, its physical properties and their measurement as well as to ALICE and those subdetectors most important for this analysis. The second chapter will explain about the measurement strategies themselves, explaining about the method and caveats of an inclusive measurement (meaning electrons from both beauty and charm hadrons decays) and a measurement of the contributions from beauty and charm hadrons separately. In the third chapter the results from these approaches will be discussed while the possibilities of future studies in this area will be explored in the fourth. In order to make the text easier to read, a glossary of frequently used terms is provided in the appendix.

1.1. Introduction to Quark-Gluon Plasma Physics

According to the well tested theory of Quantum ChromoDynamics (QCD), hadronic matter consists of quarks whose interaction is mediated by gluons. Gluons and quarks each carry color charge which is conserved in all processes. Quarks and gluons in vacuum form mesons and baryons in which the color charges cancel for an outside observer. No particle with an unbalanced color charge has been observed so far. It is thus expected that quantum chromodynamics leads to a confinement property of particles with color charge, which does not allow free colored objects [23].

In hadronic matter at high temperatures and energy densities, color charge screening effects weaken this condition somewhat. Here, a medium can be created, within which quarks are

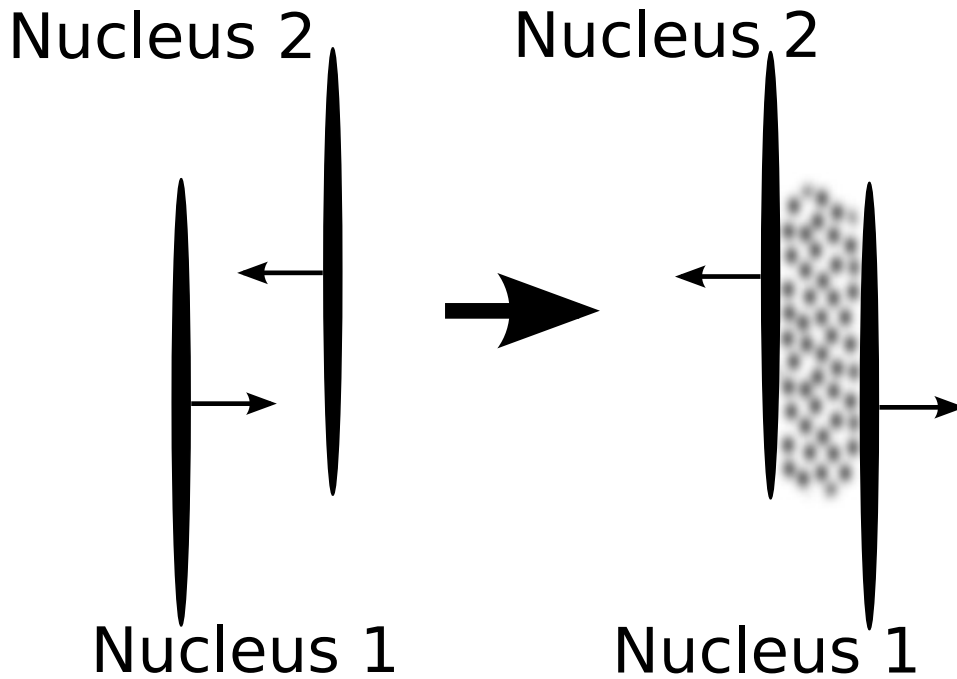


Figure 1.1.1.: Schematic of a Heavy Ion collision. Due to Lorentz contraction both nuclei appear as flat discs in the laboratory system. The nucleons in the overlap area may participate in the interaction. Nuclei outside of this area are spectators.

deconfined (not bound in hadrons). Such a medium is then called a Quark-Gluon Plasma (QGP). As a whole even such a medium must still be color-neutral.

The production of such a medium requires a process to create the high energies in a small amount of space. In nature, this state is expected to have occurred shortly after the Big Bang. Possibly, a quark-gluon plasma or a similar state of matter might exist in the core of some neutron stars. As both systems are difficult to measure directly, the only option to remain is the experimental creation [20].

The preferred method for this is the collision of heavy nuclei at high energies. Experiments of this kind have been performed for example at Super Proton Synchrotron (SPS), Relativistic Heavy Ion Collider (RHIC) and the LHC. Two colliding heavy nuclei usually have an overlapping area much larger than a single nucleon. In this case, many nucleon-nucleon interactions happen in one heavy ion collision and strongly interacting particles are produced in abundance at high energies. The resulting fireball expands and in this phase the quarks might experience deconfinement. After the energy density drops sufficiently due to the expansion, confinement sets in once again and the matter decays into color-neutral particles.

1.1.1. Approaches to Measurement

The quark-gluon plasma is produced experimentally in the collision of heavy nuclei. Typically only a certain number of nucleons participate in the collision, depending on the collision geometry. Figure 1.1.1 shows the geometry of a typical collision. In the aspherical interaction

1. Introduction

region of the overlap of the nuclei the quark-gluon plasma may be formed.

In the QGP phase of this process a number of collective phenomena can appear, depending on the degree of equilibration of the matter. If there is local thermalization, a local temperature can be assigned. It may be measured by comparing the thermally produced particle yields with respect to the particles masses [7]. Another line of inquiry concerns the equation of state of the produced system. It is interesting to understand how the QGP reacts to the pressure gradients produced by the different densities at different points and whether it behaves more like a gas (with very little remnants of the strong interaction) or like a fluid (with remnants of interaction) [18, 32]. This manifests itself in the flow of created particles with respect to the geometry of the collision. Thirdly, the melting of heavy quarkonia due to the Debye screening of the strong interaction is being investigated [15].

A different approach to getting an insight into the properties of the Quark-Gluon-Plasma is the analysis of the energy loss of particles traversing the hadronic matter. The electroweak interaction plays a secondary role here, so the important probes are quarks and gluons. A high-energy parton created in the initial scattering will traverse the hadronic medium and on the way interact with the QCD matter. Similar to bremsstrahlung in the electromagnetic interaction it can radiate off some of its energy in the form of gluons. The total effect depends not only on the mechanism itself but also on the density (and kinematics) of the medium. This effect is strong for those partons of the initial interaction, which are produced early and close to the center of the fireball. It is weaker for thermally produced particles, which follow more closely the general flow of the medium and which are produced on average later and more to the edge of the medium.

1.1.2. Measurement of Heavy Quarks

The energy loss measurement creates some difficulties as not all quarks come from the initial scattering. Light quarks can additionally be produced thermally as well as from the fragmentation of gluons. As thermal production of quarks is strongly correlated with their mass, heavy quarks are particularly interesting probes of the QGP. Charm and beauty (bottom) quarks are almost exclusively produced in the initial hard scattering processes. They traverse the whole medium and thereby experience a large part of the temporal evolution and spatial extent of the produced medium. Due to confinement they cannot be measured as heavy quarks directly. Thus they have to be measured as part of the hadrons they form after hadronization. The measurement of top quarks does not tell much about the energy loss mechanism as they decay before traversing a distance significant with respect to the size of the system. Thus charm and beauty quarks are particularly interesting probes for measuring properties of the QGP without being limited by effects from thermal production and gluon fragmentation.

Production From perturbative QCD, the leading order production process for the formation of heavy quarks is *gluon fusion*. In the Feynman graph, two gluons merge to one, which creates a quark-antiquark pair. Figure 1.1.2 shows important production processes at LHC energies. For very high collision energies, gluon interactions dominate over interactions of

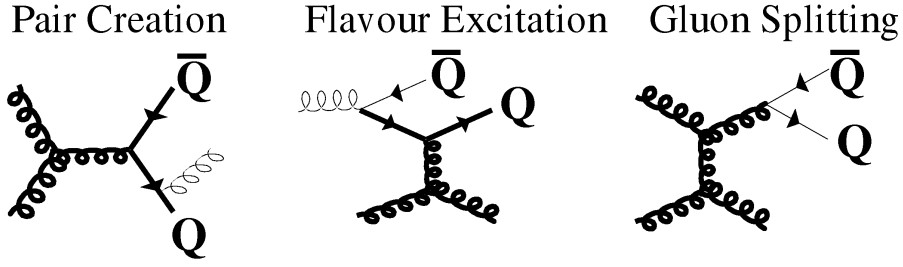


Figure 1.1.2.: Some important heavy quark production mechanisms. The leading order diagram is the pair creation via gluon fusion [21].

the quarks for the initial hard scatterings.

Energy Loss Mechanism Particles at energies close to the temperature of the surrounding medium can in interactions with it both loose energy and gain it. The discussion here is limited to particles at a high energy compared to that of the medium. These particles are the partons and gluons produced in the initial interaction. Energy loss can occur by collisions with other particles of the plasma and by induced gluon radiation. Although there is no clear consensus on the relative strength of the processes, the induced radiation is expected to be stronger [22]. A typical Feynman diagram of such a process can be seen in figure 1.1.3. Of the many available models (e.g. [8]) the BDMPS model will be discussed in slightly more detail here.

For a theoretical treatment of the induced gluon radiation, the BDMPS (Baier, Dokshitzer, Mueller, Peigné and Schiff, [9]) model assumes interaction of the parton with multiple static scattering centers. In a process similar to bremsstrahlung gluons are radiated by the interaction. At larger distances the scattering centers are screened. Multiple scattering centers may contribute coherently to the formation of a single gluon if the scattering centers are close together (the mean free path is small) compared to the formation time of the gluon. Using the approximation of high gluon energies, the general energy loss from this approach is

$$\frac{dE}{d\omega dz} = \frac{\alpha_s C_R}{\pi\omega} \sqrt{\frac{\hat{q}}{\omega}} \quad (1.1.1)$$

Here, α_s is the strong coupling constant, ω is the gluon energy and z the traversed distance. \hat{q} is the so-called gluon transport coefficient. It is a property of the medium and proportional to the density of the scattering centers within it. C_R is the Casimir color factor. Its value is $C_R = 4/3$ for quarks and $C_R = 3$ for gluons.

For heavy quarks in the quark gluon plasma at LHC energies, a different behavior is expected compared to ones from this massless approximation. The properties of the induced gluon radiation depends on the mass of the parton in such a way, that the gluon radiation of heavy quarks at low angles is reduced. This is called the dead-cone effect [22]. The spectra differ by the factor:

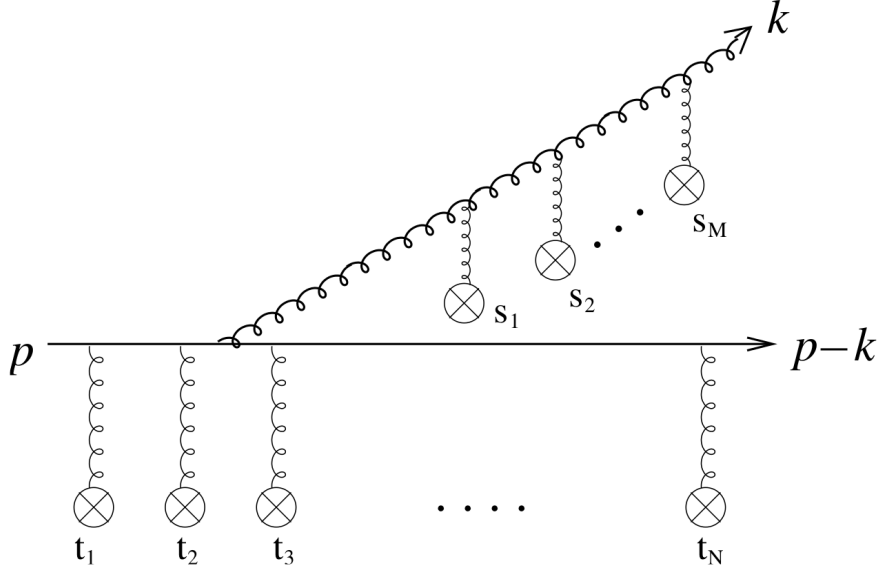


Figure 1.1.3.: Feynman Diagram of Induced Gluon Radiation [8]. Interaction of the parton with gluons (here from scattering centers t) induces radiation of a gluon, which itself interacts with the medium.

$$dP_{HQ} = dP_0 \frac{1}{\left(1 + \frac{m/E}{\theta^2}\right)} \quad (1.1.2)$$

where P_{HQ} is the heavy quark energy loss spectrum, P_0 is the spectrum for massless quarks and θ is the angle of the radiated gluon. m and E are mass and energy of the parton.

For this reason, a lower energy loss is expected for heavier quarks compared to lighter ones. For heavy flavors, a smaller energy loss is expected for b quarks compared to c quarks.

Hadronization Outside of the quark-gluon plasma, no free quarks can exist. Thus, a hadronization process has to take place before measurement. The heavy quarks will hadronize to form a meson or baryon. This process is highly nonperturbative and difficult to calculate. As the measurement is performed for the hadronized particles, the hadronization will always be a part of the signal. One possibility to avoid these complications, is to measure all particles created in the direction of the heavy quark as well together with their momenta to get a measurement which is more independent of the hadronization process. In the case of such a jet-measurement however, there is additional sensitivity to the effect of the medium on all particles of the jet within the medium. Thus, the measurements complement each other and pose different challenges for the theorists.

The most commonly formed particles from heavy quarks are the D and B mesons. Along with the quarkonia J/ψ and Υ they are the most important ones for heavy flavor measurements. The quarkonia can be additionally suppressed in the QGP due to melting of the states

1. Introduction

[25] and enhanced by recombination[13, 31]. Thus, their spectra are influenced by additional effects compared to the B and D mesons, making the theoretical prediction more difficult.

The decay channel of interest for the study is the decay of the charm and beauty hadrons into electrons:

$$\begin{aligned} H_c &\rightarrow e + X \\ H_b &\rightarrow e + X \end{aligned} \quad (1.1.3)$$

where H_c and H_b are hadrons with charm or beauty. The branching ratios for semileptonic decays are considerable: $9.6 \pm 0.4\%$ for $c \rightarrow l^+ + X$ and $20.5 \pm 0.7\%$ for $b \rightarrow l^+ + X$ [26]. The weak decays of the B and D mesons are slow compared to the decays of the quarkonia. This results in measurable decay lengths, which are an important tool for the distinction of these hadrons from other particles via displaced vertex or impact parameter analyses. Such an analysis will be described in section 2.3.

Due to the large mass of the beauty and charm hadrons, the electrons will have a significant momentum from the decay. With the additional influence of the hard spectrum of the quarks from the initial interaction, they dominate the electron spectrum at high momenta.

1.1.3. Measurable Quantities

To compare pp and Pb-Pb transverse momentum spectra for a given centrality of the collision, it would be easiest to simply take the ratio of the spectra in order to see the change between them. However, two things have to be considered first:

- The proton-proton runs used in this analysis at the LHC were performed at $\sqrt{s} = 7\text{TeV}$, while Pb-Pb is measured at $\sqrt{s_{NN}} = 2.76\text{TeV}$.
- One Pb-Pb collision consists of many nucleon-nucleon interactions compared to only one in pp.

The different energies can be taken into account by making use of the relatively good theoretical handle on the perturbative calculations of the pp process. The data can be scaled to a new center of mass energy using the ratios of the spectra from perturbative QCD calculations. The number of binary collisions can be estimated using a Glauber model. The expected number of binary collisions is then used to scale the Pb-Pb spectrum to a spectrum of nucleon-nucleon collisions instead. The resulting quantity is called the *nuclear modification factor* R_{AA} .

$$R_{AA} = \frac{1}{\langle N_{coll} \rangle} \frac{d\sigma_{Pb-Pb}/dp_t}{d\sigma_{pp}/dp_t} \quad (1.1.4)$$

where σ_x is the spectrum for the pp or Pb-Pb collision and $\langle N_{coll} \rangle$ is the expected number of binary collisions in this centrality class.

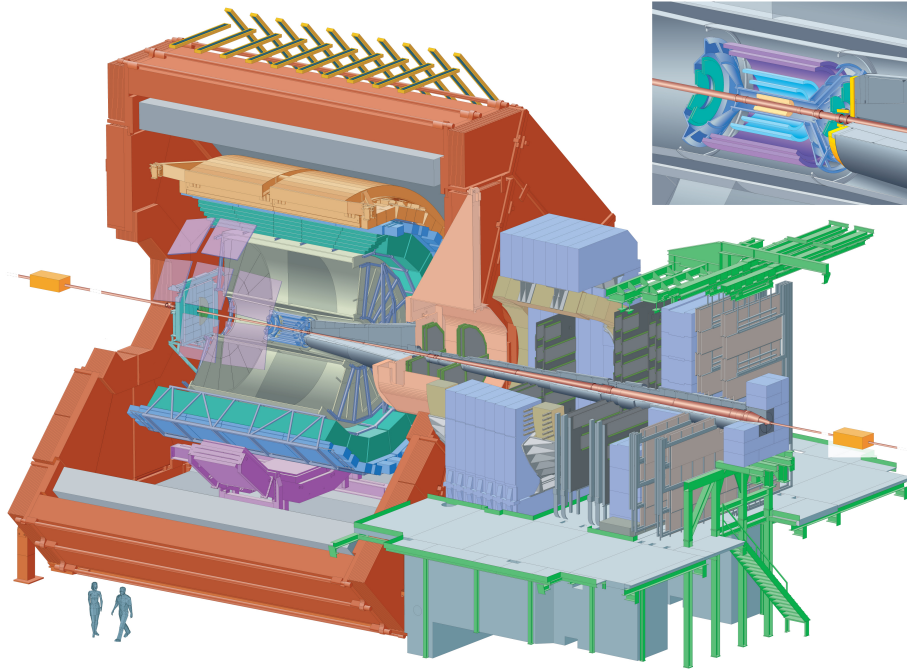


Figure 1.2.1.: Schematic of the ALICE experiment

1.2. The ALICE Experiment

Of the four big experiments at the LHC, ALICE is the one designed with the peculiarities of heavy-ion collisions in mind[27]. The detectors of ALICE are able to cope with the high multiplicities associated with Pb-Pb collisions at LHC energies. The associated requirements include good particle identification (PID), measurement and separation of many tracks at once and measurement down to low transverse momentum where also the bulk of the particles is produced.

The magnetic field is produced by a large solenoid magnet which was used before in the L3 experiment at LEP. At 0.5 T the magnetic field is lower than in other LHC experiments to enable particles at a low transverse momentum to traverse a range in the detector that is sufficient for measurement.

Broadly speaking, the experimental setup consists of two main subsystems: The central barrel and the forward muon spectrometer. Several small detectors like the VZERO detector and the Zero Degree Calorimeter (ZDC) complete the setup. The latter are used for event characterization. They enable accurate measurement of the reaction plane for the analysis of flow as well as the collision multiplicity.

The forward muon spectrometer lies behind sufficient amounts of absorptive material to receive a clean muon signal. It covers $171^\circ - 178^\circ$ of the polar angle over the full azimuth and can be used for open heavy flavor measurements as well as for quarkonia studies in the muon channel[28].

Due to the low magnetic field, it is possible to measure the decays of charmonia down

1. Introduction

to a p_t of 0 in the central barrel, which is unique within the LHC experiments. The central barrel detectors are designed to deal with the high particle multiplicities of Pb-Pb collisions and are can measure even multiplicities of $dN_{ch}/d\eta = 8000$.

A strength of ALICE are the excellent particle identification capabilities. In the central barrel, the Time of Flight detector, the Time Projection Chamber and the Transition Radiation detector provide strong separation of particle species at high multiplicities in the full azimuth in a pseudorapidity range of $|\eta| < 0.9$. Additionally, the Photon Spectrometer (PHOS), the ElectroMagnetic Calorimeter (EMCal) and the single-arm ring imaging Cherenkov detector (HMPID) work in a more limited acceptance.

The analysis of the electron spectra is done in the central barrel. In the following, the most crucial detectors for this analysis will be discussed in more detail insofar as they are relevant for the analysis.

1.2.1. The Inner Tracking System

The *Inner Tracking System* (ITS) is the innermost subdetector of the ALICE experiment. It encloses the beam pipe over the full azimuth and measures particles at a pseudorapidity of $|\eta| < 0.9$, which corresponds to $\pm 45^\circ$ relative to the reaction plane. To handle the large track densities close to the interaction vertex, the ITS consists of six layers with a high granularity for the more central ones[2].

The ITS has three main purposes:

- *Tracking* of low momentum particles, which do not reach the outer subdetectors and an improvement of the resolution for tracking in these for higher momenta.
- Determination of the *primary vertex* as well as possible secondary vertices.
- *Particle identification*, mostly for low momentum particles which do not reach the TPC.

For the measurement of heavy flavor electrons, the particle identification capabilities of the ITS do not play a large role. Here the main contributions are:

- The reduction of electrons from the conversion of photons within the detector using the spatial resolution.
- The improvement of the p_t measurement and tracking in the TPC.
- The measurement of the impact parameter, a byproduct of the measurement capabilities of production vertices. This provides additional information for flavor separation.

The six layers of the ITS consist of two Silicon Pixel Detectors (SPDs), two Silicon Drift Detectors (SDDs) and two Silicon Strip Detectors (SSDs). The measurement of the SPDs is most crucial for the determination of the impact parameter as they are the closest ($\approx 4\text{cm}$) to the beam axis.

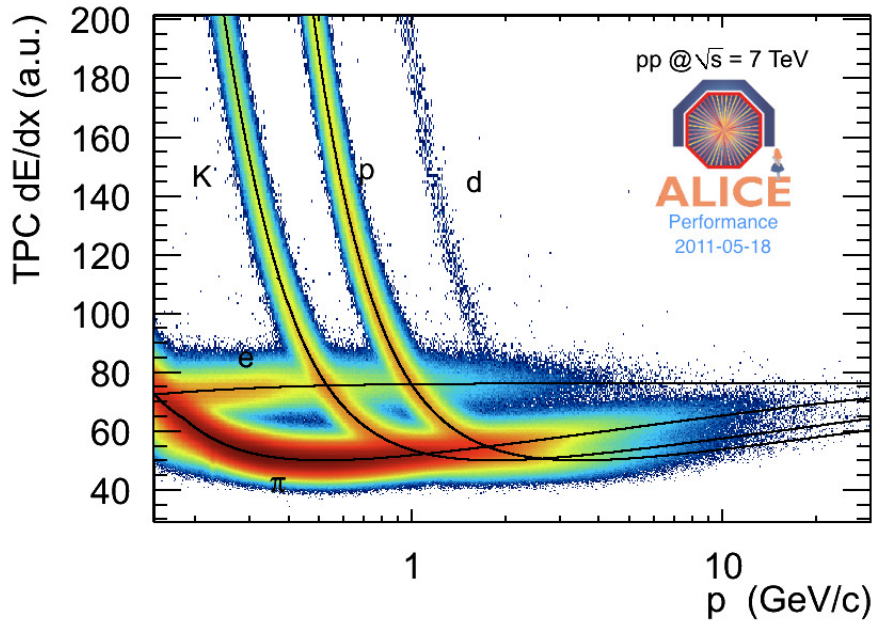


Figure 1.2.2.: TPC signal for the energy loss for different particles measured in pp collisions.

1.2.2. The Time Projection Chamber

The Time Projection Chamber (TPC) is a large gas detector, positioned around the ITS. It is the main “workhorse” of ALICE and it is crucial for almost all types of measurements at intermediate pseudorapidity and combines capabilities for tracking and particle identification. Most of the volume is taken up by the cylindrical field cage. At both ends of the cage, readout end-plates are placed[4].

The TPC measurement is based on the energy loss of charged particles traversing the gas volume. When a particle approaches a gas particle sufficiently closely it can ionize the gas creating free electrons in the process. The measurable quantity is the total ionization at different points in the detector. As a gas mixture, Ne – CO₂ – N₂ was used with the proportions of 90-10-5[6].

In contrast to the Silicon Pixel Detectors in the Inner Tracking System, the readout is spatially separated from the production point of the free charges. To read out the TPC, a homogeneous electric field is applied to the gas volume, accelerating the free electrons towards the endplates. At the endplate the field of the readout wires amplifies the signal by producing an avalanche of electrons which are then measured via the potential change in readout pads placed behind the wires.

Due to interactions with the medium, the electrons have an approximately constant velocity while traversing the gas. The time of arrival at the endplates therefore gives a measurement for the production point along the beam axis even though the readout planes only measure in two spatial dimensions. This information allows for reconstruction of the tracks at a high accuracy. The TPC tracking is particularly important for the measurement of the transverse momentum making use of the curvature of the tracks of charged particles in a magnetic field.

1. Introduction

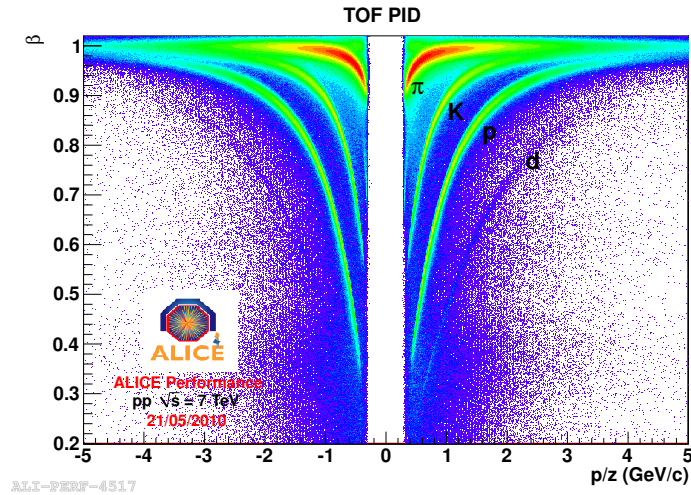


Figure 1.2.3.: TOF signal for different particles at different momenta measured in pp collisions.

The particle identification is based on the different energy loss by particles of different masses at the same momentum. The final TPC signal takes into account the measured ionization at all measured points. Figure 1.2.2 shows the energy loss distribution in the TPC for different particle types at different momenta. As with most particle identification techniques, particles of different masses have similar properties at high momenta making them difficult to distinguish. Additionally, due to the rise of the Bethe-Bloch curve at low momenta, the lines from different particles cross, making them difficult to distinguish.

The large size of the ALICE TPC makes the measurement very accurate and provides excellent particle identification from it. Still the resolution is limited and the different contributions overlap. For the analysis of single particle spectra, it is important to know in which way the lines overlap and how strong the different contributions are. This topic is explored further in 2.2.

1.2.3. The Time of Flight Detector

At the crossing points of the energy loss for different particles, the knowledge of the TPC signal is not sufficient to yield information about the particle type. Similarly at high momenta the signals overlap. Thus, some other measurable quantity has to be used to resolve the ambiguity. For low momenta, the Time of Flight detector measures the velocities β of the particles to achieve this. TOF has a design based on a Multigap Resistive Plate Chamber (MRPC) setup: Several resistive plates are stacked in direction of the particles path. A particle passing through the plates ionizes the gas between them. The signal is read out at the anode in the center of the stack and at the cathodes at the ends[3].

The signal from the Time of Flight detector for different particle types at different momenta can be seen in figure 1.2.3.

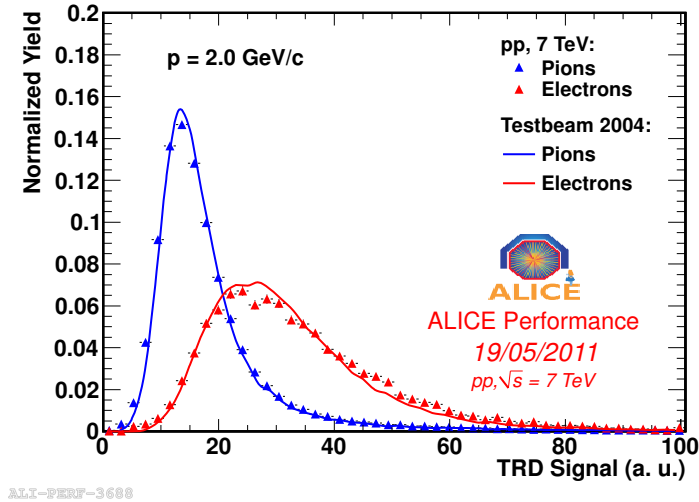


Figure 1.2.4.: TRD energy loss distribution for electrons and pions measured in pp collisions.

1.2.4. The Transition Radiation Detector

Many of the properties of charged particles measured by different types of detectors become similar at high momenta. Examples of this behavior are the velocity β , the energy loss dE/dx or the energy E . Transition radiation is an exception to this, being dependent mainly on the Lorentz factor γ . It is created when a charged particle crosses a boundary between materials of a different refractive index. In the Transition Radiation Detector (TRD), this effect is used to differentiate between pions and electrons at higher momenta, when there is little separating power from TPC and TOF measurements.

The TRD consists of six layers of detector modules. Each module contains a radiator and a gas volume. When a charged particle traverses the radiator material, photons are created from transition radiation. In the gas volume the gas is ionized by the charged particle. If photons at sufficient energy were created in the radiation material, these can create additional ionization. Thus, the TRD measures a combination of gas energy loss and production of transition radiation[5].

Figure 1.2.4 shows the integrated charge within one layer of the TRD. The separation of the distributions is stronger than for pure gas energy loss due to the addition of transition radiation. Still, the pion distribution reaches into the electron peak. The separation is done using information from all available layers using a maximum likelihood method similar to the ones discussed for fits in the next chapter.

2. Analysis of Electrons from Heavy Flavor Hadron Decays in pp at $\sqrt{s} = 7 \text{ TeV}$ and Pb-Pb at $\sqrt{s_{NN}} = 2.76 \text{ TeV}$

2.1. Analysis Strategy for the Measurement of Inclusive Heavy Flavor Electron Transverse Momentum Spectra

The inclusive measurement of heavy flavor electrons makes no distinction between electrons from charm and beauty hadrons. The transverse momentum spectra of all hadrons containing heavy quarks is measured at the same time. In this study, the preferred approach was the measurement of all electrons produced near the primary vertex. In this case not only electrons from heavy flavor decays are measured but also those from all other electron sources. Fortunately, the influence of other processes diminishes with increased transverse momentum. Still all background particles have to be considered. The basic idea of the measurement is thus[30]:

- Measure the transverse momentum spectrum of a clean electron sample
- Correct for detector efficiencies and the remainder of the contamination
- Subtract from the final spectrum the corresponding spectra of electrons from all background processes

For this purpose, it is necessary to understand the detector efficiencies very well, have a good understanding of the remaining contamination and have available a reliable spectrum for particles from the background processes.

2.1.1. Data Set, Event and Track Selection

The data for this analysis was recorded by ALICE in 2010. The detector performance from this period is particularly well understood, which is important due to the high requirements on the detector performance for this analysis. The data sample contained data corresponding to an integrated luminosity of 2.6 nb^{-1} . Quality cuts were applied to the tracks to ensure a high-quality detector response for all particles (a detailed list may be found in [30]).

2. Analysis of Electrons from Heavy Flavor Hadron Decays

For the Pb-Pb measurements, the same requirements were applied. The Pb-Pb data was taken in late 2010 and the centralities 0-80% correspond to an integrated luminosity of $2\mu\text{b}^{-1}$.

2.1.2. Electron Identification

For the electron identification, information from the TPC, TOF and TRD subdetectors were used. At the time of the measurement, seven out of a maximum of 18 supermodules of the TRD were installed. As the TRD signal is most important for high momenta, below $4\text{GeV}/c$ only the information from the TPC and from TOF was used in order to get a measurement for the full azimuth and thus with higher statistics. This is particularly important for lower momenta as the higher background subtraction amplifies the error of the final spectrum. To get a signal of high quality from the TPC, a minimum of 80 clusters for the energy loss measurement were required. For the TOF signal, a measured time of flight within 3σ of the expectation for an electron was required. For the TRD signal, the cut was performed in such a way, that the electron efficiency was at a constant 90% at all momenta[30].

2.1.3. Cocktail Estimation

Apart from the charm and beauty hadron decay electrons, the main source of electrons are photon conversions in the detector material as well as three-body Dalitz-decays of light mesons. To subtract the background particles, a transverse momentum spectrum of electrons from all significant sources has to be created with the correct weighting according to the strengths of each source. This is called an electron background cocktail. The cocktail for pp collisions at 7TeV at ALICE is shown in figure 2.1.1. It is important to note, that the number of electrons from photon conversion (conversion electrons) strongly depends on the effective detector material. Both the photons and the Dalitz electrons come to a large part from the decay of π^0 particles:

$$\begin{aligned}\pi^0 &\rightarrow \gamma\gamma & B.R. &\approx 99\% \\ \pi^0 &\rightarrow \gamma e^+e^- & B.R. &\approx 1\%\end{aligned}\tag{2.1.1}$$

The similar contribution of the two decays is due to the small effective material budget (and thus small photon conversion probability) of ALICE with the track requirements described above.

2.2. Estimating the Hadron Contamination

In general no detector will be able to perfectly identify all electrons correctly due to statistical fluctuations in the signal which are a result of the finite resolution of all physical detectors. For each mode of selection of electrons according to the detector signal (cut) there will be a certain amount of other particles remaining; additionally some fraction of the electrons will not be identified as such. The amount of misidentified non-electrons is given as the contamination of the sample. The amount of selected electrons relative to the total number

2. Analysis of Electrons from Heavy Flavor Hadron Decays

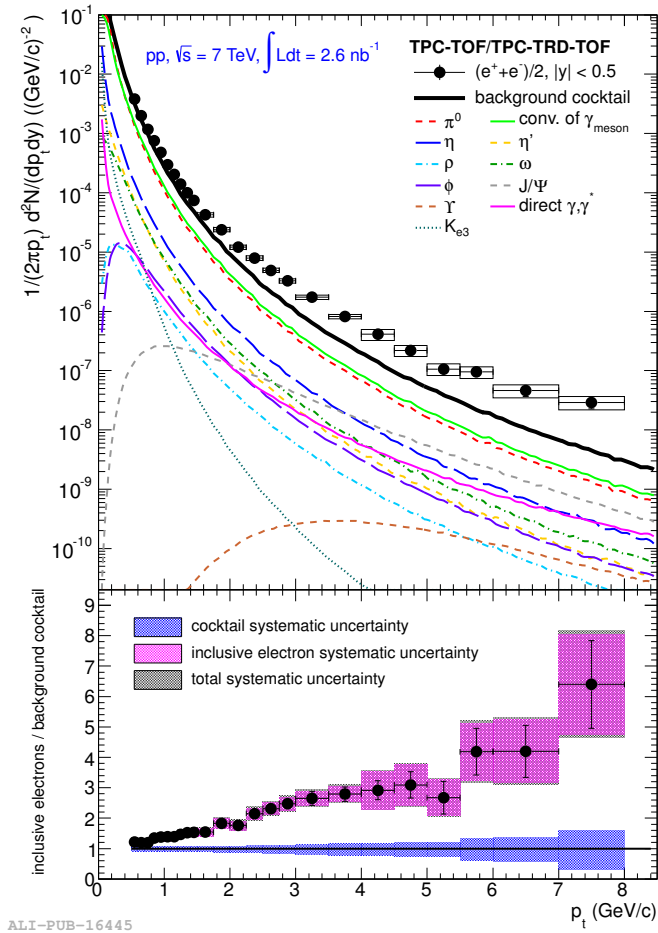


Figure 2.1.1.: Background Electron Cocktail for pp collisions at ALICE. The upper plot shows the measured electrons, the sum of the cocktail and the individual contributions. The lower plot shows the ratio of all electrons and the background cocktail. At high transverse momentum the influence of the background decreases.

2. Analysis of Electrons from Heavy Flavor Hadron Decays

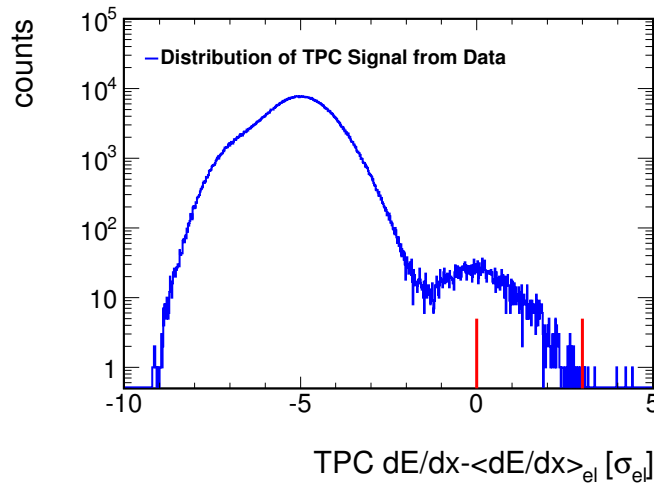


Figure 2.2.1.: The distribution of the energy loss of all particles at a momentum of $p \approx 2.6\text{GeV}/c$ in units of the width of the electron line. The electron distribution is distinguishable around 0. The red lines represent a possible cut on the signal.

is given as the efficiency of the cut. Strategies for the analysis have to make a compromise as usually a cut with a higher efficiency results at the same time in a higher contamination and vice versa. For the apprehension of an electron spectrum it is particularly important to get a good estimate for both numbers as they are necessary for the proper correction of the spectrum.

Particularly problematic is the estimation of the contamination after the cut on the specific energy loss in the Time Projection Chamber. This is closely related to the measurement of the efficiency of the same cut. The reason for this is the difficulty of finding a direct measurement of these properties as a large and clean sample of background particles would be required.

Figure 2.2.1 shows the distribution of the energy loss for different particle species in the TPC. For the purpose of selecting electrons it is useful to draw the distribution in units of the width of the electron energy loss distribution with the average electron energy loss at 0. This is a linear mapping which only shifts and stretches the distributions without changing their shape. The energy loss distribution of a particle species depends on the momentum, thus the analysis needs to be done separately for different momenta. As a selection method, a minimal and maximal energy loss for the particle is required. As the energy loss distributions of the different particles overlap it is necessary to find some way to disentangle them in order to get an estimate of the contamination and efficiency of the cut. To change the properties of the selection, mainly the lower edge of the selected region is important: The further it is lowered, the higher the contamination will be while giving a higher electron efficiency. To obtain a clean sample, the cut has to be done at a higher energy loss. As a result the distribution of the background particles has to be known far away from the center of their respective distributions. This requires a deeper understanding of the origin of these distributions which will be discussed in the following pages.

2.2.1. Energy Loss of Charged Particles in a Gas Detector

To better understand the distribution of the TPC signal for a given particle it is necessary to consider the physical processes involved. As introduced in section 1.2.2 the TPC detects particles in a large volume of gas. A particle traversing the detector interacts electromagnetically with the detector gas and in this way partially ionizes it along its path. The free electrons are projected onto the end-plates via an electrical field and amplified by the strong inhomogeneous field near the wires at the end-plates. The induced change in potential at the end-plates allows estimation of the total charge ionized and its r/φ distribution while the arrival time indicates the longitudinal production location. The signal shape is further influenced by the subsequent conversion to a digital signal for further processing. The digitized signal is then interpreted and analyzed to reconstruct the tracks of all charged particles. This process along with the applied cuts on the signal quality will influence the final distribution in the analysis further. Before going into detail about the particularities of the analysis with the ALICE TPC it is useful to consider the general processes present in the energy loss of a charged particle traversing a large volume of a gas mixture.

For the energy loss of a charged particle in a gas several statistical processes have to be considered simultaneously. The basic process is the electromagnetic interaction of the particle with a single gas particle. From one particle to the next, the particle momentum, path length in the detector, number of collisions, individual collision energy loss, types of encountered gas particles and number of produced charges can change, all of which will influence the total energy loss. To simplify the problem for analytical or numerical calculation, it is simpler to consider the case of a given path length and momentum (both of which can be measured separately) and repeat the procedure for different values of these quantities. A second simplification is the assumption that the number of ionizations from one collision is proportional to the corresponding energy deposit due to rescattering of electrons with high momenta. Finally, for a gas mixture an effective energy loss spectrum can be used.

The task is now reduced to finding the collisional energy loss distribution for a single ionization in the TPC gas and calculating from it the distribution of the energy loss for one track of the total length. If the cross section for the gas mixture is known, then the distribution of the energy loss for a fixed number n of collisions is the n -fold convolution of this energy spectrum.

$$\sigma_{tot}^n(\Delta) = \int \dots \int \delta(\Delta - E_1 - E_2 - \dots - E_n) \prod_{i=1}^n \sigma_{single}(E_i) dE_1 dE_2 \dots dE_n \quad (2.2.1)$$

or recursively

$$\sigma_{tot}^n(\Delta) = \int_0^\Delta \sigma_{tot}^{n-1}(\Delta - E) \cdot \sigma_{single}(E) dE \quad (2.2.2)$$

where Δ is the total energy loss and σ_{single} is the differential collision cross section for a single ionization. An example for the ionization spectrum of Ne gas can be found in figure 2.2.2. The ALICE TPC contains a mixture of Ne – CO₂ – N₂ with the proportions of 90-10-5.

2. Analysis of Electrons from Heavy Flavor Hadron Decays

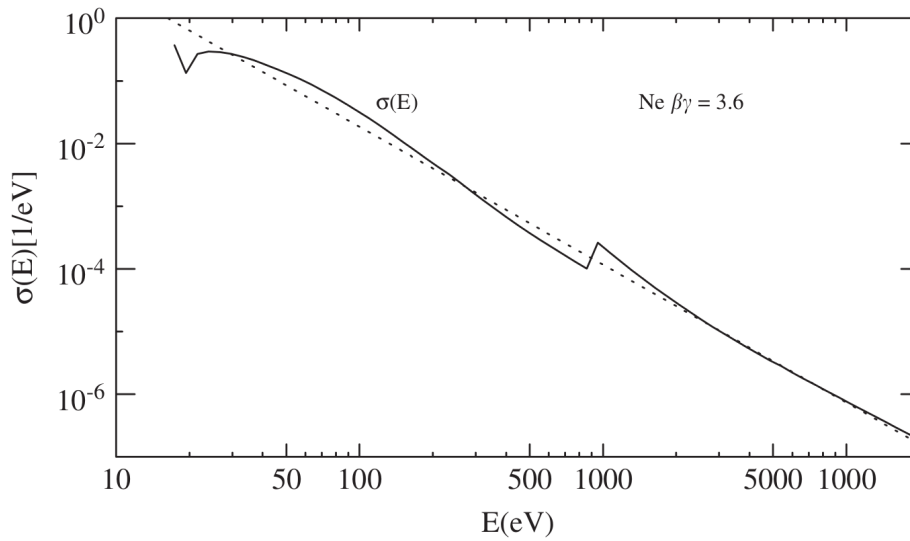


Figure 2.2.2.: Ionization Spectrum for Ne Gas as an Example (solid line). It is shown together with a modified Rutherford cross section (dotted line) [11].

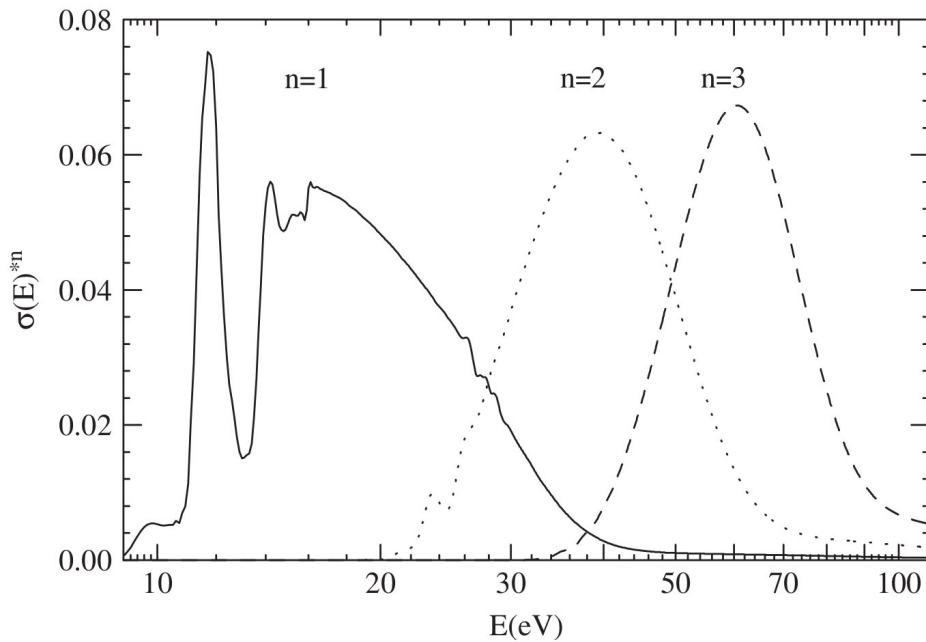


Figure 2.2.3.: Example of the ionization spectrum of a gas (P10) with one (dotted line) and two (dashed line) convolutions with itself. These represent the energy loss distribution for one, two and three collisions of the incident particle with the gas[11].

2. Analysis of Electrons from Heavy Flavor Hadron Decays

The result of such a convolution for different collision numbers is shown in figure 2.2.3. It becomes apparent that although the final shape depends on the structure of the spectrum, much of its details are hidden after successive convolutions. This effect increases as the number of collisions increases. To get an approximation for the cross section of an individual interaction, a good starting point is the interaction of the ionizing particle with a free electron instead of one bound in the gas atom. This leads to the Rutherford cross section[11]:

$$\sigma_R(E; \beta) = \frac{k_R (1 - \beta^2 E/E_{Max})}{\beta^2 E^2} \quad (2.2.3)$$

where $k_R \approx (0.15354 \text{MeV} \cdot \text{cm}^2) \cdot C \cdot \frac{Z}{A}$ with C the charge of the incident particle and Z and A the atomic number and mass number of the gas nuclei, is a constant and E_{Max} is the maximal transferable energy in a single collision.

For the ALICE Monte Carlo simulations this formula is used with a denominator of $E^{2.2}$ instead of E^2 . This modification is done to take into account the fact that the electrons are bound. It is important to point out that the total cross section is not infinite through the divergence at low energies. The low energy losses correspond classically to a large impact parameter. At large distances to the electron however, the electric force is shielded by the other charges present. Quantum mechanically, the reason for the appearance of a minimal energy loss per interaction is the fact that the electron is bound. There can be no energy loss smaller than the lowest excitation level of the target. As a result the real spectrum drops for low energy losses.

Assuming availability of a sufficiently accurate description of the energy loss in one ionization this provides a method to calculate the energy loss distribution for a fixed number of collisions in the gas. It remains to find a description for the distribution of the number of individual collisions. To find this a simple model is sufficient. The track of the particle can be thought of as being composed of many small tracklets. In each tracklet, a certain number of collisions occur. If these tracklets are made sufficiently small, most tracklets will contain no interactions with some containing one. If the interactions are independent of each other, this adds up many binomial decisions. The result is a Poisson distribution of the number of interactions:

$$P(n) = \frac{\lambda^n e^{-\lambda}}{n!} \quad (2.2.4)$$

Where λ here is the average number of collisions in the path. (See appendix A for more information on the Poisson distribution)

With these ingredients it is now in principle possible to calculate the complete energy loss distribution (or straggling function) from first principles although the repeated convolutions can be tedious:

$$f(\Delta) = \sum_{n=0}^{\infty} \frac{\lambda^n e^{-\lambda}}{n!} \sigma_{tot}^n(\Delta) \quad (2.2.5)$$

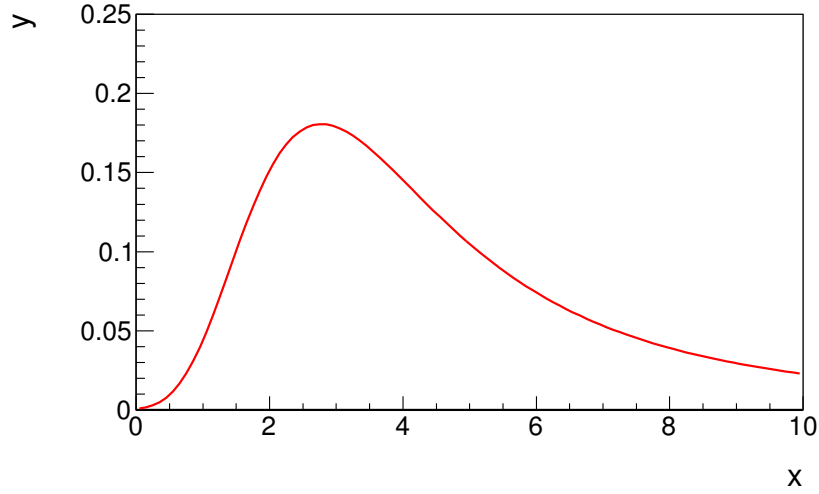


Figure 2.2.4.: Example of a Landau Distribution. Due to the long tail on the right, mean and variance of the distribution are not defined.

2.2.1.1. The Landau Approximation

Solving a series of convolutions becomes simpler if it is done in a transformed space. Landau found a solution assuming a cross section with only the $1/E^2$ -term from Rutherford and using Laplace transforms. Historically he found it by solving the transport equation [12], which should be equivalent to the formalism described above:

$$\frac{\partial f(x, \Delta)}{\partial x} = \int_0^{\infty} \omega(E) \cdot f(x, \Delta - E) dE - f(x, \Delta) \sigma_{int} \quad (2.2.6)$$

where $\sigma_{int} = \int_0^{\infty} \sigma(E) dE$ is the total collision cross section and ω is the differential cross section of a path of unit length in the material.

The result is

$$f(x, \Delta) = \frac{1}{2\pi i} \int_{c-i\infty}^{c+i\infty} e^{I(p)} dp \quad (2.2.7)$$

where

$$I(p) = p \cdot \Delta - x \cdot \int_0^{\infty} \sigma(E) \cdot (1 - e^{-p \cdot E}) \quad (2.2.8)$$

An example of the resulting distribution may be found in figure 2.2.4. This function can be calculated numerically and has found widespread use for fitting purposes. It is not possible to characterize this distribution by its mean and variance as both of these moments are

undefined due to the large tail of the distribution. Instead, the distribution can be defined by its most likely value and a parameter for the width. The reason for the divergence of mean and variance is the use of the $1/E^2$ -term of the Rutherford cross section only.

2.2.2. The ALICE TPC Signal

The total charge from the track of the particle being measured is not the same as the recorded and reconstructed TPC signal. This has two reasons: For one thing, the total charge measured at the end-plates is dependent on the read-out electronics. Secondly, the measurement does not simply yield the total charge, but also its distribution along the track. Thus by simply adding charges from all pads, some information is lost. It is recommendable to use some of this information, in particular due to the long tail of the distribution towards higher energy losses. For several particle types, these tails overlap significantly which severely limits the strengths of the particle identification. For the detector effects, it is sufficient for most applications to assume some variance in the difference between physical charge and measured signal after electronics. The second point however requires some deeper understanding.

2.2.2.1. TPC Clusters

The measured charge in the TPC readout pads is joined into so-called *clusters*. The nomenclature employed for the TPC is the following (quoted from [15])

- *Digit*: This is a digitized signal (ADC count) obtained by a sensitive pad of a detector at a certain time.
- *Cluster*: This is a set of adjacent (in space and/or in time) digits that were presumably generated by the same particle crossing the sensitive element of a detector.
- Reconstructed *space point*: This is the estimation of the position where a particle crossed the sensitive element of a detector (often done by calculating the center of gravity of the 'cluster').
- Reconstructed *track*: This is a set of five parameters (such as the curvature and the angles with respect to the coordinate axes) of the particle's trajectory together with the corresponding covariance matrix estimated at a given point in space."[sic]

Thus, clusters are collections of charge coming from the local energy loss of a single particle. These clusters are the fundamental building blocks for the final TPC signal. As they correspond to the energy loss of the particle in an effective track length, their signal should follow a Landau distribution for a series of measurements. The information from the clusters is used for the Particle IDentification (PID) and in a slightly different form also for the track reconstruction of particle in the TPC. It is important to note that not all tracks have the same number of clusters. To be used in tracking or PID, the clusters have to pass certain quality cuts. Clusters can be deemed unfit to contribute to the signal for example if they

2. Analysis of Electrons from Heavy Flavor Hadron Decays

correspond to a region where two or more particles traversed the gas. Although for tracking in many cases it is still possible to use information from both contributions, this is not done for the energy deposit measurement. As a result two particles (from separate events) may have a different number of clusters used for PID even if their paths thorough the TPC are identical. The total number of clusters measured for one particle track loosely corresponds to the total path length over which the energy is measured. A track with a small number of clusters used for PID will have a signal similar to that of a shorter measured track and thus have a worse resolution for the energy loss signal of the TPC. A worse resolution will result in a wider distribution of the final signal. The maximal number of clusters in the TPC is 159. To increase the performance of the cut on the energy loss, a minimal number of tracking and/or PID clusters can be required in the analysis. As the average number of clusters is dependent on the path length, it depends indirectly on the angle to the beam axis typically expresses by the connected pseudorapidity η . For a cut on the number of clusters care has to be taken not to change the eta distribution of the measured particles. Thus, cuts should be applied conservatively if a large η -range is measured.

In conclusion, the TPC signal is subject to a fluctuation in the effective and physical measured track length for the energy loss. The number of clusters of a track is connected to the width of the distributions. Requiring a minimal amount of clusters can increase the resolution of the detector. However, this does not solve the problem of the large tails of the distributions.

2.2.2.2. The Truncated Mean Cut

A frequently used method for removing the Landau-tail which is also employed in this instance is the *truncated mean cut*. It is based on the knowledge that in a random measurement most of the individual energy losses will still fall into the main peak of the distribution. To remove large tails, a certain fraction of ionizations with particularly high and low energy losses are removed before calculating the sum. As the individual ionizations are not available, the cut is made on the cluster level. For the asymmetric distribution it is useful to remove preferentially the higher ionizations to remove the tail. In the actual calculations, the 40% highest and 2% lowest signals were removed. As shown in figure 2.2.5 this results in a distribution for the energy loss which is approximately Gaussian.

The truncated mean cut removes a large amount of the clusters from the calculations. This removes also some information about the signal. However, it is important to note, that the information would also be lost in a simple summation of the individual cluster signals. The complete information is in the cluster signals themselves. The truncated mean cut creates a signal distribution similar to a Gaussian with a small width. This is useful for many applications, as a cut on the TPC signal gives a strong particle identification. On the other hand, it creates some problems in the calculation of the remaining contamination, which will be explored in the next few chapters.

2. Analysis of Electrons from Heavy Flavor Hadron Decays

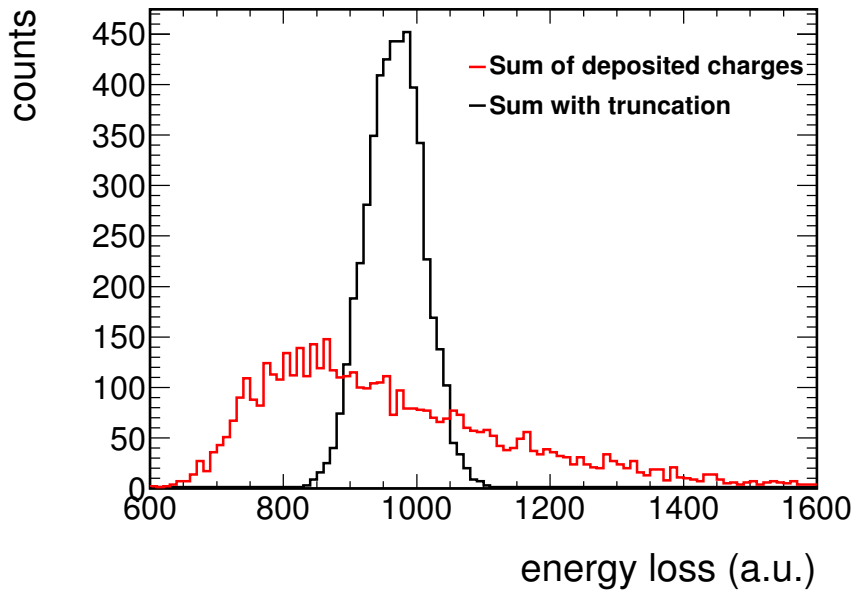


Figure 2.2.5.: Example for the truncated mean cut. The original distribution is the sum of 140 Clusters for which a Landau distribution of the charges is assumed. The truncation removes the 40% highest of these clusters similarly to the TPC truncated mean. The resulting distribution is scaled along the x-Axis to allow for easier comparison. The truncated mean cut removes the large tail of the distribution and creates a result which resembles a Gaussian.

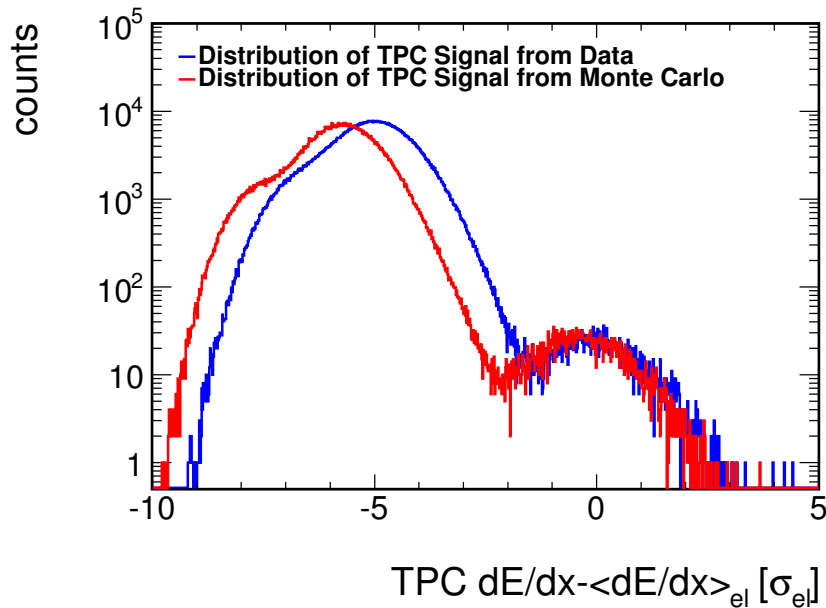


Figure 2.2.6.: Comparison of distributions of the TPC signal in data and Monte Carlo. The distributions in MC are in general slimmer than for data, overestimating the power of the TPC PID.

2.2.2.3. Monte Carlo Reproduction of the Energy Loss Distribution

The most direct way to calculate the remaining contamination after a cut on the TPC signal would be to calculate from the principles above the final distribution of the signal, preferably taking into account all detector properties as well. As this cannot be realistically achieved by analytical calculation, a Monte Carlo integration would have to be employed. Ideally this would generate similar particle spectra as in physical collisions. For each simulated collision then a complete simulation of the the detector response is performed.

Fortunately exactly these calculations exist for ALICE with all detectors and the different collision energies. As a relevant example: Simulations for proton-proton collisions at $\sqrt{s} = 7\text{TeV}$ have been performed with PYTHIA as an event generator and GEANT3 for the calculation of the detector response[16]. Similar calculations also exist for the Pb-Pb collisions using a HIJING event generator and in general they give a fairly accurate picture of the detector properties. For many calculations, corrections based on the Monte Carlo results give an accurate method to include detector effects like acceptance and efficiencies (e.g. [30]).

Unfortunately the case of the TPC signal is one of the few examples where this approach fails. Figure 2.2.6 shows the distribution of the TPC signal from the Monte Carlo simulation compared to the distribution from data. It becomes obvious, that the separation of the distributions from different particle species is stronger in the Monte Carlo simulated signals. The distribution shape is not correctly described.

2. Analysis of Electrons from Heavy Flavor Hadron Decays

For the analysis, it is important to know the contamination of the electrons. The detector simulation does not yield the desired result, so some other method has to be devised. The method presented in the following sections is based on the idea of fitting a suitable shape for the distribution shape to the data and extracting from this description the necessary information. No such method will incorporate all effects described by a detector simulation. If the contamination is low however, an approximate description might suffice. In the next section, the basic concept of binned fits will be described together with useful approaches to the description of the TPC signal distribution.

2.2.3. Fitting Binned Data

To continue, two things are necessary: A good model of the observable which contains one or more free parameters and a way to compare the model to the data. Generally speaking a fit is the variation of the free parameters in a model as to best describe a given data set. Efforts to obtain a suitable model will be discussed in the next section, while this one deals with constraining the free parameters by comparison to data. The availability of a suitable model will be assumed here.

It has previously been stated, that in a fit process the parameters of the model are tuned for the model to best describe the data set. Thus for each configuration of the parameters the agreement between the model and data set have to be compared. This raises the question: What does it mean to say, that model and data agree well or less well?

For this reason, it is necessary to find some measure of the agreement between data and the model. Two of the most commonly used measures are the χ^2 of a fit and its *likelihood*. Both concepts will be considered in more detail in the next sections. A simple example is the fit of a sampled function to a model function: The measure of agreement can be defined here as

$$\chi_{ls}^2 = \sum_{i=1}^N (f(x_i, \vec{p}) - d_i)^2 \quad (2.2.9)$$

where $f(x_i, \vec{p})$ is the value of the fit function at the coordinate of the sampling point i , while d_i is the corresponding data point. The fit function depends on the model parameters \vec{p} . In this case the χ^2 method is identical to the method of least squares.

2.2.3.1. Fitting Binned Data using the χ^2 -measure

For several independent, Gaussian distributed variables x_i with means μ_i and variances σ_i^2 , the measure

$$\chi'^2 = \sum_{i=1}^N \frac{(x_i - \mu_i)^2}{\sigma_i^2} \quad (2.2.10)$$

follows the so-called χ^2 -distribution. In the following, the expression “ χ^2 ” will be used for both the measure and the name of the distribution in all places where this does not lead

2. Analysis of Electrons from Heavy Flavor Hadron Decays

to confusion. As a measure of the agreement between model and data, μ_i will be the fit function value, while σ_i^2 usually needs to be estimated. For the least-squares method in the previous example, a fixed value for $\sigma_i^2 \equiv 1$ is assumed (the exact value is arbitrary in the sense that it does not change the minimum).

For the problem at hand, the data points are the number of entries in a given TPC signal bin at a given momentum. For each particle, there is a certain very small probability for it to create a TPC signal in the range of this bin. Thus, the distribution of the number of particles in a given bin must be Poissonian. For a Poissonian distribution, the variance in each bin is equal to the mean number of counts in the bin. This means, that a constant assumed variance will underestimate the fluctuations in bins with more counts, while overestimating the fluctuations in bins with few counts.

A possible solution for this problem is to simply set $\sigma_i^2 = \langle x_i \rangle \approx x_i$ in all bins. A similar approach will play an important role in the later sections on the measurement of the individual contributions from beauty and charm hadrons. However, the description is still not mathematically accurate, as the χ^2 -approach always assumes a Gaussian distribution within a bin. A Poisson-distribution of width $\sigma^2 = x$ only resembles a Gaussian in the limit of high bin counts. For lower counts, the distribution is skewed, thus creating some bias in the fit. This problem can be circumvented completely by choosing instead a fit method which aims at maximizing the likelihood as will be explained in more detail in the next section. It is important to note, that most issues with the statistical treatment of fitting are diminished for a larger amount of available statistics in data.

2.2.3.2. The Maximum Likelihood Method

In a very general way, a model with a given set of parameters predicts a certain probability for a given set of data points. The central idea of the maximum likelihood method is to make a model for this probability and then vary the models parameters in order to maximize it.

Assuming, the probability density function $p(x_i, \vec{\Theta})$ of the measurement i given model parameters $\vec{\Theta}$ has been obtained and the measurements are independent, the likelihood measure of the N measurements is:

$$L(\vec{x}, \vec{\Theta}) = \prod_{i=1}^N p(x_i, \vec{\Theta}) \quad (2.2.11)$$

It is convenient for calculations to maximize not the likelihood itself but its logarithm, as this transforms the product into a sum. As the logarithm is monotonous this does not change the position of the maximum. Formally the next step is to solve the *likelihood equations*

$$\frac{\partial \ln L(\vec{\Theta})}{\partial \Theta_i} = 0 \forall i \quad (2.2.12)$$

But in practice the maximal likelihood is usually found numerically. In unbinned likelihood methods, the probability $p(x_i, \vec{\Theta})$ is calculated for each individual particle measured. In the present case however, this does not yield additional information as all particles are already

2. Analysis of Electrons from Heavy Flavor Hadron Decays

only represented as bin counts. For this reason the “measurement” in this case means the number of particle counts in one bin and the summation is performed over all bins. If the model yields an expectation value for the bin of $\lambda(\vec{\Theta}, i) \equiv \lambda_i$ then the probability of a number of bin counts d_i is

$$p(d_i) = \frac{\lambda_i^{d_i} e^{-\lambda_i}}{d_i!} \quad (2.2.13)$$

this results in the likelihood function

$$\ln L(\vec{d}, \vec{\Theta}) = \sum_{i=1}^N d_i \ln \lambda_i - \lambda_i \quad (2.2.14)$$

This likelihood method uses the model itself for the estimation of the total likelihood. This fit method is used for the evaluation of the contamination after the TPC cut. It is implemented within the ROOT framework commonly used at the LHC experiments [1]. Obviously this method depends on the model used. Care must be taken here, as an inaccurate model might also yield the wrong expectation value in some bins.

If a Gaussian probability density function is used instead of the Poissonian one, this results directly in the χ^2 -method. The latter is thus a special case of the likelihood method for Gaussian fluctuations in the data.

2.2.4. Fitting the TPC Signal

With a suitable understanding of the characteristics of the TPC signal now some understanding of the properties of a cut on the same can be developed. The most important ingredient here is a sufficiently good model for the distribution of the signal for a given source, in particular for the electrons (which make up the signal) and the pions (which make up most of the background).

2.2.4.1. Gaussian Approximation Efforts

Single Gaussian Fits of the Contamination A usual first try for many problems in statistical physics is to assume that all distributions are Gaussian. Figure 2.2.5 shows that the TPC signal for a single particle species is also approximately Gaussian. The main reason for the prevalence of Gaussian distributions is the central-limit theorem: The average of several random variables with a distribution of finite mean and variance will converge to a Gaussian distribution as their number increases towards infinity. Unfortunately, a case where the condition is famously not fulfilled is the energy loss of particles in a gas detector. Due to the large tail of the Rutherfordian energy loss in one collision, the distribution will only very slowly converge to a Gaussian. Landau even assumed a cross section with divergent mean. This means that variance and mean of the distribution are not defined and there is no parameter set which will make a Landau distribution look like a Gaussian. The reason for the similarity of the TPC signal distribution to a Gaussian is *not* the central limit theorem but the truncated mean cut on the signal.

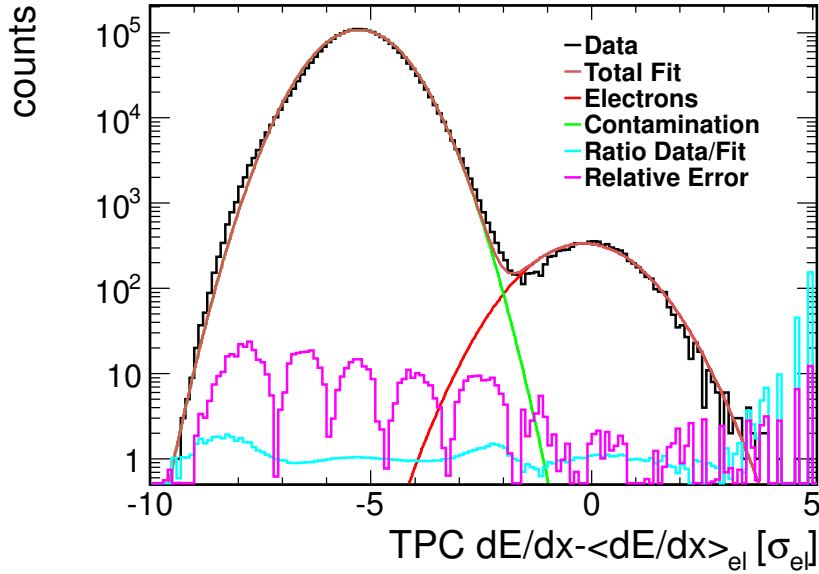


Figure 2.2.7.: Fit of the Contamination with a single Gaussian for both contamination and electron distribution. The relative error is significantly larger than expected for purely statistical errors.

Nevertheless, using a Gaussian to model the distribution of the contaminating particles might still provide some insight into the properties of the distribution. The electrons are then also fitted by a Gaussian in order to disentangle the influence of the (electron-)signal and the background in the region where both overlap.

Figure 2.2.7 shows the fit of the distribution with a single Gaussian to describe the background. Fit and data are closer together at some places while disagreeing more strongly at others. Disagreement could come both from a bad model and from statistical fluctuations. It would be interesting to know whether at some region the disagreement might be solely due to the statistical fluctuations in the data or if they surpass this and point to a problem with the model. For this purpose the *relative error* of the fit is a useful quantity. As explained in the previous chapter, the fluctuations in the bins are Poissonian. We would expect a variance in each bin of $\sigma^2 = \langle N \rangle$, with $\langle N \rangle$ given approximately by the value of the model at this point. An interesting quantity is thus

$$\frac{d_i - \lambda_i}{\sigma} \approx \frac{d_i - \lambda_i}{\sqrt{\lambda_i}} \quad (2.2.15)$$

where d_i is the number of counts in that bin, while λ_i is the value of the fit function. This describes the deviation of the fit from data in the bin relative to the expected width of the deviation. For better visibility of this quantity in a logarithmic plot, its absolute is useful for the definition of the *relative error*:

2. Analysis of Electrons from Heavy Flavor Hadron Decays

$$e_{rel} = \frac{|d_i - \lambda_i|}{\sqrt{\lambda_i}} \quad (2.2.16)$$

This assumes a symmetric distribution of the errors, which is not strictly true for the Poissonian fluctuations. However, as this quantity serves mainly as an aid for understanding the fit properties, it is still useful. It is closely related to the χ^2 measure with Poissonian variances which is the result of a summation of the squares of this quantity. The squares of this quantity should show a χ^2 -distribution (here: the mathematical distribution) for a single degree of freedom. However, the distribution of the relative error itself should be Gaussian for a perfect model with large statistics in each bin and have a width of 1. The relative error is interesting, because it provides a measure of the local fit quality which yields more information than the χ^2 -measure itself. To get rid of the local fluctuations, some method of smoothing could be applied to the distribution, e.g. through convolution with a Gaussian, but this is not required for the present study.

From figure 2.2.7 it becomes apparent that the application of a single Gaussian is insufficient to deal with the contamination. The cut on the signal has to be made at some point, where the contamination will not be particularly large, as is the case for example in the valley between the hadron and electron peaks around -1. This region however is particularly badly represented by the Gaussian model. Thus a better fit function needs to be found.

To understand the problems with this approach, it is useful to consider the different distributions of the energy loss in figure 2.2.1. There are two main issues with the approach of a single Gaussian: The distributions are not perfectly Gaussian and there are contributions from several particle species.

Fits with Multiple Gaussians The natural generalization of this fit type to include many contaminating particle types is the use of a Gaussian distribution for each. Significant numbers of particles can be expected for kaons, pions, muons, electrons and perhaps protons. The resulting fits are shown in figure 2.2.8. It is important to note two challenges for the fit here: As all distributions are Gaussian, it is not clear which distribution will correspond to which particle. Secondly, this new fit type increases the number of free parameters from 6 for two Gaussian distributions in the previous case to now 15 (amplitude, width and center for each Gaussian). Both can be solved with the careful use of constraints for the different parameters. This also makes the task of numerically finding the minimum in the 15 dimensional parameter space simpler. The techniques involved will be discussed in more detail in section 2.2.4.3. Each additional parameter decreases the stability of the fit and increases the calculation time.

In figure 2.2.8 the relative error indicates that the fit quality is very high. The errors are almost exclusively of statistical origin. The fact that the relative error is of order 1 does not indicate that there is no deviation of the fit from the model but that the systematic difference is small compared to the statistical fluctuations. Higher statistics would at some point show some deviation as the model will not incorporate every effect of the data production. The important question is now: Given a fit which reproduced the data within statistical error bars, which kind of conclusions are possible concerning the contamination?

2. Analysis of Electrons from Heavy Flavor Hadron Decays

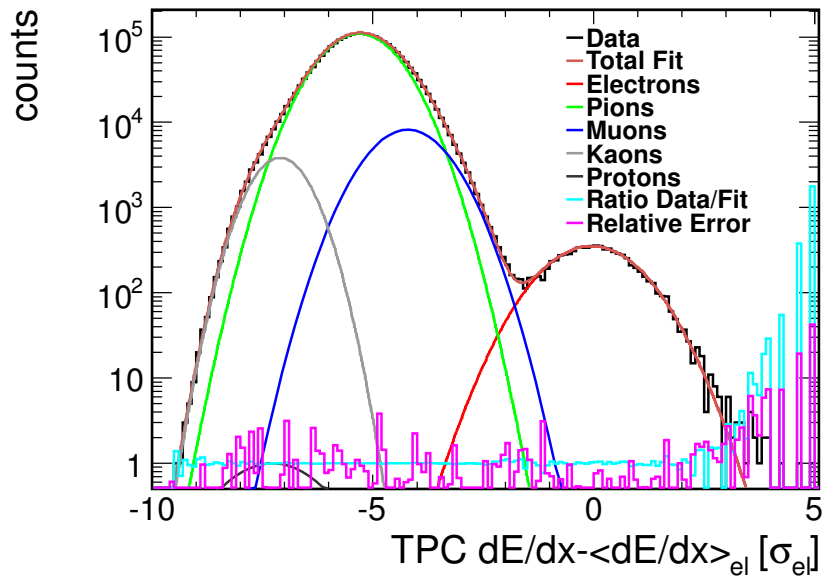


Figure 2.2.8.: Fit with 5 Gaussians. The contamination is fitted by four Gaussians, although the Gaussian for the protons does not show any influence after a cut on the TOF signal. The relative error is low, suggesting mostly statistical deviations of the data from the fit.

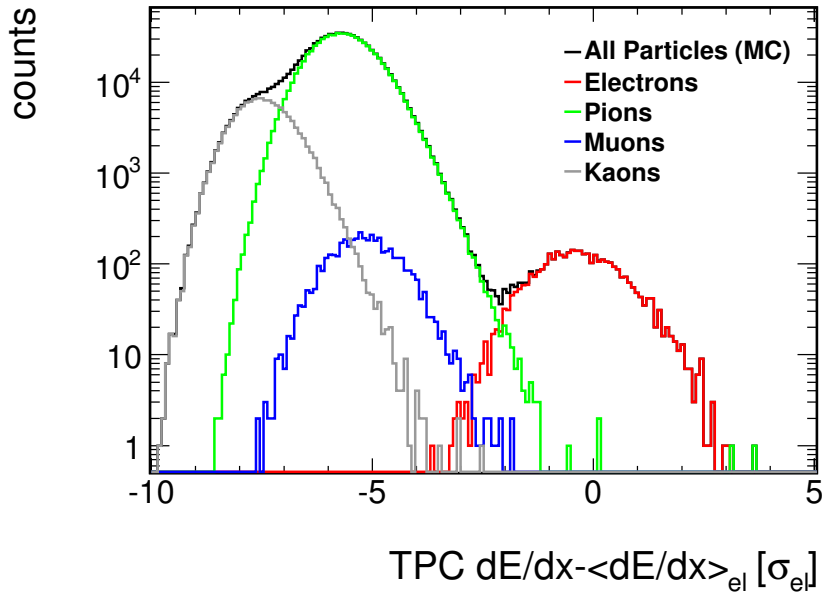


Figure 2.2.9.: The Monte Carlo Signal with Contributions from Several Particle Species. The associated momentum range is $2.5\text{GeV}/c < p < 2.7\text{GeV}/c$. The contamination of electron candidates from this sample would be dominated by pions.

Results From a fit of all background contributions over the range of the electron distribution the contamination of the electrons after a cut on the TPC signal can be calculated. Assuming the fit functions describe the actual distributions of the particles it is also possible to extract the number of particles of the different species within the momentum bin after the applied cuts on the TOF and TPC signal. One of the most important results is the number of muons this fits seems to find. According to the fit model the muons make up of the order of 5% of the pions and contribute significantly to the contamination. However this amount is much higher than expected. Figure 2.2.9 shows the expected distribution from Monte Carlo, giving only about 0.5% muons relative to pions. This would require an additional muon source. However, the MC distributions also indicate something else: The rightmost part of the contamination distribution is dominated not by muons but by the pions. This means that the tail of the pion distribution has significant influence on the contamination of the electrons and the appearance of the large muon number is due to the pion-Gaussian not adequately representing the pion tail. A better interpretation of the fit is now, that the pion line shape is being represented by the sum of two Gaussians. At all places where the pion line is dominant, this fit describes the data well. The question is now again: If the fit function has errors which can be explained by statistical variations alone, does this mean the contamination will be correctly calculated? In the analysis, the cut on the electron signal was set to the center of the electron line. Thus, a rephrasing of the question might be: Given that the description of the distribution is good in all bins where the pions are the

2. Analysis of Electrons from Heavy Flavor Hadron Decays

dominant contribution, does this allow for an estimate of the size of the pion contribution where electrons are the dominant signal?

Obviously this conclusion would be incorrect. The argument for the fit would be stronger, if a model of the involved processes served as a basis of the calculations. In this case, the agreement close to the center of the line would serve as a test of the model. It is possible, that the agreement works well simply due to the large number of free parameters and the distribution might continue in any conceivable way at the points where it does not influence the total distribution (within the electron line).

One important point remains from a general comparison with the Monte Carlo shape: The Gaussian distribution drops rather quickly far away from the center. Thus, at larger energy losses it will always underestimate the contamination. For this reason it might serve as a lower bound for the contamination if the cut is done at a high TPC signal.

2.2.4.2. Alternative Methods

To get a better estimate for the contamination, a model has to be found, which

- Does not introduce too many free parameters
- Is based on the underlying physical processes
- Can be calculated with sufficient speed to serve as a fit template

For this, there are four basic strategies:

1. Take the distribution from a direct measurement of the straggling function.
2. Use Poissonian distributions instead of Gaussian ones.
3. Calculate the energy loss distribution from first principles
4. Calculate an approximate distribution based on a modified Landau distribution

As mentioned before, the ideal would be a complete Monte Carlo simulation of the detector, but the excellent MC calculations of ALICE did not yield the correct result and it would be difficult to improve upon them.

Direct Measurements of the Straggling Function The distribution of the electron energy loss signal from the TPC contains contributions from different particle species. In the measured region it is not possible to directly extract the shape of any single distribution directly. Thus, some method of experimental discrimination must be found. A very direct way to do this, is the use of the so-called V0 samples¹. These consist of several identified particles from the decays of fully reconstructed neutral particles. They are identified by the invariant mass and cuts on the topology. The pions are identified from the decays of kaons and lambda particles:

¹Not to be confused with the V0 detectors used for the measurement of the forward particle multiplicities

2. Analysis of Electrons from Heavy Flavor Hadron Decays

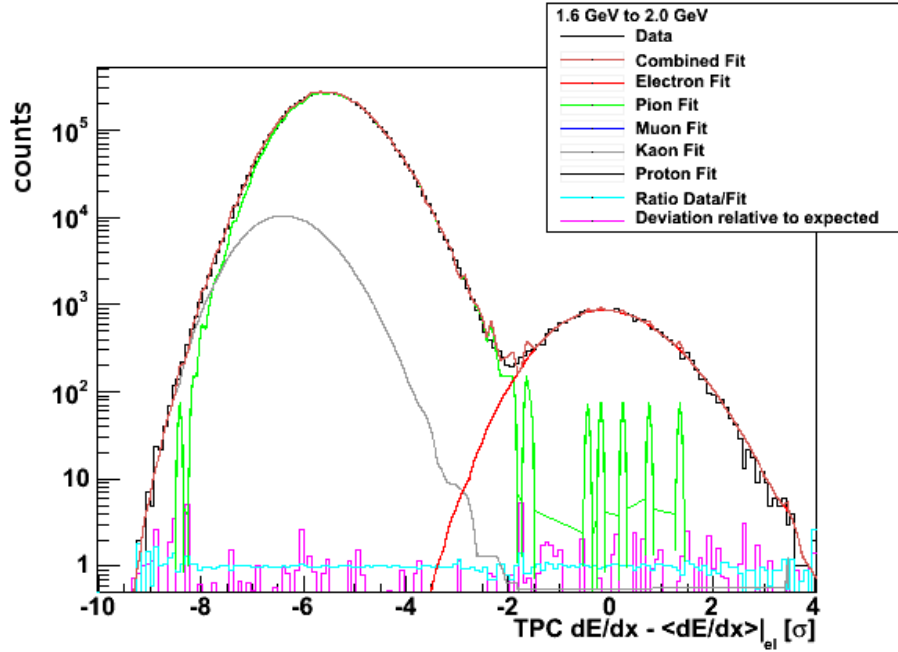


Figure 2.2.10.: Fits Using V0 Samples. The relative error is modified to take into account also fluctuations of the V0 fit template.

$$\begin{aligned}
 K_S^0 &\rightarrow \pi^- \pi^+ \\
 \Lambda &\rightarrow \pi^- p \\
 \bar{\Lambda} &\rightarrow \pi^+ \bar{p}
 \end{aligned}
 \tag{2.2.17}$$

These samples contain a very low amount of contamination by other particles and provide a useful sample for test of many detector efficiencies. Figure 2.2.10 shows the resulting fits from using the V0 distributions as a template. The obvious problem is the low statistics from the V0 sample. The final cut on the sample was at 0. There and even at lower points, the V0 sample is dominated by statistical fluctuations and perhaps even by contamination from electrons. Additionally, the spectrum for the V0 particles drops much faster than for the total number of pions. This method is therefore not useful in this context and this discussion only serves to give an explanation as to why it is not used in the present analysis.

A better approach would be to measure the full amount of pions. The ratio of pions/electrons can be increased by changing the TOF cut to preferentially select pions. However, at high momenta, this will still leave a significant amounts of electrons. In addition, also kaons and protons might be selected. If too stringent cuts are applied there also might still be the problem of low statistics at high momenta. If the goal is however, not to get the exact distribution shape but an approximation, then it might be sufficient to get the shape of the distribution at one momentum bin with high statistics and change width and center to account for differences in higher bins. As the strength of TOF is highest at low momenta, one way would be to extract the shape at a low momentum and make a TOF cut around the pion line. Figure 2.2.11 shows the extracted line shape at 800MeV as well as a fit at

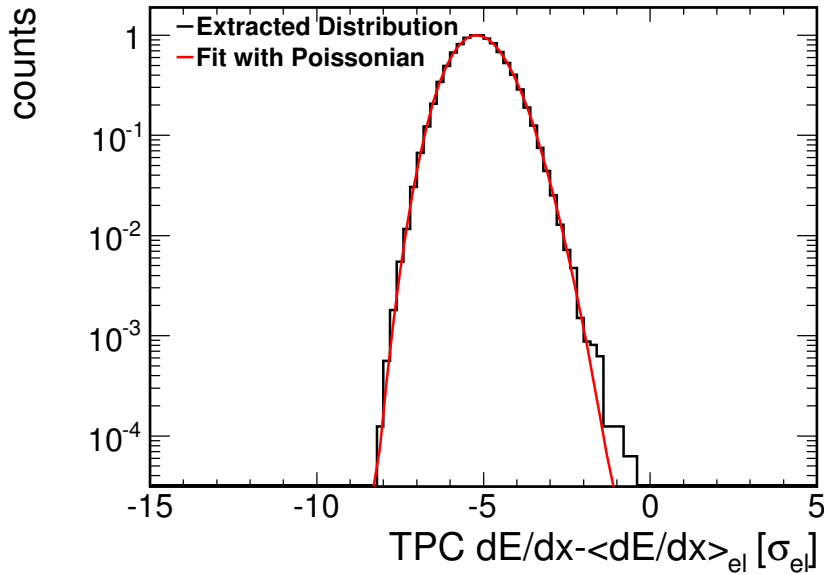


Figure 2.2.11.: Fit of the Extracted Pion Distribution at low p with a Poissonian Distribution.

intermediate momentum. In this case, width, center and amplitude of the distribution were free parameters with the function values between the bin centers given by linear interpolation. The distribution is only slightly asymmetric. This asymmetry is not sufficient to describe the final function. The reason for this is the longer path length of a low momentum particle in the TPC. This particle will lose more energy and yield on average a higher number of clusters. Thus, the extracted line may give a better approximation of the line shape than a Gaussian but it is not capable of giving a good estimate of the contamination.

Poissonian Approximation From a practical standpoint, a useful solution would be the use of a Poisson distribution instead of the Gaussian. It is skewed, has only 2 free parameters and is easily calculated. A justification for this approach might be the following: The truncated mean cut removes large clusters. This might lead to an effective cross section for individual collisions, which does not contain the high energy loss tail. The remaining distribution might be separated into two parts: Most individual collisions will yield a low energy loss. This gives a distribution of a low width around the average energy loss. The high energy loss part gives an approximately constant energy loss with a low probability. Thus, the whole distribution can be modeled as a Poissonian shifted by some constant. Thus, this model contains three free parameters: The amplitude, the average of the Poissonian and the shift due to the small ionizations.

As visible from figure 2.2.12, the Poissonian model cannot be used to describe the pions, but it can describe the distribution for pions at low momentum, described in the previous section (figure 2.2.11). Both of these distributions cannot describe the data, but they are an

2. Analysis of Electrons from Heavy Flavor Hadron Decays

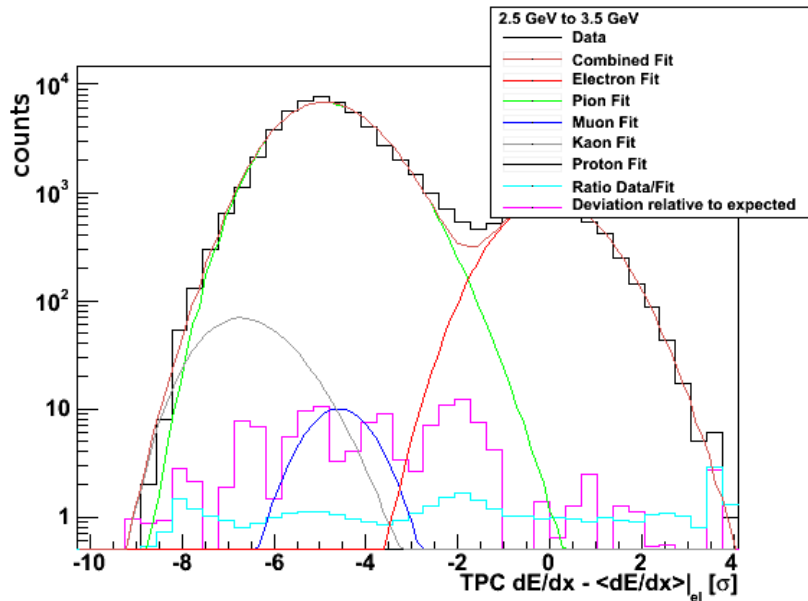


Figure 2.2.12.: Fits with Poisson Distribution for the Pions. The relative error shows large deviation compared to purely statistical fluctuations in the bins.

improvement on a single Gaussian without requiring additional free parameters. They find their use improving the fits of the kaons instead, where a low number of free parameters has precedence to a precise fit far away from the center (e.g. figure 2.2.10).

Direct Calculation As previously mentioned: The correct way for calculation would be a full Monte Carlo simulation of the energy loss and detector response but this route is not possible in the framework of this analysis. Additionally, the main difference from the Landau distribution should come from the truncated mean cut. One related method of attacking this problem would be the assumption that the truncated mean cut simply changes the effective spectrum of the energy loss and performing the calculations for this. For the effective spectrum, the high energy-loss tail should be somewhat suppressed. This suppression can be modeled by an exponential suppression or a simple cutoff. In these cases, the original spectrum was modeled simply as

$$\sigma(E) \sim \frac{1}{E^{2.2}} \quad (2.2.18)$$

There are two obvious methods for the calculation of the convolution: Monte Carlo integration and the use of a transform. Due to the similarities, both are discussed here together. For a Monte Carlo integration, a certain number of collisions is simulated with the individual energy loss gained by sampling the spectrum. The energies are added and this is repeated as long as necessary. For the transformation calculation, a fast Fourier transform was used:

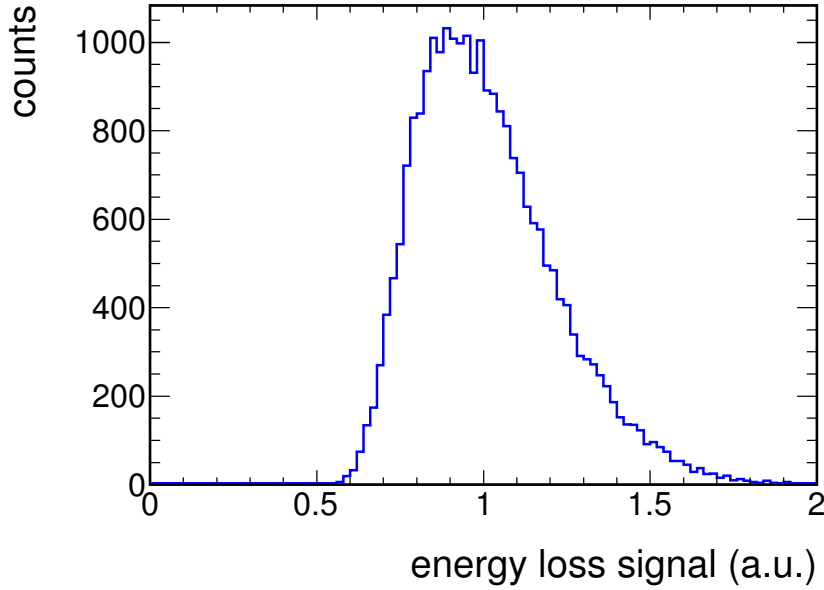


Figure 2.2.13.: Line Shape Generation Using Monte Carlo Integration

$$\begin{aligned}
 \sigma_{tot}^n(\Delta) &= \int_0^\Delta \sigma_{tot}^{n-1}(\Delta - E) \cdot \sigma_{single}(E) dE \\
 \Leftrightarrow F(\sigma_{tot}^n(\Delta)) &= F(\sigma_{single}(E)) \cdot F(\sigma_{tot}^{n-1}(\Delta)) \\
 &= F(\sigma_{single}(E))^n
 \end{aligned} \tag{2.2.19}$$

The parameters for a fit are now the lower and upper cutoff for the energy loss per collision. Depending on the cut on the number of PID clusters, a sum of the calculation for different numbers of the energy loss should be done as well as a convolution with a Gaussian to take into account the widening of the line due to effects of the read-out electronics. Although, the computation is relatively fast, both of these methods suffer from the high numerical requirements. There are methods to increase the performance but this still creates a severe workload to the fitting algorithm when it varies the parameters. The resulting signals for example parameters are given in figure 2.2.13. These methods allow inclusion of a variety of effects and should therefore be considered for future improvements. They do, however give a useful starting point for the calculations for the final model.

Modified Landau Model Without the truncated mean cut, the signal should look similar to a Landau distribution. An obvious starting point for finding a suitable model for the TPC signal would thus be a modification of this distribution to take into account the truncated mean cut. The simplest approach is a correction factor:

$$S_{TPC}(\Delta) = L(\Delta) \cdot f(\Delta) \tag{2.2.20}$$

2. Analysis of Electrons from Heavy Flavor Hadron Decays

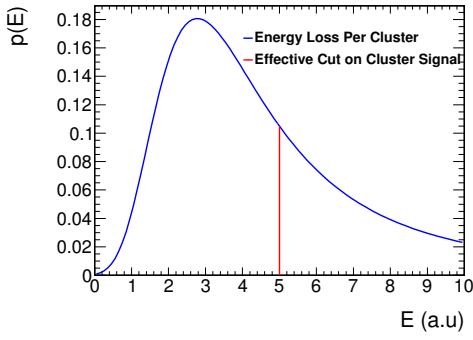


Figure 2.2.14.: In the model assumption, the truncated mean corresponds to a removal of clusters above a threshold. The distribution of energy loss in the clusters should have approximately the shape of a Landau distribution.

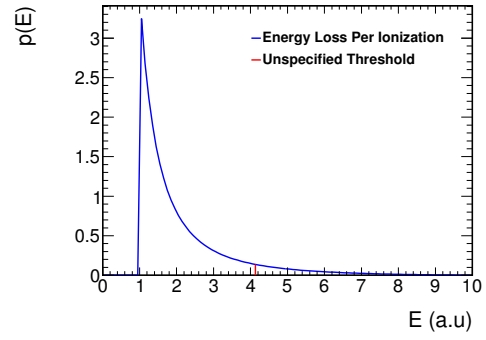


Figure 2.2.15.: Individual collisional energy losses are defined as *high* if they exceed an unspecified threshold value E_{crit} .

where S_{TPC} is the TPC signal, L is a Landau distribution and f is the correction factor. This can be motivated by a simple model: The truncated mean cut removes the 40% highest signal clusters. For each track this means, that there is a highest cluster with some signal x_{cl} . A great simplification of the problem is the assumption that the highest remaining cluster has a similar signal strength for each track. Thus, instead of cutting the highest 40% of clusters, all clusters above a certain threshold are cut. The remaining distribution is a Landau distribution for a smaller number of clusters, from which all tracks containing a cluster above the threshold are removed. $f(\Delta)$ is now the probability that a random track of energy loss Δ will *not* have a cluster with a signal above the threshold. Assuming this model describes the process accurately, it remains to find a mathematical description for $f(\Delta)$, preferably one with as few free parameters as possible. In the end, again a convolution with a Gaussian includes detector effects as mentioned before.

To estimate $f(\Delta)$, another simple model is used: Each individual ionization has an energy loss sampled from the collision spectrum. At some unspecified point E_{crit} a distinction is made: An energy loss below this point is considered a low energy loss, while an energy loss above is considered a high energy loss (The threshold mentioned earlier is not for the individual collisions but for the clusters). Assuming a low ratio of high energy loss ionizations, we can assume, that there is at most one high energy loss collision per cluster. For each high energy loss ionization, there is a chance p that this will result in a cluster above the threshold. Thus, the probability for a track to have no clusters above the threshold can be calculated as:

2. Analysis of Electrons from Heavy Flavor Hadron Decays

$$f(\Delta) = P_0(\Delta) + P_1(\Delta) \cdot p + P_2(\Delta) \cdot p^2 + P_3(\Delta) \cdot p^3 + \dots \quad (2.2.21)$$

where P_i is the probability for the track to contain i high ionizations. At each collision there is a small probability for a high ionization to occur. Thus P_i follows a Poisson distribution.

$$P_i = \frac{\lambda^i e^{-\lambda}}{i!} \quad (2.2.22)$$

with $\lambda = \lambda(\Delta)$ the expected number of high ionizations for a given average energy loss. Assuming knowledge of λ , this gives the following correction factor:

$$f(\Delta) = \sum_{i=0}^{\infty} P_i(\Delta) \cdot p^i = \sum_{i=0}^{\infty} \frac{\lambda^i e^{-\lambda}}{i!} \cdot p^i = e^{-\lambda} \sum_{i=0}^{\infty} \frac{(\lambda \cdot p)^i}{i!} = \exp((p-1) \cdot \lambda(\Delta)) \quad (2.2.23)$$

From a Taylor expansion of $\lambda(\Delta)$

$$\lambda(\Delta) = a_0 + a_1 \cdot \Delta + \dots \quad (2.2.24)$$

it is clear that the zeroth order contribution only changes the normalization of the $f(\Delta)$ distribution and thus can be combined with the amplitude of the Landau. To keep the amount of free parameters low, the assumption

$$\lambda \sim \Delta \quad (2.2.25)$$

is the simplest, introducing only one additional free parameter, which is the proportionality factor multiplied with $(p-1)$. Thus

$$f(\Delta) = \exp(-\alpha \cdot \Delta) \quad (2.2.26)$$

in this model.

Apart from the total amplitude and width and center of the Landau distribution, this introduces one additional parameter. The distribution then has to be convoluted with a Gaussian for the detector widening. In principle this introduces the width of this Gaussian as an additional parameter. However, in practice this parameter was found to be very small and it is thus set to the fixed value of 0.002 in units of the electron width. This model assumes that the cluster cut does not have to be explicitly included for a good contamination estimation. An example of a fit using this model can be found in figure 2.2.16. An interesting result is that this model achieves a description of the data similar to that of the multi-Gaussian fit. However, the description of the pions now only contains 4 free parameters compared to the previous 6. Additionally, this fit function is now based on a model with its roots in physics, making it significantly more trustworthy.

2. Analysis of Electrons from Heavy Flavor Hadron Decays

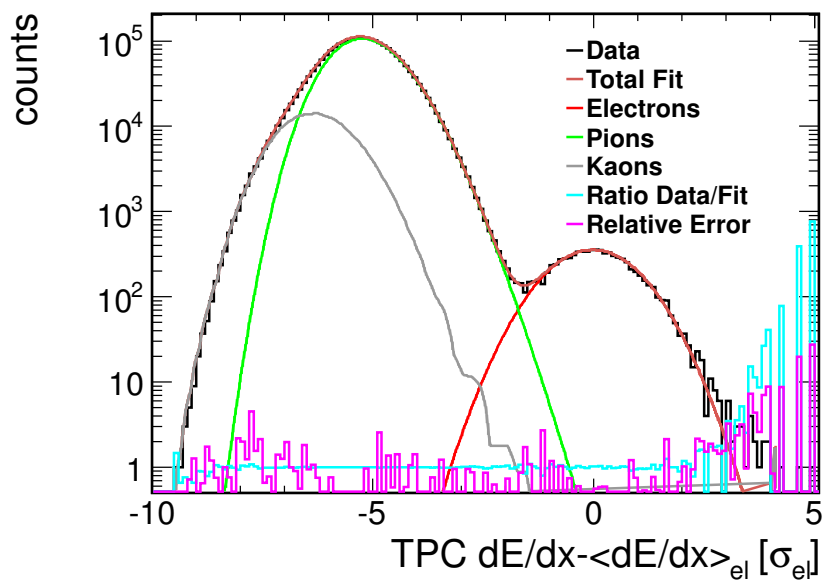


Figure 2.2.16.: Fit Using the Modified Landau Model. The relative error is consistent with statistical fluctuations. On the very right, a deviation can be seen. This is due to the approximation of the electron signal distribution by a Gaussian. The latter is not critical for the calculation of the contamination.

2.2.4.3. Refinement of the Fit Quality

With the availability of a suitable fit model and a measure of the agreement of a certain set of parameters with the data the fit becomes basically a minimization problem in the space of the parameters to be solved numerically by some minimization algorithm. For a large number of fit parameters (meaning: dimensions of the parameter space) this problem can become quite challenging for the minimization algorithm. The most obvious problem is the appearance of local minima in addition to the best fit. Additional problems appear due to ambiguities in the minima e.g. when fitting with multiple Gaussians which might be switched around. A third problem is the appearance of very wide minima, where the correct apprehension of the minimum is particularly dependent on the remaining errors of the fit model which can inflate the systematic errors. Finally, all fits are performed in bins. The fit of a finite range of variables can cause additional challenges for the correct fit.

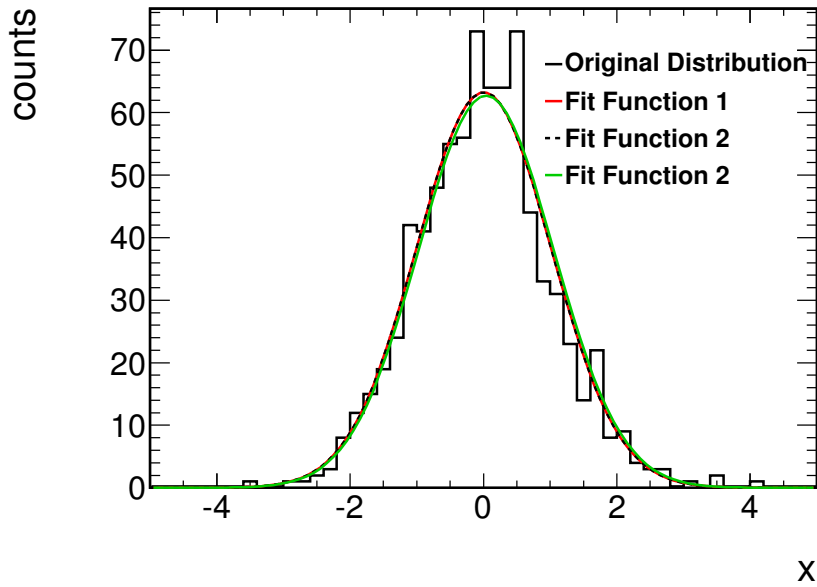
Stability Issues The parameters of the present fit are correlated. This is obvious from the fact, that it is insufficient to minimize every parameter separately. If two distributions overlap and the amplitude on one becomes larger then the amplitude of the other will generally become smaller. An obvious example is given in figure 2.2.17. A Gaussian distribution is fitted by a Gaussian. This fit works better or worse depending on the parametrization of the Gaussians. If the parameters are highly correlated then the fit becomes more difficult.

This is particularly important for the pion component of the fit. The functional form in this coordinate system is according to the derivation (without the convolution with a Gaussian):

$$S_{TPC}(x) = A \cdot L(x, \sigma, c_0) \cdot \exp(-\alpha \cdot (x - x_0)) \quad (2.2.27)$$

where A , σ , c and α are the free parameter giving the total amplitude, width and center of the Landau and the free parameter in the exponential. x_0 would be the x value in the coordinate system corresponding to zero ionization. It is important to note that the actual value is not particularly important, as any change in this variable can be compensated by a change in the amplitude. However, α is strongly correlated with the amplitude, center and width of the total distribution. x_0 can be used to partially decorrelate α from A , which should be the strongest correlation. It would be best to set x_0 to the current maximum of the function. However this is not analytically calculable. Thus x_0 was set to $c_0 - 8.5$ as an approximation of the center obtained through trial-and-error.

In particular for the multi-Gaussian fit the same minimum appears, if the parameters of two Gaussians are exchanged, as they have the same functional shape. It is preferable to have some control over which of these minima is found. Additionally a fit in a high-dimensional parameter space has to be guaranteed. One way to achieve this is to find starting values close to the desired minimum and put sufficient constraints on them. A guess for the starting values of the center is provided by a spline fit of the most likely value of the TPC signal as drawn in 1.2.2. This is the equivalent of a Bethe-Bloch-Curve for the case of the TPC signal. The mayor difference is that the Bethe-Bloch-curve describes the change of the average energy loss (assuming a Rutherfordian ionization cross section), which is very different from the most likely energy loss. After a truncated mean cut however, both are



#	Function Definition	Calls by Fitter	Final Status
1	$p_0 \cdot \text{Gauss}(x, \text{center} = p_1, \text{width} = p_2)$	336	<i>Converged</i>
2	$p_0 \cdot p_1 \cdot \text{Gauss}(x, \text{center} = p_1, \text{width} = p_2)$	1347	<i>Converged</i>
3	$p_0 \cdot p_1^5 \cdot \text{Gauss}(x, \text{center} = p_1, \text{width} = p_2)$	1345	<i>Call Limit</i>

Figure 2.2.17.: Example of Stability Problems due to Correlations of Parameters. Although for only 3 free parameters the fitter finds a reasonable fit for all functions, those with stronger correlations between the parameters perform worse in the example. The starting parameters were chosen to produce identical starting distributions.

2. Analysis of Electrons from Heavy Flavor Hadron Decays

much closer together. Assuming the same number of ionizations for each particle type, but a different average energy loss, the ratio of the centers can be approximated by the ratios of the absolute TPC signals. The parameter ranges still need to be kept sufficiently wide to make sure the inaccuracies of the estimates do not influence the fit result.

The methods mentioned above make the multi-Gaussian fit significantly more stable. The modified Landau fit however still requires some tuning for completely new types of data samples (e.g. different production periods or collision types). The parameters of the electron Gaussian are also constrained to obtain a good fit.

Line Widening As previously mentioned, the fit is performed in momentum bins. Consequently a momentum range has to be considered when calculating the fit functions. All distributions of the TPC signal are in principle dependent on the momentum. This dependence is small for the electrons, as the coordinate system is defined relative to their width and center. In principle, the shape of the other contributions has to be integrated over the momentum range taking into account the different amplitudes:

$$f_{bin}(x) = \int_{p_{min}}^{p_{max}} N(p) \cdot f(x, a_i(p)) dp \quad (2.2.28)$$

where f_{bin} is the distribution of the energy loss from this source in one bin, $f(x, a_i(p))$ is the distribution at a given momentum with the momentum dependent fit parameters $a_i(p)$ and the relative amplitudes $N(p)$ given by the momentum spectrum of the source. p_{min} and p_{max} are the momenta at the lower and higher edge of the bin. This introduces an infinite amount of new parameters in each bin, so some approximations have to be done. The spectrum is not a priori known, in fact it is the result of the whole analysis. By choosing small bin sizes in momentum relative to the change in the function shape, most effects can be neglected. In this case, the strongest effect should come from the change in the center of the distribution.

$$f_{bin}(x) \approx \int_{p_{min}}^{p_{max}} f(x, x_0(p)) dp \quad (2.2.29)$$

Changes in width and amplitude are therefore neglected as secondary effects over the momentum range of the bin. The total shape will only depend on this effect relatively weakly. Thus the fit would not be able to constrain the change in center well. In order to circumvent this and not to introduce additional parameters, the spline approximation for the centers is used to give the difference in center between the start and end of the bin. This quantity is called ϵ . For small bin sizes the center should depend on the momentum approximately linearly:

$$f_{bin}(x) \approx \int_{p_{min}}^{p_{max}} f \left(x, x_0(p) = x_0(p_{min}) + \epsilon \cdot \frac{p - p_{min}}{p_{max} - p_{min}} \right) dp \quad (2.2.30)$$

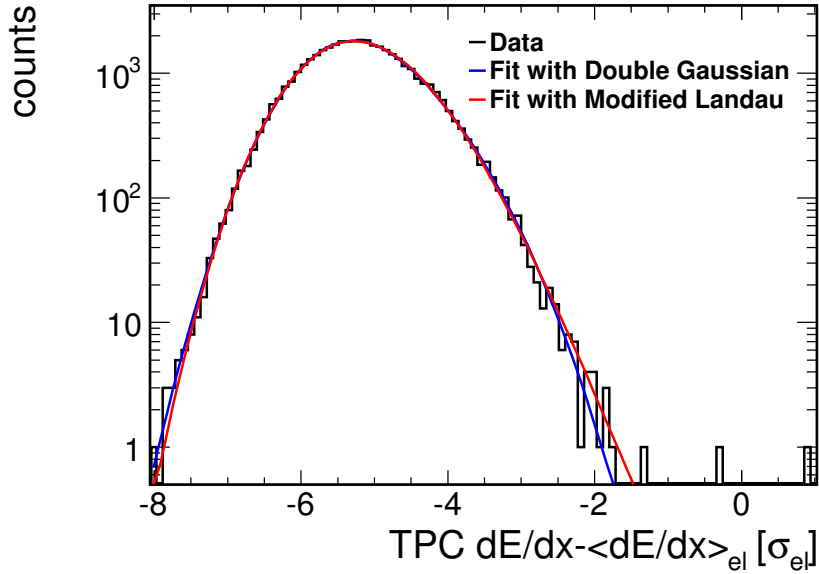


Figure 2.2.18.: A fit of V0 pions using a double Gaussian and a modified Landau distribution. To the very right, the modified Landau fit gives a higher value than the fit with two Gaussians.

In practice, the parameter ϵ is small: $\epsilon_{\text{pion}} \approx 0.025$ for a 200MeV momentum bin at $\approx 2\text{GeV}$. Thus the approximations are justified. For the purposes of a fit, a full numerical integration is computationally very expensive. Thus, the function values for equidistant points is sampled in the actual calculations. The effect is currently only included for the multi-Gaussian fit method, and there only for the pion-distribution as for the modified Landau widening is already included via the convolution with a Gaussian. In conclusion, this effect is small for most cases, except for one very important one described in the next section.

Line Crossing Figure 1.2.2 shows the positions of the distributions of the energy loss for different particles in the TPC. At some momentum, the particles produce a minimal ionization. Below this point, the energy loss increases due to the larger interaction time of the charged particles. Above, it increases again due to the relativistic change of the electric field, the relativistic rise. This means, that at low momenta, the average energy loss of heavier particles will become equal to that of the electrons. In this context, this will be called a *line crossing*. At this point, none of the approximations mentioned in the previous section can be applied. This is important at the crossing point of the protons at $\approx 1\text{GeV}$. A similar problem occurs for the kaons. The result is a contamination with unclear systematic errors. As the TPC cannot effectively suppress the protons here, the contamination is of the order of the remainder of the TOF cut.

Graph

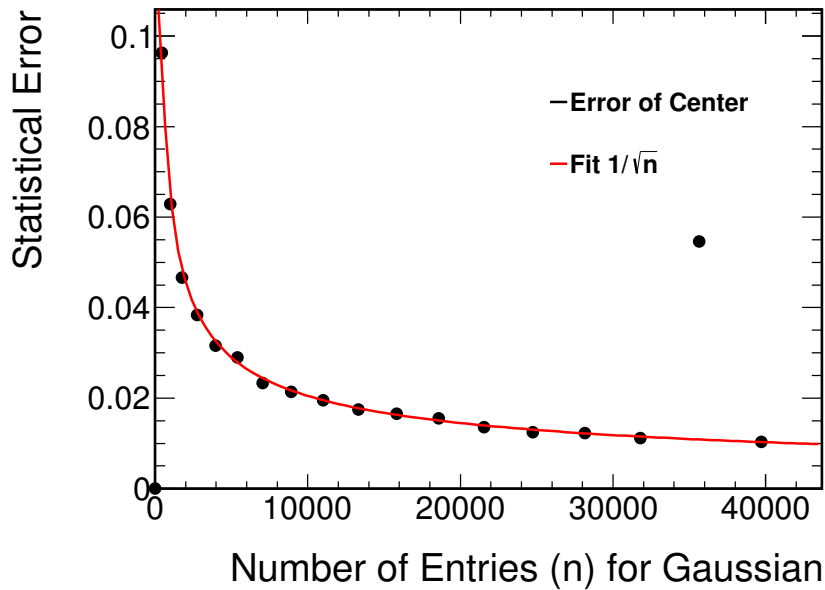


Figure 2.2.19.: Error on the Center of the Electron line fitted with a function of the form a/\sqrt{n} .

Error Sources To compare the results which could come from the fits of the multi-Gaussian method with those of the modified Landau fit, it is helpful to make a fit of the V0 pions using both. This is shown in figure 2.2.18. For a large signal value, the double Gaussian will fall as the square of an exponential, while the modified Landau will fall slightly stronger than a regular exponential. If all quantities are extracted with both fit types, this gives an idea of the systematics from the modeling of the contamination.

A similar approach is possible for the determination of the center of the electron line: The center will be lower for the Gaussian fit, as the electron distribution has to account for some of the pions while the center will be a bit higher for the the Landau fits which take up more of the distribution between the peaks.

For the estimation of the electron centers some care has to be taken. The electrons are already well in the region of the relativistic rise for the relevant momenta. The pions are at the beginning of the rise. For higher momenta, the distributions overlap more strongly (figure 1.2.2). Even more importantly, the spectrum of electrons drops for higher momenta. Thus, the determination of the center is best at low momenta. Still, it would be preferable to take the average of several bins to get the true center. Thus, a weighted average is the best option. This raises the question, what these weights should be. Assuming, the fits with the double Gaussian and modified Landau give a similar result, the statistical error on the electron center is primarily determined by the electron statistics. It is thus interesting to get the dependence of the electron center (and width) on the number of electrons. Within an approximation this can be determined by a Monte Carlo integration. It is assumed, that the

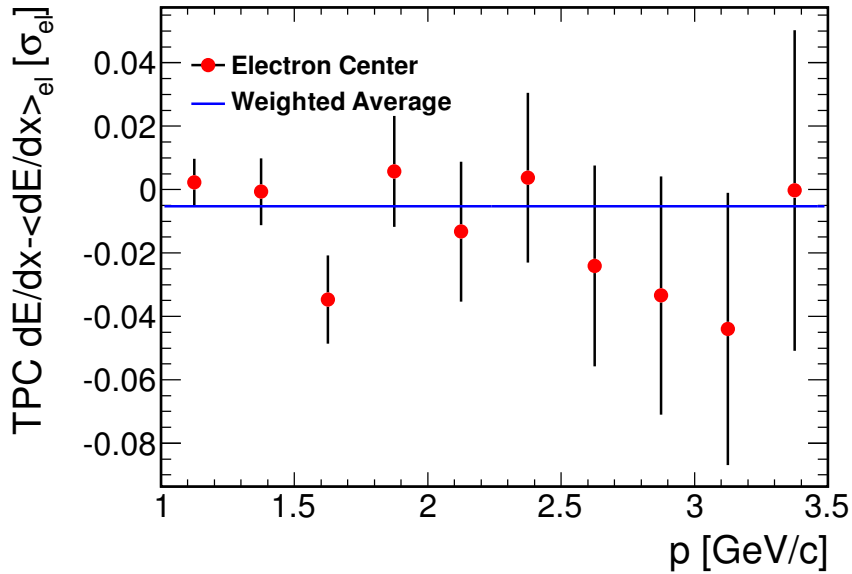


Figure 2.2.20.: Electron Centers measured at different momenta. The error bars come from the estimation based on the number of electrons. The blue line is the weighted average of the bins.

effective fit range is about -1 to 2 in units of the electron width relative to the center of the electron line. The lower limit comes from the influence of the contamination, the upper one from the problem of fitting the electrons far from the center due to the non-Gaussian shape of their distribution. A Gaussian distribution of width 1 and center 0 is sampled a certain number of times and the resulting distribution fitted with a Gaussian. The centers and widths of this process again form a distribution which is fitted with another Gaussian. The resulting widths of the distributions for a different number of sampled points is given in figure 2.2.19. The resulting errors are Poissonian in their dependence on the sample size. This dependence is used to assign a weight to each bin for the determination of the centers. At high momenta, the influence of the pion distribution becomes large, thus the average is done over the lower bins.

2.2.5. Fit Results

2.2.5.1. Electron Centers

The exact point of the cut in the TPC signal depends on the requirements for the efficiency and contamination of the resulting sample. The current choice for the cut is the center of the electron line. In the coordinate system used here this corresponds to a cut at about 0. At this point the electron distribution is at its maximum. For this reason, the efficiency correction is very dependent on the exact knowledge of the actual center of the electron

2. Analysis of Electrons from Heavy Flavor Hadron Decays

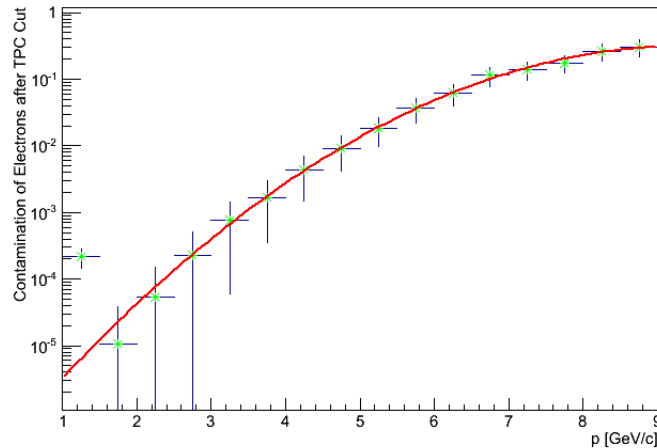


Figure 2.2.21.: Dependence of contamination on momentum for a setup with and without a cut on the TRD signal. The fit is purely phenomenological and without physical motivation. Error bars are for the Poissonian fluctuations of the contamination based on the expected number of contaminating particles.

distribution. Figure 2.2.20 shows the resulting electron centers from a fit using the modified Landau function.

The center of the electron line varies with the eta range due to detector effects which are not included in the calculation of the TPC signal. To limit the influence from this effect, for the final measurement the η -range was limited to $|\eta| < 0.5$ for the cocktail subtraction method.

2.2.5.2. Contamination and Efficiency

For a cut along the measured electron center, the efficiency is constant at about 50%. The contamination however, varies with the momentum. Figure 2.2.21 shows the dependence of the contamination on the momentum. The results are given for the use of a TPC+TOF measurement strategy. To make the fit more stable, the electron center and width are fixed to the values obtained via the method of the previous section.

With a handle on the hadron contamination, it is possible to access the spectra of electrons from the decays of particles containing heavy quarks. Doing this in pp and Pb-Pb collisions provides some information about the energy loss of heavy quarks. Still preferable even would be a measurement of the individual contributions. The reasons for this and a method for the measurement will be described in the next subchapter.

2. Analysis of Electrons from Heavy Flavor Hadron Decays

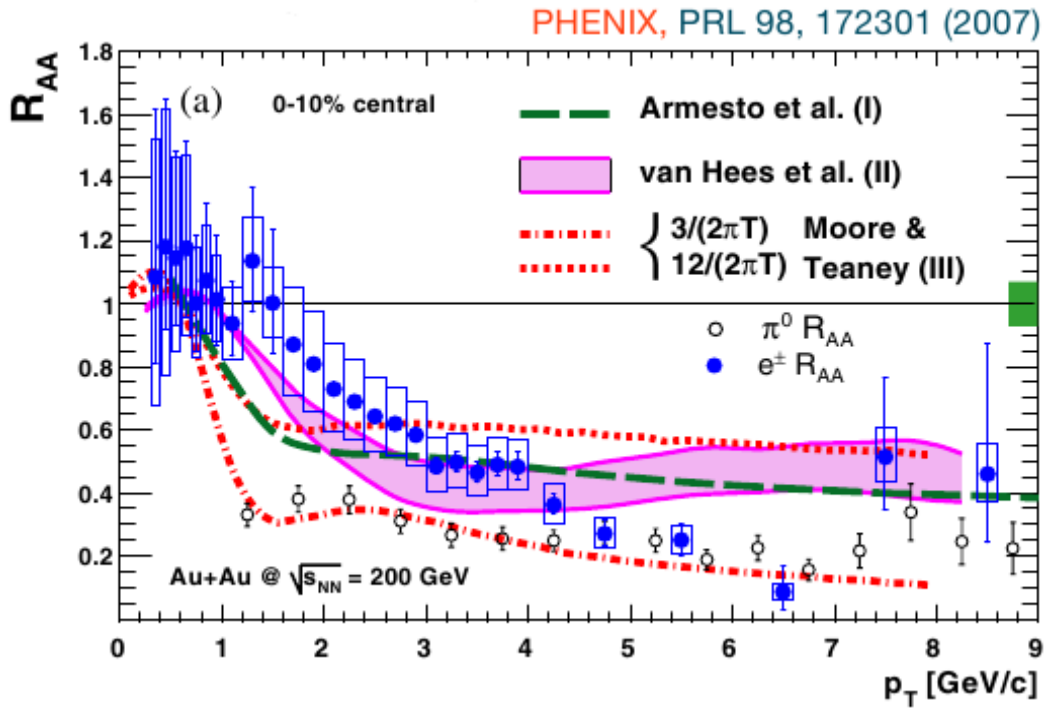


Figure 2.3.1.: Heavy flavor electron measurement by PHENIX at RHIC.[19] For higher transverse momenta, the nuclear modification factor for electrons from the decay of beauty and charm hadrons is similar to that of the pions.

2.3. Measurement of Electrons from Beauty Decays

2.3.1. The RHIC Heavy Quark Energy Loss Puzzle

Theory predicts a stronger energy loss for gluons compared to quarks and for lighter quarks compared to heavier ones. Assuming this effect is dominant over others, the expectation for a measurement of the nuclear modification factor would be

$$R_{AA}^{\pi} < R_{AA}^D < R_{AA}^B \quad (2.3.1)$$

Surprisingly, measurements of the electron modification factor at RHIC paint a different picture (figure 2.3.1). For the higher p_t -part of the diagram, the nuclear modification factor for the total number of electrons from charm and beauty hadron decays is similar to that of the pions and less than predicted by most theoretical calculations. Apart from the question of whether electrons at the LHC exhibit similar behavior, it is also important to ask what the contribution from beauty and charm quarks is to this effect. It is possible that the lighter charm quark behaves more like a light quark and thus some assumptions for the energy loss are invalid. Or theory fails to describe the energy loss for all heavy quarks for example by wrongly estimating competing effects.

To actually measure the different distributions from the two heavy quark flavors in the electron channel requires some ingenuity in the measurement. In a similar approach as for the inclusive measurement, one of the contributions might be estimated as a cocktail and then subtracted to gain the other. The availability of independent D meson spectra from ALICE measurements in the hadronic decay channel[29] makes this a viable approach. The decay of D mesons from the measured spectrum can be simulated to gain a spectrum of electrons from charm hadrons. By itself however, this method gives large error bars due to the large background contribution. Additionally it would be good to have a method which is independent of the measurement of the D mesons, perhaps even of the complete electron cocktail. One such more direct approach will be presented in the following subchapters. It is important to note that both methods are connected by the use of the impact parameter. Where this connection is important, it will be noted in the following sections.

No matter how high the quality of a PID setup is, it will not be able to measure a difference between electrons from one source and another. Thus, some new quantity has to be found to separate the electrons from the decays of beauty hadrons from the others, at least stochastically. For this purpose a quantity needs to be used for differentiation, which shows a sufficient dependence on the source and is a property of the measurement of a single electron.

2.3.2. The Impact Parameter

2.3.2.1. Decay Vertices

Apart from their masses, one particularly differentiating characteristic of many types charm and beauty hadrons is their large decay length. To make use of this, measurements which measure all decay particles usually also require a minimal distance of the decay vertex to the

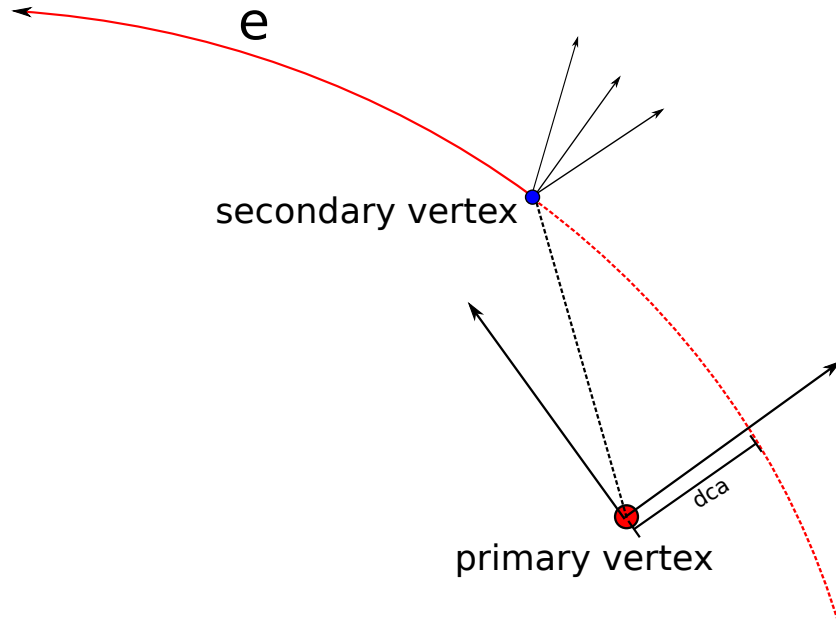


Figure 2.3.2.: Definition of the Impact Parameter. The Distance of Closest Approach (dca) is connected to the impact parameter, which also takes into account the direction of the particle's momentum.

primary vertex to reduce the background. c and b quarks hadronize at the primary vertex to form mainly D and B mesons. These have a much longer decay length than for example uncharged pions, whose Dalitz decays form a large part of the electron background:

Particle	Semielectronic Decay Example	Total Decay Length $c\tau$
π^0	$\pi^0 \rightarrow e^+e^-\gamma$	25.2nm
D^+	$D^+ \rightarrow \bar{K}^0 e^+ \nu_e$	312 μ m
D^0	$D^0 \rightarrow K^- e^+ \nu_e$	123 μ m
B^+	$B^+ \rightarrow \bar{D}^0 e^+ \nu_e$	491 μ m
B^0	$B^0 \rightarrow D^- e^+ \nu_e$	457 μ m

A differentiating property of the D and B mesons is thus their long lifetime. However, the decay vertex is not accessible via the electron channel. A connected quantity, the impact parameter is explained in the next section.

2.3.2.2. The Impact Parameter

The subdetectors of ALICE reconstruct the tracks for most charged particles in the acceptance of the central barrel. For those points where there is no immediate measurement, knowledge

2. Analysis of Electrons from Heavy Flavor Hadron Decays

of the momentum and magnetic field allow estimation of the path. For particles produced at or very close to the primary vertex, the reconstruction should yield a track which crosses the primary vertex within the accuracy of the detectors. For particles produced away from the primary vertex, the reconstructed track will usually not be compatible with crossing the collision point. If the detectors have a greater accuracy, particles produced closer to the primary vertex still be have a track inconsistent with production at the primary vertex. The impact parameter gives a measure for this inconsistency. The impact parameter is defined as the distance of closest approach of a particle's reconstructed track to the primary vertex. For the present analysis, it is calculated only in the plane perpendicular to the beam axis. Figure 2.3.2 shows the definition a bit more clearly: For each particle a coordinate system is constructed with the y-axis parallel to the momentum of the particle. The x-axis is perpendicular. The impact parameter is the difference between the y-coordinate of the particle path and the primary vertex. Thus, the impact parameter can be positive or negative, depending on whether the particle passes the primary vertex on the left or right side.

Figure 2.3.2 shows an example of the impact parameter for a charged particle decaying at a finite (wrt. resolution) distance from the primary vertex. The direction of the particle is determined by the momentum of the mother particle and the angle of the decay wrt. the direction of the mother particle in its center of mass system. Its path is also influenced by the magnetic field within the detector. If a line is imagined along the flight path of the mother particle, this can be used to show the dependence of the impact parameter distribution on charge. For every thinkable decay, there is also possible the decay mirrored on this line with all particles exchanged for their antiparticles. In this case however, the impact parameter will switch its sign. Thus, the distribution of the impact parameter for any source, particle or combination of particles is the mirrored version of that distribution for the antiparticles. For this reason, in the present analysis, instead of the impact parameter itself, often the impact parameter multiplied by the charge of the particle is used. This way all particles from a certain source follow the same distribution.

In general, the angle between mother particle and decay product will depend on the mass of the mother and its momentum. For a higher mass and lower momentum, the decay product will have a larger angle to the mother and therefore a larger impact parameter. This will be examined for some important contributions in the next section.

A related quantity is the so-called impact parameter significance, where for each track the measured impact parameter is divided by the error on the measurement of this impact parameter.

2.3.2.3. Contributing Processes

The sample of electron candidates after the PID described previously contains particles from several contributing sources. The ones of primary interest are the electrons from the decays of charm and beauty hadrons. Apart from this, there is some contamination by non-electrons in addition to the electrons from other sources. As previously mentioned, the background comes mainly from the decays of light mesons, which either decay into electrons directly via a three-body Dalitz decay or decay into photons, which are converted into electrons via pair-production in the detector material. For the distinction of background and signal using the

2. Analysis of Electrons from Heavy Flavor Hadron Decays

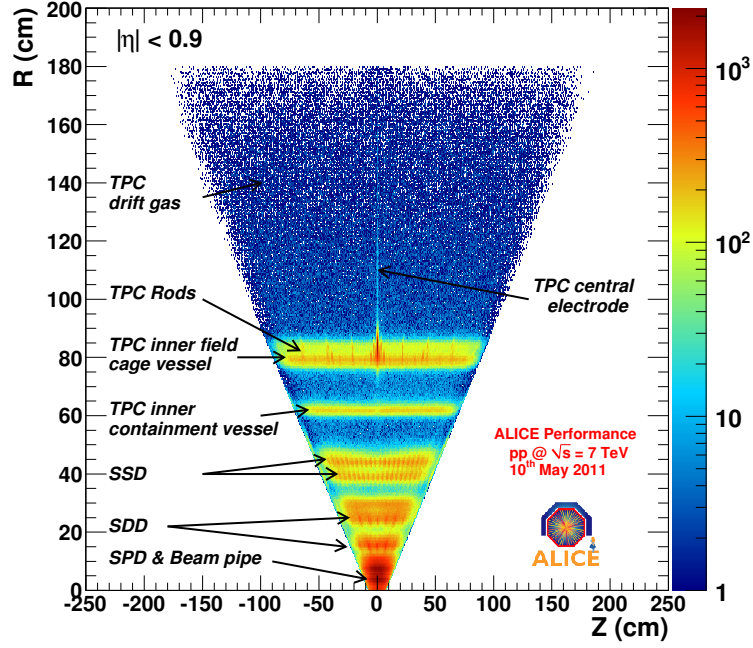


Figure 2.3.3.: Production points of Conversion electrons at different radii within the ALICE detector.

impact parameter information, the main interest is in the impact parameter distribution of these sources. The light mesons decay almost instantly and have no measurable flight path. Thus, the impact parameter distribution may be separated into five main contributions:

- Electrons from beauty hadron decays
- Electrons from charm hadron decays
- Electrons from the primary vertex
- Electrons from photon conversion in the detector material
- non-electronic background particles, mostly from the primary vertex

The measured impact parameter distribution for particles from the primary vertex is determined mainly by the resolution of the detectors. It is important to note that the resulting distribution is not Gaussian. These electrons are mainly from Dalitz decays in the considered momentum range and will in this context often be referred to as *Dalitz electrons*.

Electrons from photon conversion have zero angle between the momentum of the mother particle and the electron-positron pair. The impact parameter is determined mainly by the influence of the magnetic field. A simple calculation gives the connection:

$$\langle d_0 \rangle = \sqrt{\frac{p_t^2}{q^2 B^2} + R^2} - \frac{p_t}{|q| B} \approx \frac{R^2 B |q|}{2p_t} \quad (2.3.2)$$

2. Analysis of Electrons from Heavy Flavor Hadron Decays

where $\langle d_0 \rangle$ is the expected value of the impact parameter, p_t is the transverse momentum, B is the magnetic field and R is the radius of the production vertex. For a field of 0.5T, a production vertex of $R = 4\text{cm}$ and an electrons momentum of $1\text{GeV}/c$ this yields an impact parameter of about $120\mu\text{m}$. The actual measured value is again smeared by the detector resolution. Figure 2.3.3 shows the different production points of conversion photons in the detector. To limit the effective radiation length in the measurement, a hit in the centermost layer of the ITS was required as in the measurement of inclusive electrons. This gives a similar yield of electrons from photon conversion and from the primary vertex.

Electrons from beauty and charm hadron decays can decay into directions other than the flight path of the mother particle. For heavier particles, this angle can be larger. At a fixed momentum however, $\beta\gamma c\tau$, the average decay radius will be smaller for particles with higher mass. These effects compete. The main effect for differences in measured impact parameter is still the lifetime of the mother particle $c\tau$. Neglecting the influence of the magnetic field, the following approximation yields a typical impact parameter for particles from heavy meson decays[21]:

$$\langle d_0 \rangle = \frac{c\tau}{\sqrt{1 + \left(\frac{m_{B/D}}{p_{B/D}}\right)^2}} \quad (2.3.3)$$

where $m_{B/D}$ and $p_{B/D}$ are mass and momentum of the mother particle. For the purpose of the estimation $\eta = 0$ and therefore $p = p_t$ was assumed. Particles with larger mass thus have a smaller impact parameter all other properties being equal. For the measured momentum ranges, the electrons from beauty hadron decays will still have a larger average impact parameter than those from other sources due to the long lifetime of the B mesons. For a B^+ at $p = 3\text{GeV}/c$ the above formula yields a typical impact parameter of about $252\mu\text{m}$. The shapes of the distribution are very different: For the background electrons, the impact parameter is the expected impact parameter convoluted with the resolution. For the beauty and charm hadrons additionally the production vertex is exponentially distributed. Very large impact parameters will almost exclusively be due to the decay of beauty and charm hadrons.

These simple approximations are not sufficient to give the required accuracy for the measurement. Therefore a better estimate for the actual distributions is necessary. This is a prerequisite for selecting a measurement strategy.

2.3.2.4. Modeling the IP Shapes

The shapes of the impact parameter distributions in a p_t bin depend on the decay vertex, the decay kinematics, the magnetic field and the detector resolution. To a lesser extent there is also a dependence on the spectrum of the mother particle. The latter dependence is small for a small change in the spectrum. The mentioned effects are difficult to include in a purely analytical calculation. The measurement strategy presented here is thus based on the shapes of impact parameter distributions provided by Monte Carlo simulations of the detector. These contain all effects mentioned previously. For the modeling a good reproduction of the measured impact parameter shapes is crucial. For the TPC signal distribution, the Monte Carlo result did not yield a compatible result, so this assumption requires some explanation.

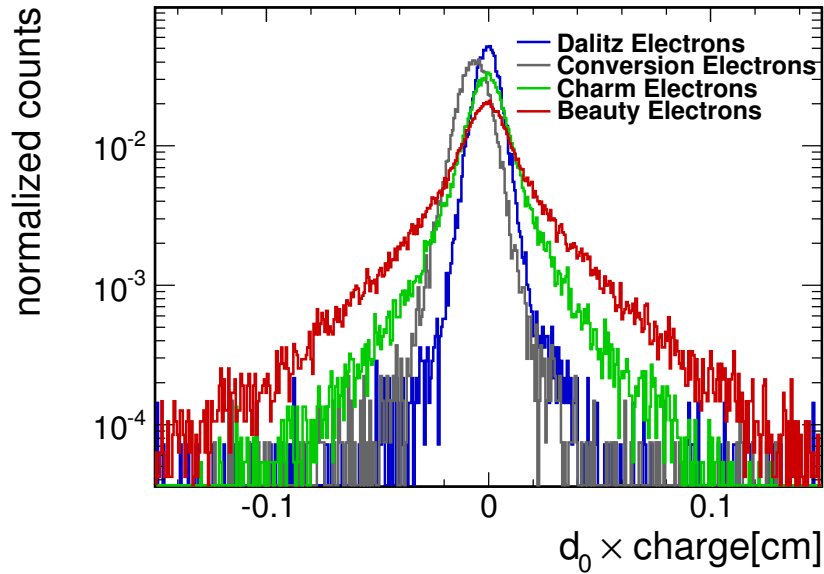


Figure 2.3.4.: Distribution of the Impact Parameter for Different Sources at $1.3\text{GeV}/c < p_t < 2.5\text{GeV}/c$ according to Monte Carlo.

The main ingredients for the decay vertex is the application of the exponential decay law, the input of the correct decay length, and the calculation of the factor $\beta\gamma$ requiring the correct mass. The calculation of the actual impact parameter requires also the inclusion of the magnetic field using the Lorentz force. All of these are well-understood phenomena, which can be easily calculated. The main difficulties lie in the description of the detector resolution and the resulting smearing of the distribution. Using the impact parameter itself instead of the impact parameter significance reduces this dependence somewhat as the heavy flavor electrons impact parameter is less sensitive to these. Figure 2.3.4 shows the normalized distributions of the impact parameter for the four electron sources.

2.3.3. A Beauty Hadron Decay Electron Measurement Strategy

Having identified the impact parameter as a distinguishing quantity for the source of the electron it remains to choose a strategy of using this information to find the spectrum for electrons from heavy flavor decays.

A strategy close in spirit to the method of finding the inclusive heavy flavor electrons through subtraction of a cocktail of background electrons is the *impact parameter cut method*[17]. Like for the inclusive electrons, the background contributions are subtracted. The electrons from the D decays are calculated using a measurement of the hadronic decays of D mesons. The measured particles are decayed in Monte Carlo to get D electron spectrum. As the name implies, the distribution is cut by requiring a minimal impact parameter. This

2. Analysis of Electrons from Heavy Flavor Hadron Decays

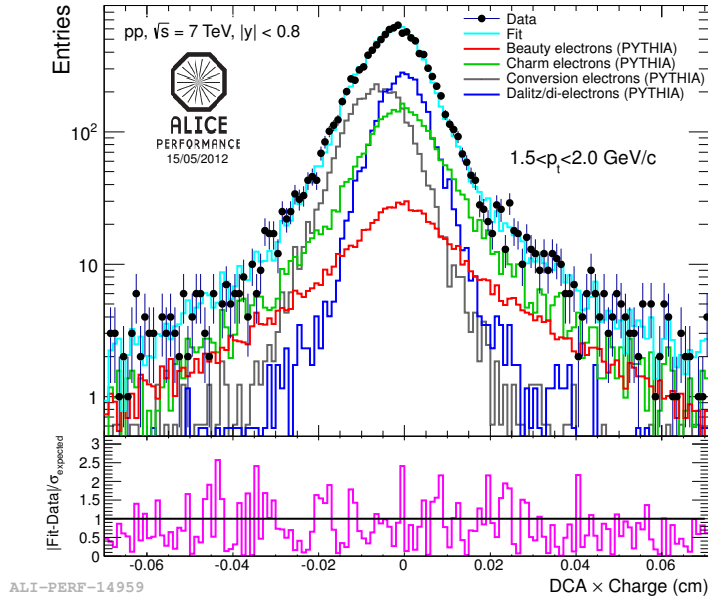


Figure 2.3.5.: Example of a fit using the modified χ^2 method. The relative error takes fluctuations in the templates into account in addition to those from data.

removes most of the background electrons and preferentially selects electrons from beauty hadron decays to such from charm hadrons. This greatly increases the signal to reduce the statistical and systematic errors due to the estimation of the background.

A more direct method and the one which will be developed in more detail in this thesis is the *impact parameter fit method*. This method aims at decomposing the total impact parameter distribution into the different components by constructing the same distribution as a sum of the individual impact parameter distributions of the different sources. This decomposition is done via a fit using the distributions provided by Monte Carlo simulations as templates.

Data set, event and track selection are for the most part identical to those described in section 2.1.1. The mayor difference is the use of a larger pseudorapidity range $|\eta| < 0.8$. This became possible due to a new correction for the TPC signal removing an η -dependence of the same. The TPC+TOF analysis strategy was used over the whole momentum range.

2.3.4. Fits with Monte Carlo Templates

The use of binned templates from Monte Carlo simulations requires some care with the fitting. A simple evaluation of the histograms as a function like in the binned fits of the dE/dx distribution will not yield the required result. The correct treatment of the use of Monte Carlo templates will be the topic of the next sections.

2.3.4.1. A Modified χ^2 Method

The most important difference between fits with an analytical function and with Monte Carlo generated templates is the statistical fluctuations of the latter. If they are not created with infinite (or very large) statistics, the templates will show statistical variations around the expectation value for each bin. Thus even if the correct parameters are used, bins with a large number of entries will show large deviations from the data. This makes the estimation of a χ^2 or likelihood difficult and the extrema of these functions might change. It is thus necessary to switch to a measure of the fit quality which takes into account the fluctuations of the templates as well as of the original function.

One important property of these fits is that they are all the sum of scaled templates. Width and center of the fit functions are not free parameters. Thus the fit function might be written as follows (within one p_t bin):

$$\begin{aligned} f_{fit}(d_0, p_i) &= p_{Dalitz} N_{Dalitz}(d_0) + p_{Conv.} N_{Conversion}(d_0) \\ &\quad + p_D N_D(d_0) + p_B N_B(d_0) \\ &= \sum_{source} p_{source} N_{source}(d_0) \end{aligned} \quad (2.3.4)$$

where $N_i(d_0)$ is the number of entries in the impact parameter bin for one source and p_i is the corresponding fit parameter. Neglecting the non-electronic contamination there are 4 free parameters in this calculation. The distribution of the number of entries in one bin in each of the impact parameter bins of the templates is again Poissonian.

This allows for a modification of the χ^2 method in order to take this into account. The expected standard deviation within one bin is the quadratic sum of all contributions:

$$\sigma_{total}^2 = \sigma_{data}^2 + \sigma_{fits}^2 \quad (2.3.5)$$

The standard deviation from the distribution of one source is the standard deviation from the statistical fluctuation of the template scaled by the multiplicative factor:

$$\sigma_{fit,source} = \sigma_{template,source} \cdot p_{source} \quad (2.3.6)$$

Using the properties of the Poissonian distribution, this yields:

$$\begin{aligned} \sigma_{total}^2 &= \sigma_{data}^2 + \sum_{source} (\sigma_{template,source} \cdot p_{source})^2 \\ &= \langle N_{data} \rangle + \sum_{source} \langle N_{template,source} \rangle \cdot p_{source}^2 \end{aligned} \quad (2.3.7)$$

within each bin. The resulting measure is

$$\chi^2 = \sum_{bins} \frac{(N_{data}(bin) - f_{fit}(bin))^2}{\sigma_{total}^2(bin)} \quad (2.3.8)$$

2. Analysis of Electrons from Heavy Flavor Hadron Decays

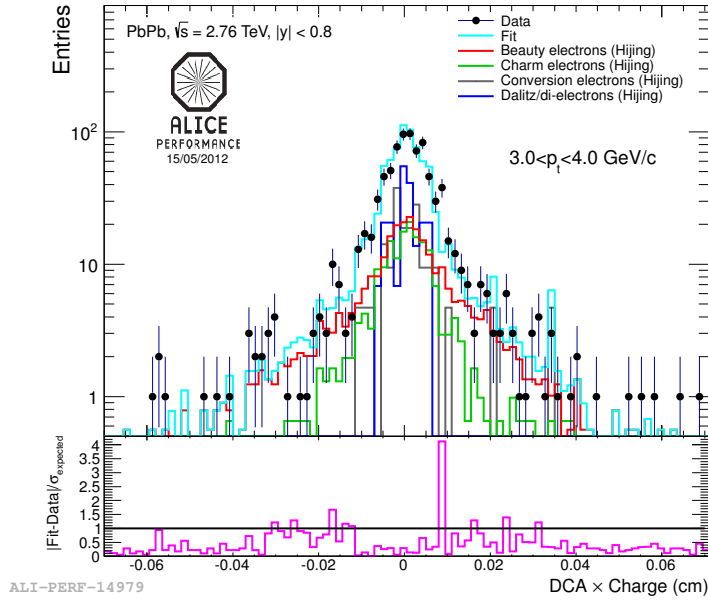


Figure 2.3.6.: Example of fit for peripheral (60-80%) Pb-Pb collisions.

If this modified χ^2 is minimized then also the fluctuations of the templates are taken into account. An example of a resulting fit is shown in figure 2.3.5. As mentioned in section 2.2.3.1 this approach creates some challenges in particular if the statistics within the bins are low. Most importantly, within each bin the assumption is made that $\sigma = \sqrt{\langle N \rangle} \approx \sqrt{N}$, which for bins with few entries gives large fluctuations in the expected standard deviation. To alleviate this problem somewhat, a minimal standard deviation was chosen as $\sigma^2 \geq 7$ for pp collisions. Challenges arising from the low statistics and from the use of a minimal standard deviation will be discussed in more detail in sections 2.3.4.3 and 2.3.4.5.

2.3.4.2. Likelihood Method

One major drawback of using χ^2 as a measure of the correspondence between fit and data is the use of a Gaussian distribution for the modeling of the fluctuations even if it is scaled to the same width as the corresponding Poissonian. A second problem is the assumption that $N \approx \langle N \rangle$ in each bin. A nice remedy would be the inclusion of the template fluctuations in a likelihood method as for the binned fits with analytical functions. Within the ROOT framework such a method has been implemented [10]. The correct application of this method is currently being investigated.

2.3.4.3. Information Content of the Diagrams

Figure 2.3.6 shows an example of a fit for peripheral Pb-Pb. The large fluctuations in both data and MC compared to small fluctuations in data only for the fit of the TPC signal show that this measurement is much more strongly constrained by the available amount of

2. Analysis of Electrons from Heavy Flavor Hadron Decays

statistics. This requires not only a very good understanding of the statistical errors involved but also makes important an understanding of how the maximal amount of information might be retrieved from the data.

As an example, a single bin of one distribution with content N gives an estimation for the expectation value of N with a width of $\sqrt{\langle N \rangle}$ (Poissonian statistics). If the same bin contains also content from another distribution M with known expectation μ_M , then the total number of counts is $N + M$. The guess for the average number of signal particles is $N + M - \mu_m$. The statistical error (assuming high statistics for Gaussian error propagation) is then $\sigma \approx \sqrt{\mu_N + \mu_M}$ which severely decreases the amount of information which can be retrieved from this bin, particularly if the background is large.

The information of the diagrams is not just in the bin counts themselves but also in the shape of the distributions. From the physical properties of the impact parameter, the distribution should drop monotonously from the maximum towards higher or lower impact parameters. More simply put: If all bins within a certain range contain a similar number of contents and one contains significantly less, this will be most likely the result of a downward fluctuation. Bins at a similar point on the impact parameter axis should have a similar expectation value. The fit methods introduced above do not take this into account. If all bins were scrambled and put into a different order, the fit result would not be affected. For the calculation of the likelihood or χ^2 , only the bin and the content of the templates is considered at each point with no regard for the neighboring bins. Thus, this information about the shape of the distribution is lost. For want of analytical templates for the distributions there are two main possibilities of keeping this information: Rebinning and the application of a smoothing algorithm.

The application of a smoothing algorithm connects neighboring bins. There are several ways to smooth diagrams. Most involve some weighted averaging over local bins. An example of this is the convolution with a Gaussian distribution. Smoothing algorithms do however pose some additional problems which are difficult to address:

- If the smoothing algorithm does not assume a shape of the resulting function beforehand, it might change the shape. A convolution with a Gaussian for example will remove all details of the original shape which are smaller than the width of the Gaussian. This is especially problematic for distributions with sharp peaks and low statistics, where strong smoothing would be necessary but would also smooth out the peak.
- Smoothing as a weighted averaging of several local bins decreases the fluctuations in this region. This change is difficult to correctly include in the calculation of the χ^2 . For samples with larger statistics this is usually less of a problem as the template after smoothing can be treated like an analytical function.

The second main way to use the information of the neighboring bins is to simply add them up. By using a larger bin size, the information of neighboring bins is used in a very direct manner. Thus bigger bins keep more information about the shape in environments with a small gradient.

A second source of information loss is the use of a minimal σ . This means that for the calculation of the χ^2 a bin where the minimal variance is applied is considered at a smaller

2. Analysis of Electrons from Heavy Flavor Hadron Decays

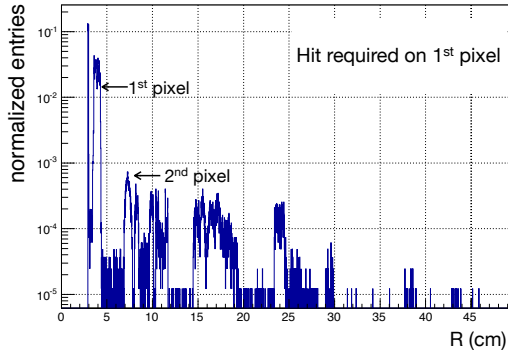


Figure 2.3.7.: Conversion Electron Production Radii with First Pixel Requirement[24].

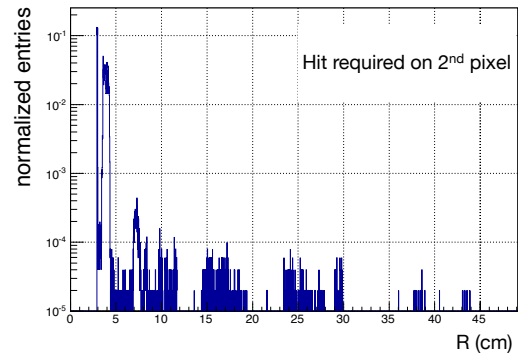


Figure 2.3.8.: Conversion Electron Production Radii with First and Second Pixel Requirement[24].

weight. If we split the sum 2.3.8 into one part where the minimal σ is used and one with sufficient bin counts per bin to avoid this, then the contribution from the latter part is the same as before, while the contribution from the low statistics part is smaller. Thus the part with more statistics will be most important for the fit with the other part giving less additional information than it would with exact knowledge of σ for each bin.

For lower statistics in data and the Monte Carlo samples, the minimal variance will apply to a larger part of the fit range. To get a good overall fit, a sufficient range of the fit is required where the minimal variance does not come into effect. Thus, for samples with lower statistics, a lower minimal variance might have to be used in order to obtain sufficient information from the sample.

2.3.4.4. Issues with the Conversion Electrons

Of the electrons which do not come from heavy flavor decays, the conversion electrons have the widest impact parameter distribution. As explained before, the average impact parameter of conversion electrons depends approximately quadratically on the production radius and is smeared out around that point. The production takes place in the detector material, mainly in the beam pipe and the layers of the Inner Tracking System (see figure 2.3.3). To make the method as sensitive as possible, it is important to keep the different distributions as distinct as possible. For the conversion electrons this means removing as many of the particles produced far from the primary vertex as possible. For a detector with perfect tracking this could be achieved by requiring a signal on the first pixel. In this case, only those conversion electrons appear, which were produced in the beam pipe and within the first ITS layer itself. For a finite tracking resolution however, some conversion electrons produced in the more peripheral layers will be connected to independent hits in the first layer. These misidentified tracks from production in the first layer will have a much higher average impact parameter. For high multiplicities tracks from even further out may be included within the cut. This causes some background for the measurement which decreases the sensitivity of the measurement

- even if it is correctly reproduced by Monte Carlo for the templates. Figure 2.3.8 shows the production vertices of electrons from electron conversions with the requirement of a hit in the first pixel. To decrease the number of particles from production vertices further out, additionally a hit on the second pixel was required for the analysis. The resulting distribution can be seen in figure 2.3.8. This decreases the amount of electrons from conversions outside the first pixel significantly.

2.3.4.5. Error Estimation

For a fit method like the one presented, the sources of errors are manifold. In particular a careful treatment of the statistical errors is important as these are especially large for large contributions from other sources to the impact parameter distribution. In particular for the comparison with theoretical predictions systematic errors are important, especially if there are many bins in p_t for the spectrum as they are not independent of the other bins and cannot be decreased by averaging or fitting.

An important source of errors is the use of the modified χ^2 -method for fitting. The reason for this is mainly the use of approximations for the calculations, which are at the edge of their validity at the available statistics in data. Important points to consider are:

- The approximation of a Gaussian distribution shape when the shape should be Poissonian within any χ^2 - based method in general
- The approximation of the variance by $\sigma^2 = \langle N \rangle \approx N$, which is only true in the limit of infinite statistics
- The lower limit on the variance introduced in 2.3.4.1

In particular for the systematic errors the errors from misrepresentation of the impact parameter distributions by Monte Carlo are important.

Error Sources When the variance within a bin is estimated by $\sigma^2 \approx N$ this creates a bias for the fit. The contribution to the total χ^2 from each bin is

$$\frac{(N_{data} - f_{fit})^2}{\sigma_{total}^2} \quad (2.3.9)$$

Under the assumption of infinite statistics for the templates this means that bins with a downward fluctuation for the data are given a larger weight (smaller expected σ) than bins with an upward fluctuation. This will give the fit a bias towards lower amplitudes (figure 2.3.9). Similarly, fluctuations in the templates will yield a variance, which is lower than the one from the hypothetical mean of the bin contents in infinite similarly created samples. Thus, for low bins, some bias is created by the assumption $\langle N \rangle \approx N$. Additionally it is not clear, what the expected variance for a bin with zero counts should be. For this reason, a minimal variance was introduced.

The introduction of a minimal variance is again a source of errors. For the systematics, putting the same weight on bins of different expectation value creates several types of biases.

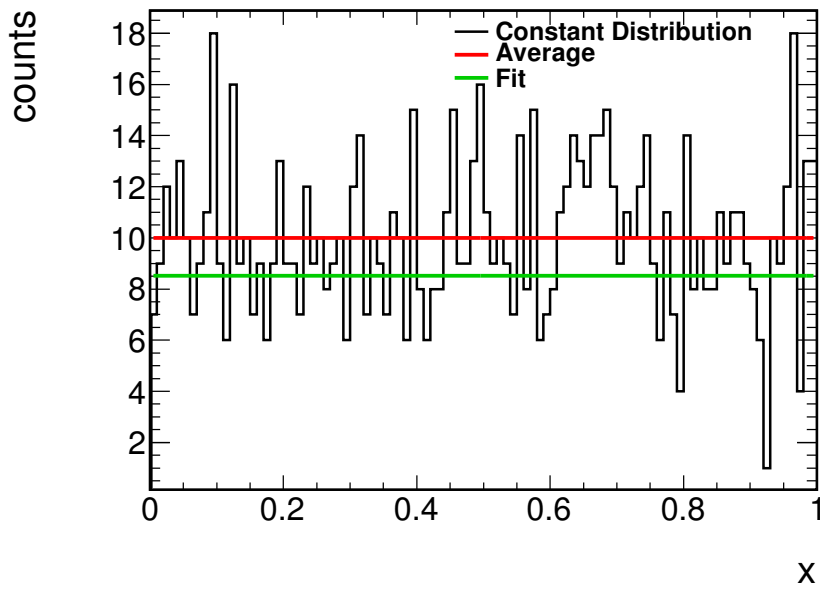


Figure 2.3.9.: Bias through the approximation $\sigma^2 = \langle N \rangle \approx N$. A flat distribution is fitted. The expectation value for the counts in each bin is given by the red line. The χ^2 method estimates a lower σ for bins with less entries and thus gives them a higher weight even though the expectation value for each bin is equal. The resulting fit is quite a bit below the average.

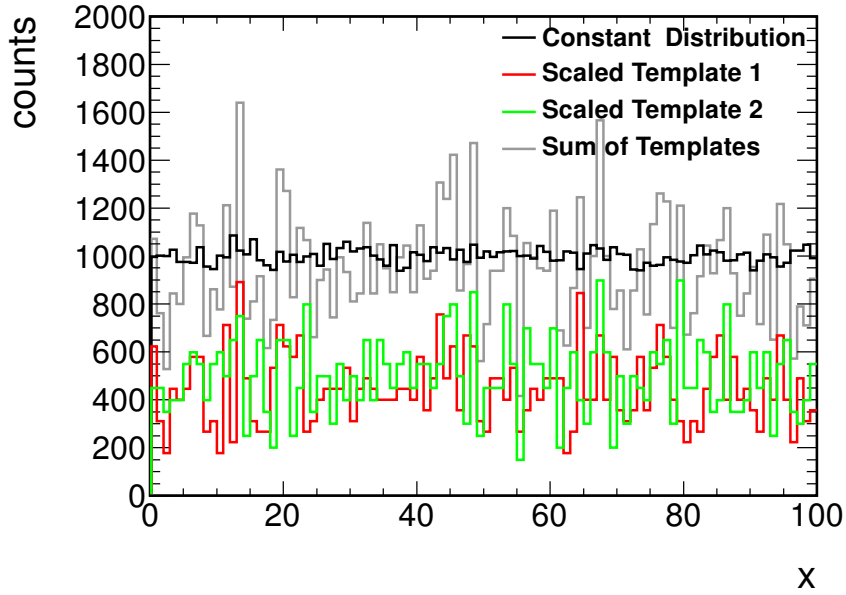


Figure 2.3.10.: Equalizing of the contributions for a fixed expected variance. All distributions are produced from constant distributions. The templates have equal, low statistics. Although there is no unique analytical solution for adding two numbers to a third one, the fit will usually find a minimum at a point where both prefactors are similar, to decrease the total variance of the resulting function. If the expected variance is set to $\sigma_{source} = \sqrt{\langle N_{source} \rangle}$, then this problem disappears. In this example, the data distribution has high statistics compared to the fit templates. The templates are scaled to the contributions they give for the final fit.

2. Analysis of Electrons from Heavy Flavor Hadron Decays

One that is easy to calculate is the averaging of the fluctuations. For a fixed expected variance, the total χ^2 is calculated as:

$$\chi^2 \sim \sum_{bins} (N_{data}(bin) - f_{fit}(bin))^2 \quad (2.3.10)$$

When the contributions are added, the resulting contribution has a standard deviation, which is the quadratic sum of the variances from the contributing functions. However, all contributions are scaled by the fit prefactor:

$$\sigma_{total}^2 = \sigma_{data}^2 + \sum_{source} (\sigma_{template,source} \cdot p_{source})^2 \quad (2.3.11)$$

For a large amount of data, σ_{data} is negligible as the prefactors are large. For the variance, the prefactors appear quadratically. For the fit function:

$$f = \sum_{source} p_{source} \cdot N_{source} \quad (2.3.12)$$

they appear only linearly. Thus, if all sources have equal statistics, there will be a bias towards keeping the contributions from them equal, to decrease the total fluctuations from the final fit. If one source has more statistics over the range, its prefactor will be biased towards higher values to keep σ_{total} small. An example of this behavior can be found in figure 2.3.10. The effect is obvious for high data statistics, but it should appear in a similar form if they are lower.

As mentioned in 2.3.4.3, the introduction of a minimal variance decreases the effective fit range, as the bins where the minimal variance comes into effect have a lower weight. A decreased effective fit range will increase the statistical error, thus the use of a minimal expected variance gives rise to both systematic errors as well as increasing the statistical ones.

The majority of the errors from the understanding of the detectors is very similar to those of the cocktail subtraction method for finding the inclusive spectrum of heavy flavor electrons. The main difference is the dependence on the measurement of the impact parameter. In particular it is important, how well Monte Carlo and the measured distributions of the impact parameter match. If the fit functions are very similar, then even a small change in the function can have a strong impact on the final result of the measurement. To find such problems there are two viable approaches: Efforts to directly measure the differences and checks for consistency of the final result with a correct representation by Monte Carlo.

Some methods for the analysis of these error sources will be presented in the next paragraphs.

Treatment of Statistical Errors For most fitting applications, the statistical variation of the fit parameters is calculated using the second derivative of the likelihood estimator. This approach makes use of the CRAMÉR-RAO Inequality to connect the variance of the estimator with the Fisher information. In this way the width of the minimum of the likelihood

2. Analysis of Electrons from Heavy Flavor Hadron Decays

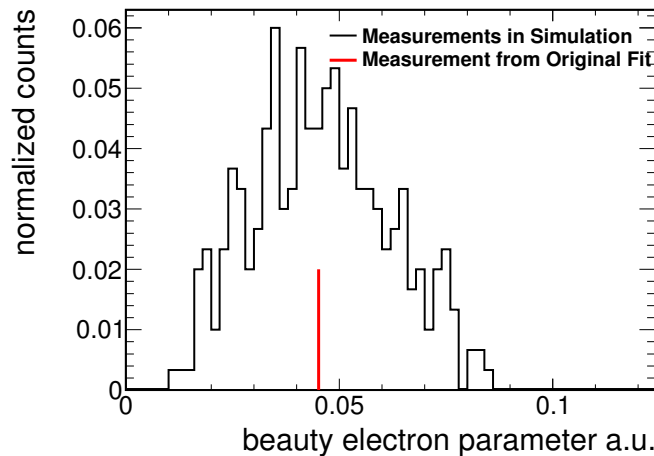


Figure 2.3.11.: Distribution of the fit parameter for 300 tests with a toy model. The red line shows the measured parameter. The width of this distribution estimates the statistical error of the fit while the offset of the mean gives an approximation for the part of the systematic error which is caused by the bias of the fit method.

measure gives the variance of the connected parameters. In its simplest form this approach assumes an unbiased measurement.

Due to the fact that for low statistics the χ^2 method is not unbiased, some more reliable method has to be used to estimate the statistical errors, preferably one which can also be used to estimate the systematic errors from the fit method. One simple way to get the statistical errors would be to perform the same measurement several times and look at the variation of the results. Obviously it is not feasible to split the sample into many for this purpose as this would increase the statistical errors greatly.

A useful alternative is the use of a toy model in order to simulate the important properties of the process. If the distributions were known perfectly as well as the correct fit parameters, the process would be very simple: The distributions are added with the correct prefactors to get the same ratios as in data. The resulting distribution can then be sampled to create a sample of the same size as the one used from the actual measurement. In the same way samples are created from the individual distributions to simulate the templates from Monte Carlo simulations. The fit of these templates to the data gives a certain value for the parameter of interest, although it will not usually be the same. If this process is repeated many times, creating new sampled (and thus independent) distributions each time, the result is a distribution of the measured parameter. This distribution yields the complete information about the statistical errors as well as the bias due to the fit.

In reality, neither the true ratios of the electrons from different sources are known, nor are the fit functions known. The only available data is a sampling of the distributions and the estimate for the true values from the fit. To get an approximation for the errors, the

2. Analysis of Electrons from Heavy Flavor Hadron Decays

results from the fit can be used instead of the unknown true values. For the distributions the direct use of the Monte Carlo templates poses some problems. The tails of the distributions have large relative fluctuations. This gives some correlation between the sampled data and the sampled fit distributions. To alleviate this problem a bit, instead the distribution over a larger p_t range can be used. In this case, the sampled distributions are more independent of each other and of the distribution in the fit. The disadvantage is the fact that the shape of the distributions changes with momentum. Thus, there will be some uncertainty to the error for larger bins. In the limit of infinite statistics for the Monte Carlo samples, only the distributions from one bin at the current momentum need to be used and the error estimation will be exact in the limit of infinite tries.

For an unbiased fit, the distribution of the fit parameter will have its center at the fit value of the original fit. The width of the distribution is the statistical error of the measurement. If the fit method produces a bias, the center will be shifted away from the input value for the parameter. In this case the difference of the mean of the fits with the simulated data and templates will give an approximation for the systematic error due to the bias from the fit method.

As explained in 2.3.4.3, a lower amount of statistics will increase both the statistical and systematic errors. For pp data the statistical error is typically of the order of 30% for the yield of electrons from beauty hadron decays. The statistical error depends on the statistics of the total sample, the statistics of each template and on the ratios of the number of particles from the different sources.

Treatment of Systematic Errors There are three main classes of systematic errors:

- Errors from detector and cut efficiencies
- Errors from bias due to the fit method
- Errors from a misrepresentation of the impact parameter distribution by Monte Carlo

The errors from the detector and cut efficiencies can be found using the methods developed for the cocktail method for the identification of the electrons from beauty hadron decays. An estimation for the systematic errors from the bias of the fit method is a byproduct of the analysis of the statistical errors as explained in the previous section.

The error from inaccuracies in the detector simulation remains to be determined. The calculation of the decay kinematics is reasonably simple. Thus this will not be a significant source of errors. The main difficulty lies in the correct estimation of the detector resolution. Figure 2.3.12 shows the resolution for data and Monte Carlo for all particles passing TPC quality requirements. There is a slight difference. This will particularly influence the distributions of conversion and Dalitz electrons as their shape is to a large part determined by the resolution of the detector. Although it is difficult to estimate the exact effect from this inaccuracy, due to the many possible changes in shape of the distributions, the difference in resolution is small overall and thus the main effect should lie in the relative amplitudes of the Dalitz and conversion electron contributions.

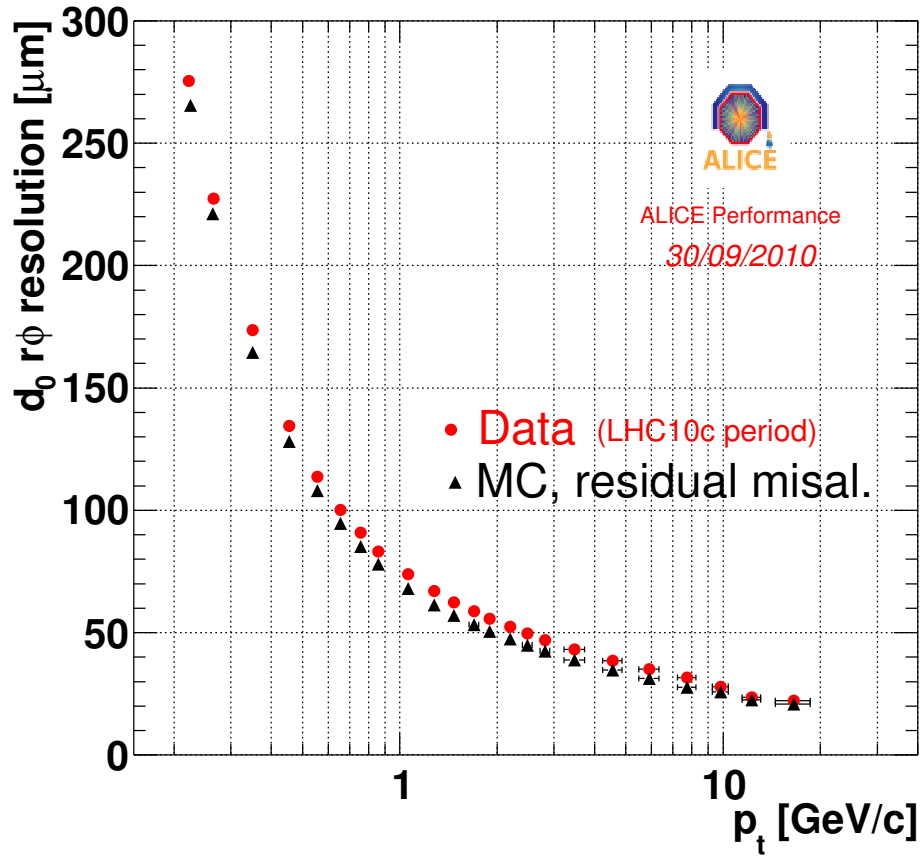


Figure 2.3.12.: The Impact Parameter Resolution of ALICE. The red line represents the resolution of the data, the black one gives the resolution from Monte Carlo.

2. Analysis of Electrons from Heavy Flavor Hadron Decays

Additionally, errors on the efficiency and acceptance corrections as well as theoretical uncertainties should be similar for the cocktail method and the impact parameter fit method as they influence the general electron distribution.

3. Results and Discussion

3.1. Results in pp

The estimation of the remaining contamination after the cut on the TPC signal is a prerequisite for the extraction of the transverse momentum spectrum of electrons from heavy flavor hadron decays using the cocktail method. The main interest in the spectrum from pp collisions in ALICE is the reference this provides for Pb-Pb collisions to get an insight into the properties of heavy ion collisions in general and the quark-gluon plasma especially. Nevertheless a spectrum from pp provides in itself also an important testing ground for the theory of quantum chromodynamics.

For the pp collisions at $\sqrt{s} = 7$ TeV with the measurement strategy discussed in the text, the remaining contamination of the electron candidates by non-electrons is less than 3% at $p_t = 8$ GeV (figure 3.1.1 shows the contamination for the TPC-TOF-TRD strategy). The amount is negligible compared to the systematic and statistical uncertainties from other effects. The modeling of the contamination with the approach described in this thesis strongly reduces the uncertainty from the contamination. For the resulting transverse momentum spectrum, the remaining contamination was included as part of the systematic error. Figure 3.1.2 shows the spectrum for electrons from beauty and charm hadron decays with the presented method together with a spectrum based on a TPC-EMCal measurement strategy[30]. The red points represent the measured data points from the strategy discussed in this study. Statistical and systematic uncertainties are given. Towards high momenta, the errors increase due to the decreased acceptance of the TPC-TRD-TOF setup compared to the TPC-TOF one. For low momenta, the influence of the cocktail increases (figure 2.1.1). This again increases the errors due to the subtraction of two numbers of similar size.

For the measurement of the individual contributions to the electron spectrum from beauty and charm hadron decays, the pp measurement also provides a testing ground for impact parameter fit method as several independent measurements exist to compare to. In principle, the fit method measures at the same time the influences of four different distributions. With sufficient statistics even additional contributions like the non-electronic contamination might be identified. This is the reason for the ample opportunity for comparison with independent measurements. Particularly interesting cases are:

- The measurement of all heavy flavor electrons using the cocktail method
- The measurement of electrons from beauty hadron decays using the impact parameter cut method

Figure 3.1.3 shows the comparison to the measurement of heavy flavor electrons using the cocktail method. The spectrum is obtained by simply adding the spectra for the charm and

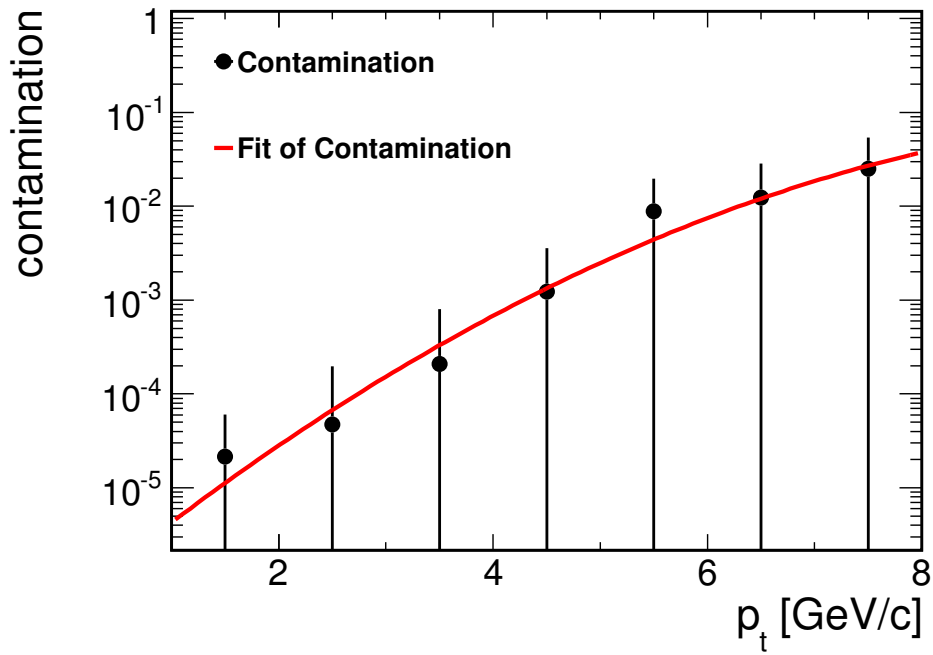


Figure 3.1.1.: Contamination from a TPC+TRD+TOF measurement strategy in the cocktail method. The error bars are expected Poissonian fluctuations of the number of contaminating particles.

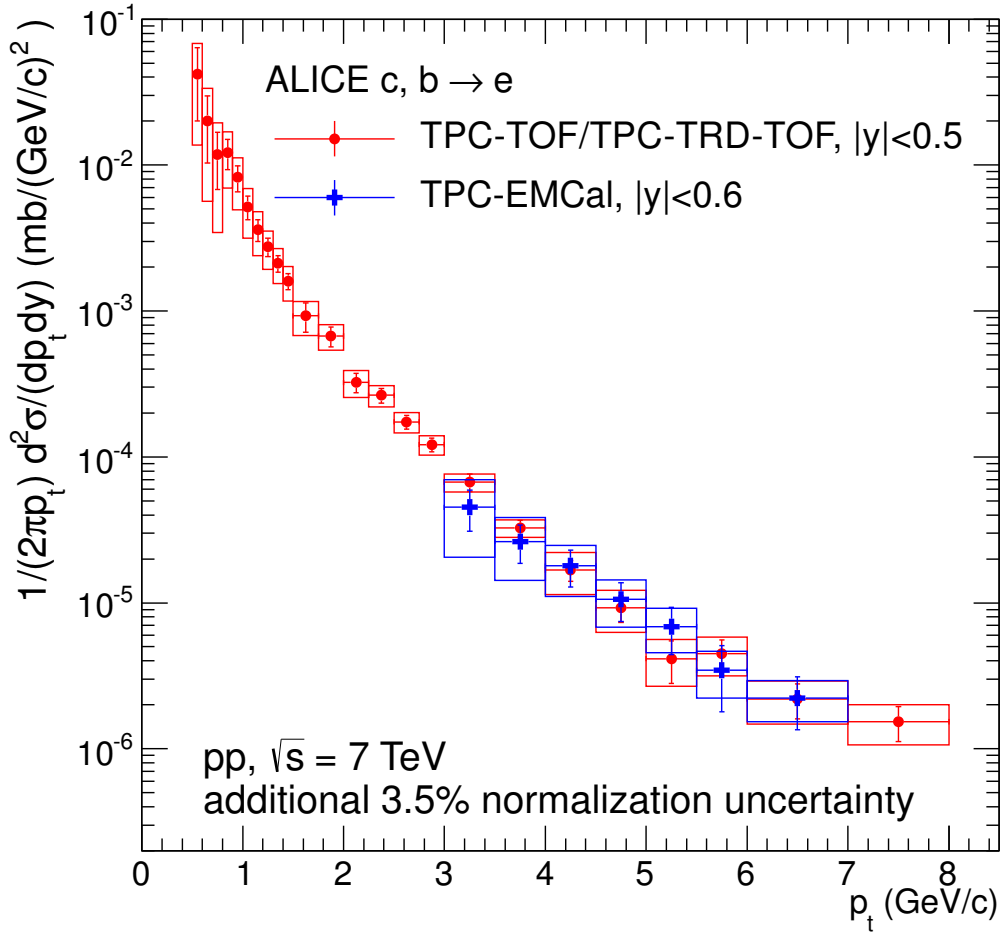


Figure 3.1.2.: The transverse momentum spectrum for electrons from the decay of charm and beauty hadrons using the cocktail method. Also shown are the results from the related method using the Electromagnetic Calorimeter (EMcal).[30]

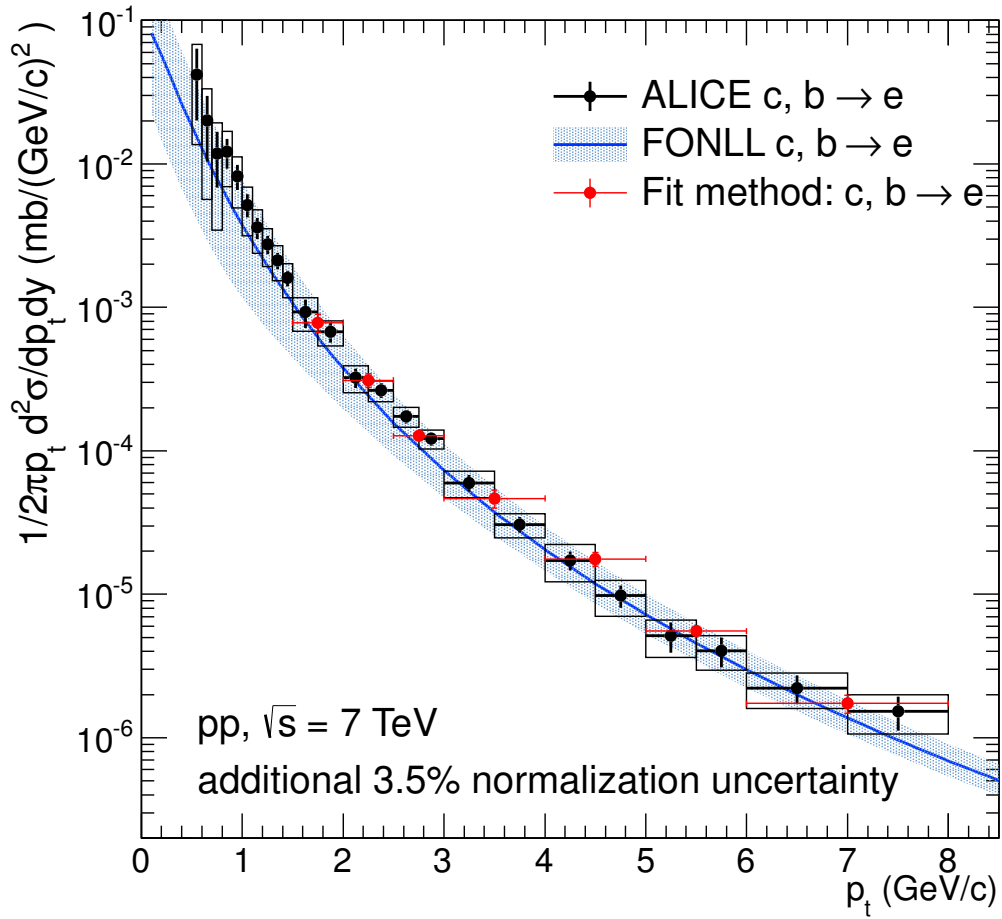


Figure 3.1.3.: Comparison of the heavy flavor electron spectrum in pp for the cocktail method and the impact parameter fit method. Both measurements agree within uncertainties with each other and with the theoretical predictions.

3. Results and Discussion

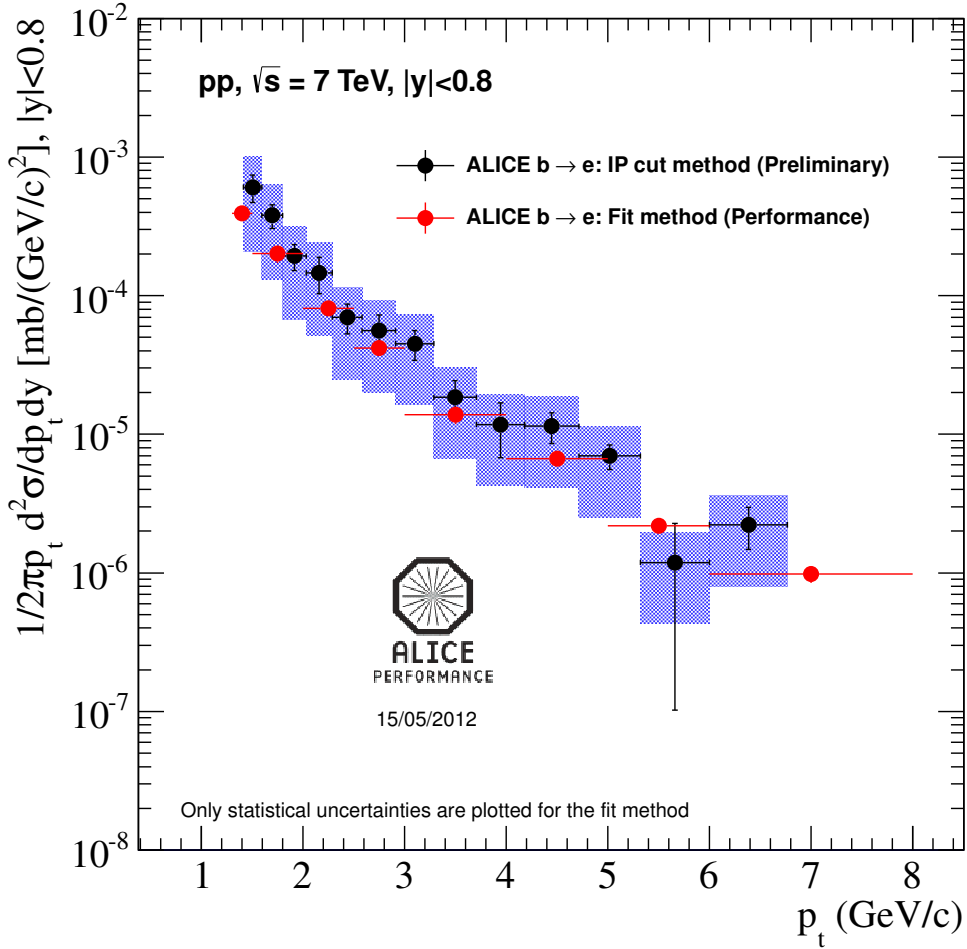


Figure 3.1.4.: Comparison of results from the impact parameter fit and cut methods. The systematic error bars from the fit and cut method should be similar.

beauty contributions obtained by the fit. Generally the p_t bin width for the fit method will be larger than for other methods because of the strong dependence of the errors on statistics. The plot shows the transverse momentum spectrum for the two measurements together with theoretical predictions based on FONLL calculations[14]. The measurements agree well with the theoretical prediction and with each other.

Figure 3.1.4 shows the comparison to the impact parameter cut method [17]. Apart from the systematic uncertainty of the D meson spectra used in the impact parameter cut method and the fit bias, the systematic uncertainties for both methods are similar. Again, the two methods show close agreement within the uncertainties.

The methods use very similar approaches to the PID and track selection. Thus they are applied to almost the same sample of electrons. It is important to stress however, that the cocktail method and the impact parameter cut method depend to a large degree on

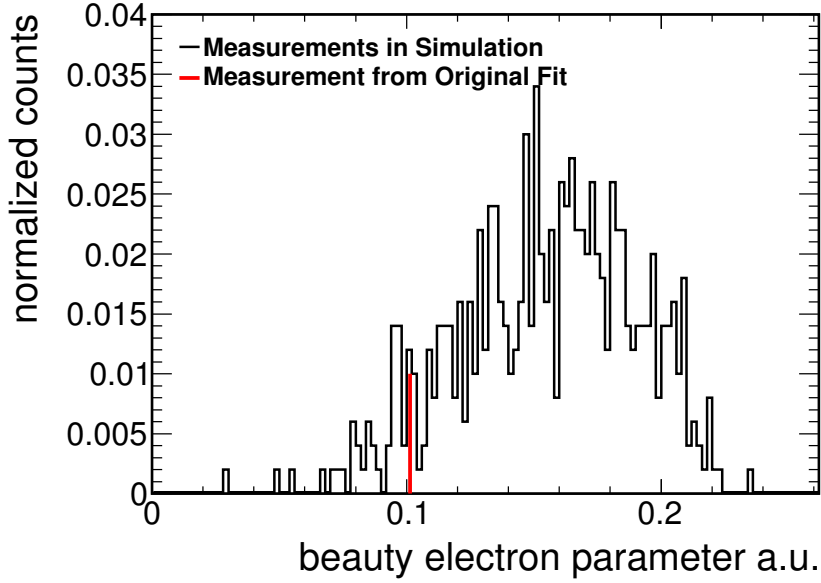


Figure 3.2.1.: Example for the estimated distribution of fit values for a fit at $3\text{GeV}/c < p_t < 4\text{GeV}/c$ in Pb-Pb with 500 simulations. The red line shows the measured value which is the starting point for the simulation. The centrality is 60-90%.

separately measured spectra (the π^0 measurements for the cocktail itself and the D meson measurements). The fact, that the impact parameter fit method is independent on such measurements means that the resulting spectra are to a large part independent. The close agreement between the methods thus provides a strong argument for the power of the impact parameter cut method developed within this thesis and justifies application also for the measurements in Pb-Pb collisions with this approach.

3.2. Results in Pb-Pb

In figure 3.2.1, the result from the error estimation (from section 2.3.4.5) for a high transverse momentum bin in Pb-Pb is shown. This graph estimates the distribution of the value for a fit parameter for a given true value. The width of the distribution estimates the statistical error, while the difference between the input value and the mean gives an estimation for the bias. The bias in bins at higher transverse momentum is of a size similar to the statistical error. This is due to the low amount of statistics analyzed for this study. For large uncertainties the error estimation will become more inaccurate.

An uncorrected spectrum based on this fit is shown in figure 3.2.2. This figure shows both the measured raw spectra for electrons from beauty and from charm hadrons decays with the impact parameter fit method. Although the spectra can be calculated with the method, it is obvious from the error analysis described above, that the data points at higher momenta

3. Results and Discussion

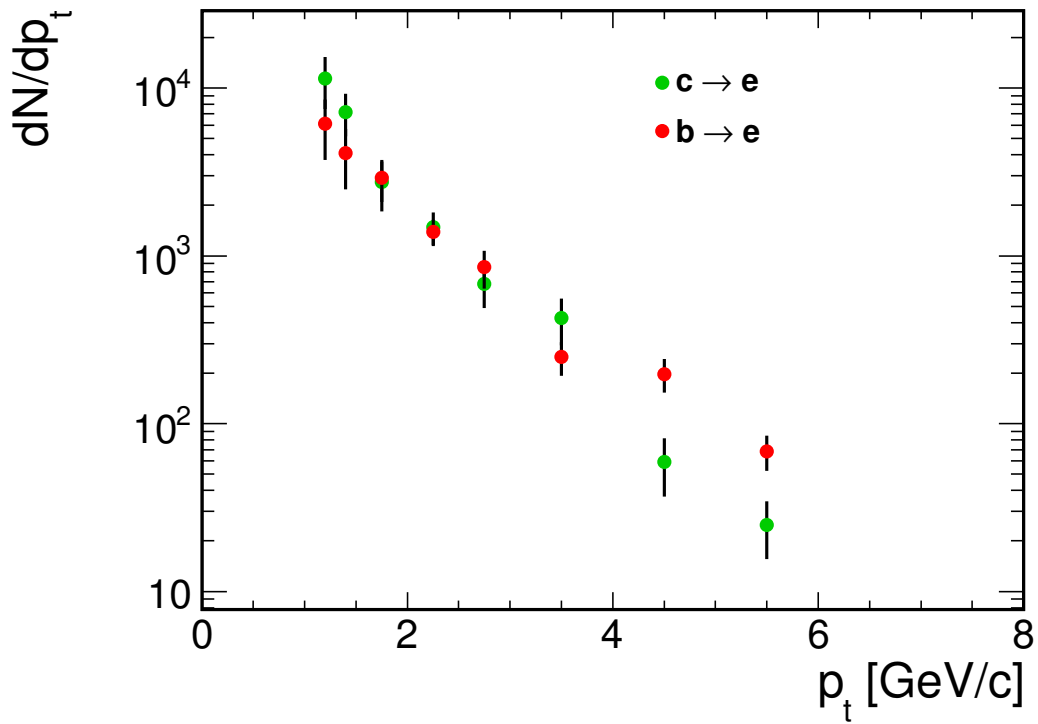


Figure 3.2.2.: Raw spectra for electrons from charm and beauty hadrons in Pb-Pb collisions with 60-90% centrality. Only statistical error bars are shown.

3. Results and Discussion

have additionally significant systematic errors which are difficult to estimate precisely without an increase in statistics. In addition, the sample of electron candidates in Pb-Pb contains a larger amount of non-electronic contamination. For a similar amount of statistics as for the pp case and with a similar amount of contamination, the measurements should work equally well.

Both problems can be solved with an increase in statistics: This decreases the statistical errors themselves. Additionally the fit bias is decreased and at the same time increased the strength of the approximation for the bias and statistical errors. For the measurement of a nuclear modification factor, the spectra in pp and Pb-Pb collisions are compared, the resulting uncertainties depend on both the uncertainties of the pp measurement and the one from Pb-Pb. Thus a low total value of the uncertainties and good approximation of both are important and will be enabled by a moderate increase in available statistics.

4. Summary and Outlook

4.1. Summary

In this thesis, two methods for the extraction of the transverse momentum spectra of electrons from the decays of beauty and charm hadrons were presented: The cocktail method for measuring the combined spectrum and the impact parameter fit method for measuring the individual contributions. For the cocktail method, a model for the distribution of the TPC signal was introduced, which was then applied to estimate the contamination of the electron candidates by non-electrons. For the measurement of the individual contributions from charm and beauty hadron decays, a method was introduced which is based on a fit of the impact parameter distributions.

The cocktail method is based on the subtraction of a cocktail representing background processes from an inclusive electron spectrum. This requires accurate knowledge of the contamination of the electron candidates identified by the particle identification strategy. For this purpose the modeling of the distribution of the TPC signal proved to be very powerful. It provided both the remaining contamination and remaining signal after a cut on the TPC signal. This is valuable to obtain a spectrum of high quality as it helps reduce the systematic uncertainty of the method from the estimation of the hadron contamination and the efficiency of the cut on the TPC signal. Different approaches for this purpose were discussed. The best estimation was reached by using a modified Landau distribution, which models the influence of a truncated mean cut on a cluster level by introducing a correction function. For the latter, a falling exponential function was derived as a simple approximation.

For the measurement of the individual electron contributions from charm and beauty hadron decays, the impact parameter was used as a differentiating quantity. The method presented here is based on a fit of the shapes of impact parameter distributions for different electron sources on the distribution of the impact parameter for all electron candidates. The shapes of the individual distributions were extracted from Monte Carlo simulations of the detector.

For the fit itself, a modified χ^2 -minimization method was used to take into account the statistical fluctuations from the templates as well as those from data. This method can produce a bias for small statistics in the used data or Monte Carlo samples making a thorough analysis of the statistical and systematic uncertainties necessary.

For the pp case, the available statistics produce systematic uncertainties which do not dominate the statistical uncertainty. The resulting spectrum for electrons from the decays of beauty hadrons agree well with those from the measurement based on the impact parameter cut method.

The fit supplies immediately also the transverse momentum spectra of the electrons from

4. Summary and Outlook

other sources. This allows also a comparison with other measurements. In particular, the spectrum for electrons from charm and beauty decays hadrons together agrees well with the one extracted via the cocktail method. The close agreement of the results from the different methods suggests applicability of the impact parameter cut method also for Pb-Pb measurements.

For Pb-Pb the currently available statistics for the Monte Carlo simulations are lower than for the pp case. This creates systematic errors of at least similar size than the statistical ones for the higher transverse momenta. The spectrum for the electrons from beauty hadron decays thus has systematic errors which are difficult to estimate with the currently available statistics. A raw spectrum was extracted with the same approach as for the pp case. However, the lower statistics make it difficult to obtain a good estimation for the systematic error.

4.2. Outlook

The main possible improvement of the measurement of the electrons from beauty hadron decays will come from an availability of more statistics in Monte Carlo for the Pb-Pb case. Currently additional data is being analyzed which will help greatly in this matter. To decrease the uncertainties even further, measurements from the second Pb-Pb collision run at $\sqrt{s_{NN}} = 2.76$ TeV in 2011 might provide even more statistics for the future. In this measurement period, parts of the TPC were used at a lower voltage, decreasing the separation of the signal distributions and thereby increasing the contamination. Thus, measurements here will require use of the impact parameter distribution from non-electrons as a fifth distribution. This distribution may be fitted with the same method, or fixed to the value provided by the contamination estimation introduced in this thesis.

Additional improvements can be made by using a model based on a Poissonian distribution for the fit. This might be done using the `TFractionFitter`[10] class of `root` or the `RooFit` framework.

To present a value for the nuclear modification factor small uncertainties for measurements in pp and Pb-Pb are important. Thus, a precise knowledge of the influence of a difference in impact parameter distributions from Monte Carlo and data is a prerequisite. Although the differences are small, it is difficult to calculate the propagation of this error to the fits with high precision. Efforts to estimate this effect will further increase the confidence in this method in the future.

To decrease the bias due to low statistics, a nonlinear type of binning can be applied for the impact parameter. This way, at points of a strong change of the distribution (e.g. close to the peak), a smaller binning might be used than for larger impact parameter values, where the increase in statistics per bin would increase the available information. This way, bias from low statistics might be decreased. It is however necessary to take care with this type of approach in order not to introduce a new type of bias.

With sufficiently low uncertainties on the transverse momentum spectra in pp and Pb-Pb, calculation of the nuclear modification factor with good accuracy will be the next step. This will enable the separation of the contributions from the beauty and charm quark energy loss in the quark-gluon plasma and also the comparison to the nuclear modification factor of

4. Summary and Outlook

pions.

When the fit in Pb-Pb performs sufficiently well, the method can immediately be applied to also measure the v_2 for the contributing sources. An estimate for this highly interesting quantity can be obtained by measuring separately the electrons within the reaction plane and perpendicular to it. This approach merely halves the statistics for the data electrons while the full Monte Carlo sample can still be used.

A. Notes on the Poisson Distribution

The Poisson distribution is by far the most important basic distribution for the purposes of this analysis. Thus, it deserves some more elaboration.

Mathematically, the Poisson distribution is an approximation of the binomial distribution. The binomial distribution results from performing n independent experiments with two possible outcomes. It describes the number of positive outcomes. The Poisson distribution is the approximation of this distribution in the limit of infinite trials with a fixed expectation value. The binomial distribution for n experiments with a probability for a positive outcome p and k total positive outcomes is

$$p(k) = \binom{n}{k} p^k (1-p)^{n-k} \quad (\text{A.0.1})$$

with $\lambda = p \cdot n$ the expectation value fixed, this can be approximated for $n \rightarrow \infty$ as

$$\begin{aligned} p(k) &= \frac{n!}{k!(n-k)!} p^k (1-p)^{n-k} &= \frac{n!}{k!(n-k)!} \left(\frac{\lambda}{n}\right)^k \left(1 - \frac{\lambda}{n}\right)^n \left(1 - \frac{\lambda}{n}\right)^{-k} \\ &= \frac{\lambda^k}{k!} \frac{n!}{(n-k)! n^k} \left(1 - \frac{\lambda}{n}\right)^n \left(1 - \frac{\lambda}{n}\right)^{-k} &= \frac{\lambda^k}{k!} \left(1 - \frac{\lambda}{n}\right)^n \frac{n(n-1)\dots(n-k+1)}{n^k} \left(1 - \frac{\lambda}{n}\right)^{-k} \\ &\approx \frac{\lambda^k}{k!} \cdot e^{-\lambda} \cdot 1 \cdot 1 &= \frac{e^{-\lambda} \lambda^k}{k!} \end{aligned} \quad (\text{A.0.2})$$

This is the Poisson distribution.

Assuming a fixed number of produced particles in total, each particle is produced according to the same laws. If the data is binned in some way, there is a certain probability, that a particle will fall into a certain bin according to the way the bins are defined. Usually, the probability for a particle to be in one particular bin is very small. Thus for several hypothetical repetitions of the experiment, the distribution of the number of counts in the bin are Poissonian. Accordingly, Poissonian fluctuations will appear in almost all cases, where the contents of a bin can be classified as integer “counts” of some sort.

A Poisson distribution is defined by a single parameter, λ . This parameter is equal to the distributions mean and also to its variance.

For fitting purposes, the calculation of the factorial is computationally too expensive. Additionally, often a shifted and/or stretched version might be useful. A simple way to solve these problems is to use Stirling’s approximation:

$$n! \sim \sqrt{2\pi n} \left(\frac{n}{e}\right)^n (1 + \mathcal{O}(n^{-1})) \quad (\text{A.0.3})$$

Thus

A. Notes on the Poisson Distribution

$$p(k) = \frac{e^{-\lambda} \lambda^k}{k!} \approx \exp\left(k - \lambda + k \log \frac{\lambda}{k} - \frac{1}{2} \log(2\pi k)\right) \quad (\text{A.0.4})$$

which after using $k \rightarrow (x-x_0)/\sigma$ gives a smooth approximation of a Poissonian serviceable for fitting, when $\lambda \gg 1$.

B. Centrality Selection

To gain an understanding about the influence of the medium on the electron spectrum the basic strategy of the measurement is the comparison of the spectra from pp collisions and from Pb-Pb collisions. The largest volume of produced medium and thus the strongest effect on the spectrum is expected for head-on collisions of the Pb nuclei. It is thus useful to do the comparison separately for different geometries of the collision. For this reason a measure of the centrality of the collision has to be used. A very useful measure for this purpose is the particle production: For the more central collisions of the nuclei, on average more individual nucleon-nucleon collisions will happen. This will produce a higher number of total particles. Thus the number of particles is highly correlated with the centrality of the collision. At ALICE, the number of particles is measured by the VZERO detectors. These are located close to the beam axis to measure the bulk of produced particles. According to the VZERO signal, the collisions can be grouped into different centrality classes (figure B.0.1).

B. Centrality Selection

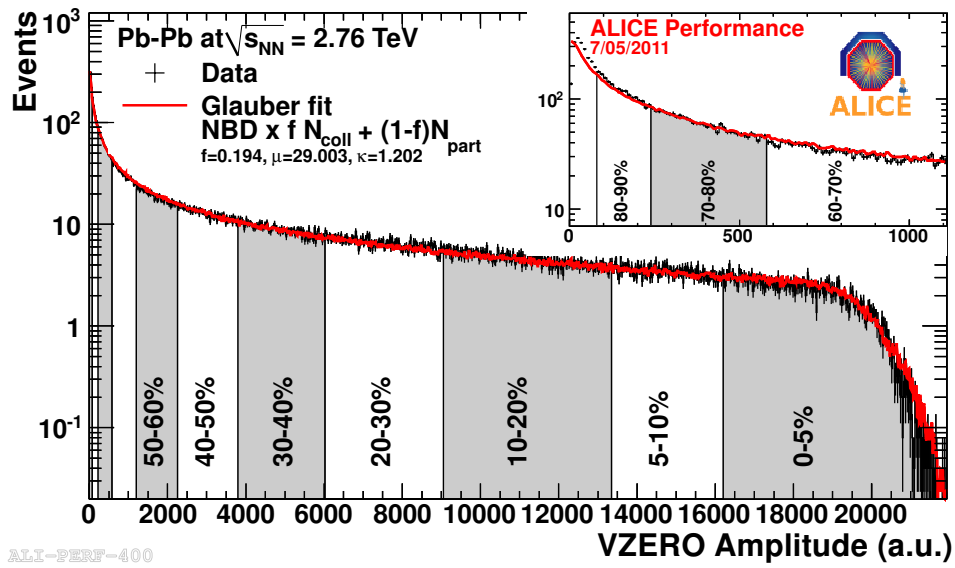


Figure B.0.1.: Distribution of the VZERO signal for Pb-Pb collisions at ALICE. The fit is done with a Glauber model, which estimates the number of binary collisions using an approximation of the nucleons as solid balls with a projected area according to their collision cross section and randomly distributed within the nucleus.

C. Glossary of Terms

In this short overview, some terms will be explained again to reduce the time spent looking for the first appearance in the text.

Beauty Hadron A hadron with a b quark as a valence quark.

Bias (of an estimator) The difference between the mean of the estimator and the true value of the estimated variable. The total error of a measurement thus has a statistical contribution (which can be reduced by repeating the experiment many times) and a contribution from the bias (which cannot be reduced without changing the estimator).

Charm Hadron A hadron with a c quark as a valence quark.

Cocktail Method A method for obtaining electrons from the decays of beauty and charm hadrons. It is based on the subtraction of a cocktail of electrons from background processes from the measured electron sample to obtain the transverse momentum spectrum.

Contamination If selection criteria have been applied to select preferentially one type of particle, the contamination is the amount of other types of particles remaining in the sample relative to the remaining number of signal particles.

Cut The application of selection criteria, disregarding particles with a signal which does not fulfill the selection criteria. The limiting signal strength itself is also sometimes called a cut.

Conversion Electron An electron from photon conversion in the detector material.

χ^2 -Method A fit method, which strives to minimize $\chi^2 = \sum_i (x_i - f_i)^2 / \sigma_i^2$, where x_i is the data point i , f_i is the corresponding model prediction and σ_i is the standard deviation assumed at this point. The method requires some model input for σ_i . It is closely connected with the maximum likelihood method.

Dalitz Electron In the context of the impact parameter distributions any electron produced at the primary vertex. Often these come from Dalitz decays of light mesons.

C. Glossary of Terms

Efficiency If selection criteria have been applied to select preferentially one type of particle, the contamination is the amount of signal particles remaining in the sample relative to the initial number of signal particles. Increasing the efficiency in some way often increases the contamination as well.

Gluon Transport Coefficient This is a commonly used quantity to quantify the medium in energy loss calculations for the quark-gluon-plasma. It can be interpreted as the average squared momentum transfer per unit path length between the fast parton and the medium.

Hidden Heavy Flavor Bound states of a heavy quark with its antiquark, e.g. J/ψ , Υ .

Impact Parameter The distance of closest approach of a particle to the primary vertex. It can be positive or negative depending on the position of the closest approach relative to the particle momentum and the magnetic field.

Impact Parameter Cut Method A method for preferentially selecting electron from beauty hadron decays via the requirement of a minimal impact parameter.

Impact Parameter Fit Method A method for separating different distributions to the electron spectrum via a fit of the impact parameter distribution.

ITS Inner Tracking System, a subdetector of ALICE. Being the closest detector to the beam pipe, this silicon detector measures the displacement of secondary vertices and tracks particles down to low p_t .

Jet Particles from a collision produced in high number with momenta within a small solid angle. Jet measurements are complementary to measurements of single particle spectra in the sense that they alleviate some calculational difficulties while posing new ones.

Likelihood Method An approach to fitting. It depends on a previously assumed probability distribution for the data vector for a given (fixed) set of model parameters. The fit value is the parameter set for which the probability of the data vector is maximal. This is often used in connection with a Poissonian probability distribution for binned fits. For a Gaussian pdf, this approach instead leads to the χ^2 method.

Open Heavy Flavor Mesons or baryons containing heavy valence quarks without the corresponding antiquarks, e.g. B and D mesons.

PID Particle IDentification. The preferential selection of particles of a certain type.

QCD Quantum ChromoDynamics. The theory of strong interactions.

C. Glossary of Terms

QGP Quark-Gluon Plasma. A state of hadronic matter characterized by the deconfinement of quarks.

Relative Error For a fit in the context of this analysis: The difference of the fit function in this bin to the data, relative to the standard deviation. The standard deviation is approximated by assuming Poissonian fluctuations of all measured bins.

TOF Time Of Flight detector, a subdetector of ALICE. It measures the velocity of particles, improving PID at low momenta.

TPC Time Projection Chamber, a Subdetector of ALICE. It measures the momentum of charged particles and the ionization trail they leave in the detector gas.

TRD Transition Radiation Detector, a subdetector of ALICE. It measures the ionization of the detector gas by charged particles in addition to the ionization by transition radiation created by particles with a high γ .

Bibliography

- [1] ROOT: <http://root.cern.ch/drupal/>.
- [2] ALICE Collaboration. ALICE Inner Tracking System Technical Design Report, ALICE TDR 4. Technical report, CERN / LHCC 99-12.
- [3] ALICE Collaboration. ALICE Time of Flight System Technical Design Report, ALICE TDR 8. Technical report, CERN / LHCC 2002-016.
- [4] ALICE Collaboration. ALICE Time Projection Chamber Technical Design Report, ALICE TDR 7. Technical report, CERN/LHCC 2000-001.
- [5] ALICE Collaboration. ALICE Transition Radiation Detector Technical Design Report, ALICE TDR 9. Technical report, CERN/LHCC 2001-021.
- [6] J. Alme et al. The ALICE TPC, a large 3-dimensional tracking device with fast readout for ultra-high multiplicity events. *Nuclear Instruments and Methods in Physics Research A*, 622:316–367, October 2010.
- [7] A. Andronic, P. Braun-Munzinger, and J. Stachel. Hadron production in central nucleus-nucleus collisions at chemical freeze-out. *Nuclear Physics A*, 772(3-4):167 – 199, 2006.
- [8] N. Armesto, B. Cole, C. Gale, W. A. Horowitz, P. Jacobs, S. Jeon, M. van Leeuwen, A. Majumder, B. Muller, G.-Y. Qin, C. A. Salgado, B. Schenke, M. Verweij, X.-N. Wang, and U. A. Wiedemann. Comparison of Jet Quenching Formalisms for a Quark-Gluon Plasma "Brick". *ArXiv e-prints*, June 2011.
- [9] R. Baier, Yu.L. Dokshitzer, A.H. Mueller, S. Peigné, and D. Schiff. Radiative energy loss of high energy quarks and gluons in a finite-volume quark-gluon plasma. *Nuclear Physics B*, 483(1-2):291 – 320, 1997.
- [10] Roger Barlow and Christine Beeston. Fitting using finite monte carlo samples. *Computer Physics Communications*, 77(2):219 – 228, 1993.
- [11] Hans Bichsel. A method to improve tracking and particle identification in TPCs and silicon detectors. *Nuclear Instruments and Methods in Physics Research Section A: Accelerators, Spectrometers, Detectors and Associated Equipment*, 562(1):154 – 197, 2006.
- [12] Hans Bichsel and Roberta P. Saxon. Comparison of calculational methods for straggling in thin absorbers. *Phys. Rev. A*, 11:1286–1296, Apr 1975.

Bibliography

- [13] P. Braun-Munzinger and J. Stachel. (non)thermal aspects of charmonium production and a new look at J/ψ suppression. *Physics Letters B*, 490(3-4):196 – 202, 2000.
- [14] Matteo Cacciari, Mario Greco, and Paolo Nason. The p_T spectrum in heavy-flavour hadroproduction. *Journal of High Energy Physics*, 1998(05):007, 1998.
- [15] ALICE Collaboration, B Alessandro, et al. Alice: Physics performance report, volume ii. *Journal of Physics G: Nuclear and Particle Physics*, 32(10):1295, 2006.
- [16] ALICE Collaboration, F Carminati, P Foka, P Giubellino, A Morsch, G Paic, J-P Revol, K Safarik, Y Schutz, and U A Wiedemann. Alice: Physics performance report, volume i. *Journal of Physics G: Nuclear and Particle Physics*, 30(11):1517, 2004.
- [17] The ALICE Collaboration. Measurement of electrons from beauty hadron decays in pp collisions at $\sqrt{s} = 7$ TeV. Article in preparation.
- [18] The ALICE Collaboration. Elliptic flow of charged particles in pb-pb collisions at $\sqrt{s_{NN}} = 2.76$ TeV. *Phys. Rev. Lett.*, 105:252302, Dec 2010.
- [19] The PHENIX Collaboration. Energy loss and flow of heavy quarks in Au + Au collisions at $\sqrt{s_{NN}} = 200$ GeV. *Phys. Rev. Lett.*, 98:172301, Apr 2007.
- [20] Lázló P. Csernai. *Introduction to Relativistic Heavy Ion Collisions*. 2008.
- [21] Andrea Dainese. Charm production and in-medium QCD energy loss in nucleus nucleus collisions with ALICE: A Performance study. 2003.
- [22] Yu.L Dokshitzer and D.E Kharzeev. Heavy-quark colorimetry of qcd matter. *Physics Letters B*, 519(3-4):199 – 206, 2001.
- [23] E.M. Henley and A.L. Garcia. *Subatomic physics*. World Scientific, 2007.
- [24] MinJung Kweon. private communication.
- [25] T. Matsui and H. Satz. J/ψ suppression by quark-gluon plasma formation. *Physics Letters B*, 178(4):416 – 422, 1986.
- [26] K Nakamura and Particle Data Group. Review of particle physics. *Journal of Physics G: Nuclear and Particle Physics*, 37(7A):075021, 2010.
- [27] The ALICE Collaboration. The ALICE experiment at the CERN LHC. *Journal of Instrumentation*, 3(08):S08002, 2008.
- [28] The ALICE Collaboration. Heavy flavour decay muon production at forward rapidity in proton-proton collisions at $\sqrt{s} = 7$ TeV. *Physics Letters B*, 708(3-5):265 – 275, 2012.
- [29] The ALICE Collaboration. Measurement of charm production at central rapidity in proton-proton collisions at $\sqrt{s} = 7$ TeV. *JHEP*, 1201:128, 2012.

Bibliography

- [30] The ALICE Collaboration. Measurement of electrons from semileptonic heavy-flavour hadron decays in pp collisions at $\sqrt{s} = 7$ TeV. *ArXiv e-prints*, May 2012.
- [31] Thews, Robert L. and Schroedter, Martin and Rafelski, Johann. Enhanced J/ψ production in deconfined quark matter. *Phys. Rev. C*, 63:054905, Apr 2001.
- [32] W.A. Zajc. The fluid nature of quark-gluon plasma. *Nuclear Physics A*, 805(1-4):283c – 294c, 2008. INPC 2007: Proceedings of the 23rd International Nuclear Physics Conference.

Bibliography

Erklärung:

Ich versichere, dass ich diese Arbeit selbstständig verfasst habe und keine anderen als die angegebenen Quellen und Hilfsmittel benutzt habe.

Heidelberg, den 30.6.2012

.....